

INTERNATIONAL ENERGY AGENCY
Energy conservation in buildings and
community systems programme

27th AIVC Conference

Technologies & Sustainable Policies for a Radical Decrease of the Energy Consumption in Buildings

The International Journal of Ventilation
Special Edition – June 2007



Air Infiltration and Ventilation Centre
Operating Agent and Management
INIVE EEIG
Boulevard Poincaré 79
B-1060 Brussels
Belgium

The International
Journal of Ventilation

Volume 6 Number 1
June 2007

ISSN 1473 - 3315

Special Edition:
EPIC AIVC Conference – Technologies and
Sustainable Policies for a Radical Decrease of
Energy Consumption in Buildings

Contents

| | |
|--|----|
| Editorial | 1 |
| Monitoring Results of a Naturally Ventilated and Passively Cooled Office Building in Frankfurt, Germany: Wagner A, Kleber M and Parker C. | 3 |
| Flow Pattern Effects on Night Cooling Ventilation: Lissen JMS, Fernández JAS, Sánchez de la Flor FJ, Domínguez SÁ and Pardo ÁR. | 21 |
| Numerical Evaluation of Earth to Air Heat Exchangers and Heat Recovery Ventilation Systems: Chlela F, Husaunndee A, Riederer P and Inard C. | 31 |
| Urban Canyon Influence on Building Natural Ventilation: Syrios K and Hunt GR. | 43 |
| Study of the Air Flow Structure in Cross-Ventilated Rooms based on a Full-Scale Model Experiment: Nishizawa S, Sawachi T, Narita K, Kiyota N and Seto H. | 51 |
| Vent DisCourse - Development of Educational Material on Energy Efficient Ventilation of Buildings: Kolokotroni M, Shilliday J, Liddament M, Santamouris M, Farrou I, Seppanen O, Brown R, Parker J and Guarracino G. | 61 |
| Application of the PHACES Tool in the Design of Natural Ventilation for Passive Cooling: El Mankibi M and Michel P. | 69 |
| Exergy Analysis as an Assessment Tool of Heat Recovery of Dwelling Ventilation Systems: Sakulpipatsin P, Boelman EC and Cauberg JJM. | 77 |
| Potential of Natural Ventilation in a Tropical Climate: Bastos LEG and Barroso-Krause C. | 87 |
| The Real Life Efficiency of Gas Phase Filters Used in General Ventilation and their Influence on the Indoor Air Quality of an Office Building: Ginestet A and Pugnet D. | 95 |

Editorial Board

- Prof. Francis Allard** (*LEPTAB, Université de La Rochelle, France*);
Dr. Hazim Awbi (*School of Construction Management and Engineering, University of Reading, UK*);
Prof. Jim Axley (*Yale School of Architecture, US*);
Prof. Richard Aynsley (*Delta T Corporation, Lexington, Kentucky, US*);
Dr. Malcolm Cook (*Inst. of Energy and Sustainable Development, De Montfort University, Leicester, UK*);
Dr. Angelo Delsante (*Building, Construction and Engineering CSIRO, Australia*);
Michael Donn (*Centre for Building Performance Research, Victoria University, Wellington New Zealand*);
Dr. Rodger Edwards (*Dept. of Building Engineering, UMIST, UK*);
Dr. David Etheridge (*University of Nottingham, UK*);
Prof. Ing. Gian Vincenzo Fracastoro (*Dipartimento di Energetica Politecnico di Torino, Italy*);
Prof. Fariborz Haghighat (*Dept. of Building, Civil and Environmental Eng, Concordia University, Canada*);
Prof. Per Heiselberg (*Hybrid Ventilation Centre, Aalborg University, Denmark*);
Dr. Gary Hunt (*Dept. of Civil & Environmental Engineering Imperial College, UK*);
Prof. Yi Jiang (*Dept. of Building Science & Technology Tsinghua University, China*);
Prof. Miroslav Jicha (*Faculty of Mechanical Engineering, Brno University of Technology, Czech Republic*);
Prof. Shinsuke Kato (*Industrial Institute of Science, University of Tokyo, Japan*);
Dr. Maria Kolokotroni (*Brunel University, UK*);
Dr. Yuguo Li (*University of Hong Kong, China*);
Dr. Alfred Moser (*Air & Climate, Dept of Architecture ETH-Zentrum LOW E2, Zurich, Switzerland*);
Prof. Tadj Oreszczyn (*Bartlett School of Graduate Studies, University College, London, UK*);
Dr. Claude-Alain Roulet (*Ecole Polytechnique Fédérale de Lausanne, Swiss Fed. Inst. of Technology*);
Prof. Mats Sandberg (*Indoor Environment and Ventilation, Dept. of the Built Environment, HIG, Gävle, Sweden*);
Prof. Mat Santamouris (*Associate Professor of Energy Physics, University of Athens, Greece*);
Prof. Olli Seppänen (*Inst. of Heating, Ventilating and Air Cond. Helsinki University of Technology, Finland*);
Dr. (John) Chia Yu Shaw (*Inst. for Research in Construction, National Research Council, Canada*);
Dr. Jerzy Sowa (*Warsaw University of Technology, Institute of Heating and Ventilation, Poland*);
Prof. Hiroshi Yoshino (*Tohoku University, Dept. of Architecture and Building Sciences, Japan*);
Dr. Jianshun “Jensen” Zhang (*Director, Energy and Indoor Environmental Systems, Syracuse University, US*).

Editor: Prof. Martin W. Liddament (*VEETECH Ltd. UK*)

© VEETECH Ltd. 2007 (Ventilation Energy and Environmental Technology). No part of this Journal may be uploaded on to the world wide web or any other public access system without the express permission of the publisher.

Published by: VEETECH Ltd.
7A Barclay's Venture Centre,
The University of Warwick Science Park,
Sir William Lyons Road,
COVENTRY
United Kingdom
CV4 7EZ

Tel: +44(0) 118 9477231

Email: mliddament@ijoint.org.uk

Web: www.ijoint.org.uk

Cover Design: Zoe Lawson, *Wyatt International Ltd.*

Paper: Rey Superior, *Manufactured from wood managed according to PEFC.*

Binding of printed edition: Kew Bookbinding.

E-Edition: This Journal is available on-line via Atypon and major providers.

Disclaimer: The views expressed in this Journal need not necessarily reflect those of the Publisher or of the Editorial Board. Information published in the International Journal of Ventilation is intended for research purposes only and is not validated for legal applications.

International Journal of Ventilation

Special Edition: EPIC AIVC Conference - Technologies and Sustainable Policies for a Radical Decrease of Energy Consumption in Buildings

Guest Editorial

The common EPIC – AIVC Conference was organized in Lyon France between 22 to 24th of November 2006. A very high number of excellent papers were presented and the conference was regarded as being of high scientific quality.

More than 80 of the papers presented at the Conference dealt with ventilation studies and most of these reported very interesting and innovative results. Among the best papers, we have selected 10 which we believe merit publication in the International Journal of Ventilation.

All invited papers were rewritten to fit the standards of the Journal and are fully reviewed. The papers cover to the following topics:

- Monitoring Results of Naturally Ventilated Buildings;
- Night Cooling Ventilation;
- Earth to Air Heat Exchangers and Heat Recovery Systems;
- Natural Ventilation in Urban Canyons;
- Air Flow Structures in Cross Ventilated Rooms;
- Ventilation and Education;
- Natural Ventilation and Control Systems;
- Exergy Analysis of Ventilation Systems;
- Natural Ventilation in Tropic Climates;
- The Influence of Gas Phase Filters on IAQ.

I would like to thank all authors for the excellent work they have undertaken and for the effort they have put in order to develop as much as possible the quality of this special issue. Finally, I would like to thank Martin Liddament, who encouraged us to prepare this special issue and agreed to publish these papers.

Professor Mat Santamouris
Steering Group Member - Air Infiltration and Ventilation Centre

Monitoring Results of a Naturally Ventilated and Passively Cooled Office Building in Frankfurt, Germany

Andreas Wagner¹, Michael Klebe¹ and Christopher Parker²

¹Division of Building Science, University of Karlsruhe, Englerstr.7, 76131 Karlsruhe, Germany

²Student at Purdue University who worked for this study at the University of Karlsruhe as a research scholar

Abstract

Ventilation, cooling and air-conditioning contribute significantly to the energy consumption of many existing office buildings, particularly when primary energy factors are taken into account. "Lean" building concepts however can diminish this energy consumption by natural ventilation and passive cooling strategies. Compared to fully air-conditioned buildings the resulting indoor temperatures float in a broader band during summer and might exceed the boundaries for thermal comfort for short periods. This paper presents the monitoring results of a naturally ventilated and passively cooled bank building in Germany and shows that, even during the very hot summer of 2003, the indoor climate could be held in an acceptable range by only passive means if the rooms were operated properly. The air quality was shown to be high with natural ventilation. Investigations on the night ventilation strategy revealed an incorrect implementation of design parameters in the building management system. Further optimization potential for nocturnal airflow was found by simulations based on recorded data. The low total primary energy consumption for heating, cooling, ventilation and lighting of $115 \text{ kWh m}^{-2}\text{a}^{-1}$ confirmed an excellent performance of the building. Monitoring proved to be a necessary and efficient way to optimize the building's operation.

Key words: natural ventilation, passive cooling, night ventilation, energy efficiency, thermal comfort, indoor air quality, monitoring, case study.

1. Introduction

In commercial buildings the energy consumption for ventilation, cooling or air-conditioning very often accounts for 50% or more of the total electricity consumption for technical building services. With the introduction of the European "Energy Performance of Buildings Directive" in 2001 a strong incentive was given to decrease this energy consumption by appropriate building design and integrated energy concepts. Such "lean" building strategies include natural ventilation (at least) outside the heating season and passive cooling during summer. Additionally these buildings present a high insulation standard and a high amount of daylight available at the workspaces. These measures ensure high indoor air quality as well as thermal and visual comfort.

Already in 1995 the German Ministry of Economics and Technology (former Ministry of Economy and Labour) initiated the funding programme EnBau (1995) to support the realisation and evaluation of new energy-efficient commercial buildings with the features mentioned above and new building

technologies. Funding is restricted to buildings with a predicted primary energy consumption for heating, cooling, ventilation and lighting of not more than $100 \text{ kWh m}^{-2}\text{a}^{-1}$ which is less than at least a third of the consumption of existing buildings. So far 23 demonstration buildings have been realised and monitored thoroughly; results show that the ambitious target could be reached by the majority of the buildings with investment costs that are in the same range as the costs of conventional projects (Voss et al, 2006).

In this paper the "East Arcade" of the KfW bank in Frankfurt, Germany, is presented which was funded in the programme from 2003 to 2005. In addition to the limitation on total primary energy consumption, the thermal comfort conditions for this naturally ventilated and passively cooled building were fixed to a maximum indoor temperature of 26°C with outdoor temperatures up to 32°C . Above that, a minimum temperature difference between outside and inside of 6 Kelvin should be kept. It was agreed that these limits should not be exceeded by more than 60 hours per year during working hours.



Figure 1. View of the KfW building from south-east (© Architekten RKW Rhode Kellermann Wawrowsky).

2. Building and Energy Concept

The “East Arcade”, a new extension building of the KfW bank group, is situated in the middle of Frankfurt, Germany (Figure 1). The 7 storey high building, which was completed in 2002, has a net floor area of 8585 m² for approximately 300 employees. Five floors with office rooms and two upper floors with apartments are grouped around an atrium in the centre of the building, which is used for night ventilation for all passively cooled offices.

The energy-related features of the building include a high insulation standard with a mean U-value of the

building envelope of 0.54 W/m²K and a form factor of 0.25 m⁻¹. The offices are situated along the perimeter zone of the building and windows reach up to the ceiling resulting in high daylight coefficients at the workspaces. Conference rooms are adjacent to the atrium and receive daylight as well. Artificial lighting in the building is automatically controlled as a function of presence of the occupants and available daylight on the desk. Natural ventilation was realized for the offices on the eastern and western façades with manually operable windows and skylights and by appropriate design of the room depth (single-side ventilation). The occupants can either determine the opening times of the windows or skylights individually or activate the skylights via a control panel in each office resulting in a 3 minute opening time.

Moderate glazing ratios on the façades, windows of low energy transmittance but high selectivity (38% total solar energy transmittance, 68% daylight transmittance) and an efficient external shading system with optional daylight transmittance in the upper part minimise external heat loads during summer. In the offices only TFT screens with a low heat emission are used for the computers. Natural night ventilation plays a major role in the passive cooling concept. For this purpose the skylights in the façade and towards the hallways are opened automatically during the night allowing the discharge of the internal building mass (concrete ceilings in the office rooms without any suspension) by the stack effect in the centralised atrium (Figure 2).

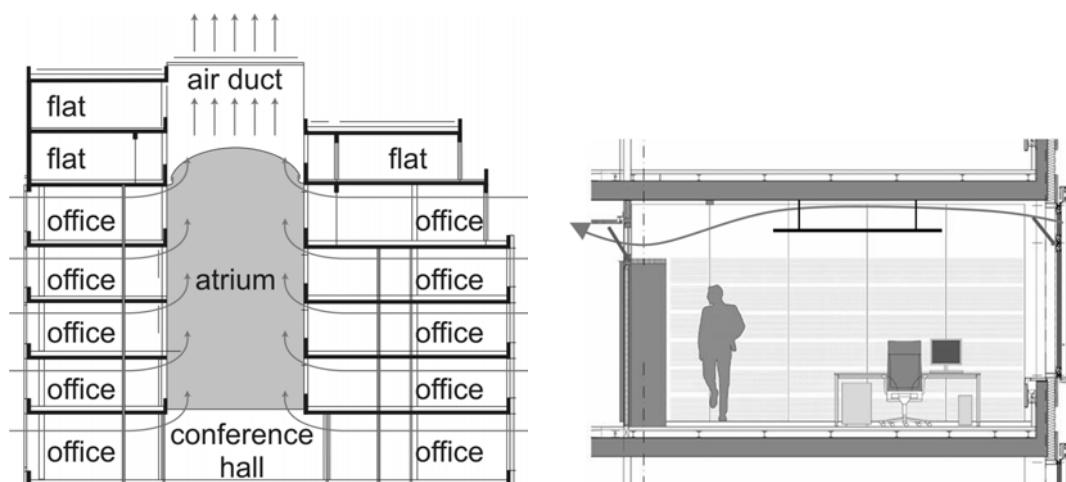


Figure 2: Left: Cross section of the KfW building with the central atrium showing the paths of the airflow during night ventilation (©EnBau). Right: Section through an office showing the open skylights during night ventilation (© ip5 ingenieurpartnerschaft).

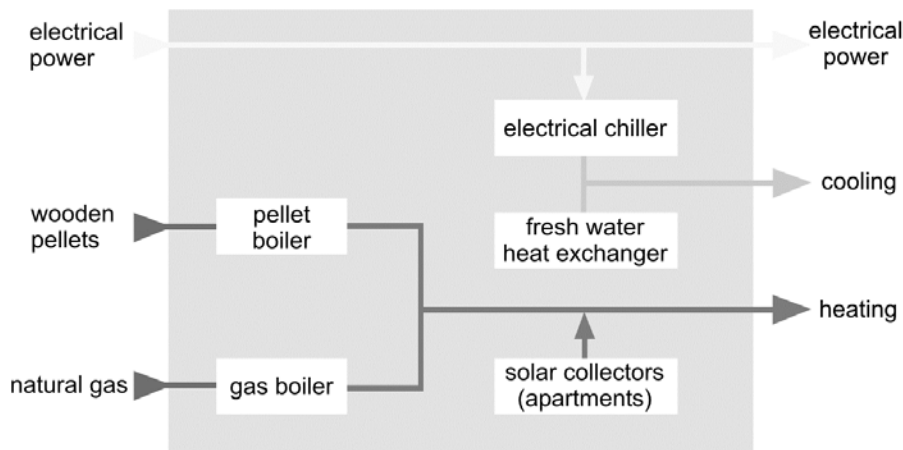


Figure 3. Scheme of the energy concept of the KfW bank building (© EnBau).

In offices where air-conditioning is necessary due to high internal loads and their location towards a noisy street (about 20% of all rooms, mostly situated along the south façade) the cooling loads are mainly covered by tab water cooling, backed by a conventional compressor water chiller. Heating energy is provided by a boiler fired with wood pellets and a condensation boiler for peak loads. A thermal solar system contributes to the hot water demand of the canteen and the apartments. The energy supply concept of the building is shown in Figure 3.

3. Results and Discussion

The operation of the technical equipment for heating, ventilation, cooling and lighting as well as the indoor climate conditions were monitored from May 2003 to December 2005, using about 300 sensors in the technical building services systems and different office rooms. The main circuits for heat and cold supply were equipped with heat meters and the large consumers of electricity with electric meters. In the offices air temperature, two ceiling temperatures and CO₂-concentration (only in a few rooms) were measured. Additionally, the position of the sun blinds as well as the state of the windows and the skylights were recorded to provide information about the building control. Continuous data were recorded in 10-minute-intervals, event data like the opening of a window were recorded in real-time. The data were written into different text files on a computer in the bank building and transferred into a database on the university server every night. In the following sections, results of the energy consumption and thermal comfort conditions

are shown and discussed. Special emphasis is given to the night ventilation strategy and its impact on passive cooling.

3.1 Energy Consumption of the Building

Figure 4 shows the primary energy consumption of the building over the whole monitoring period. It decreases continuously and almost reaches the targeted 100 kWh m⁻²a⁻¹ in the third year if only energy for heating, ventilation, cooling and lighting is considered (as required by the funding programme). Reasons for exceeding the target in the first two years are explained below. Even if the target was not met, the energy performance of the KfW building is outstanding compared to usually built office buildings in Germany with a primary energy consumption between 400 and 700 kWh m⁻²a⁻¹ (Voss et al, 2006).

Regarding the total primary energy consumption, heating and cooling of the IT systems show the highest contributions. The portion of heating is even higher if final energy consumption is taken as a basis (the primary energy factor of biomass is 0.2 according to the German standard). One of the reasons for this was the permanent year-round heat demand of two hot water boilers which caused a constantly high supply temperature of up to 90°C in the heating distribution system even during the summer. An improvement can only be achieved by modifying the system design. The second reason was the pellet boiler: unusual high exhaust temperatures indicated that the efficiency of the boiler was too low and led to a higher consumption of the wooden pellets. The boiler has to be replaced by an appropriately sized one in order to reach the

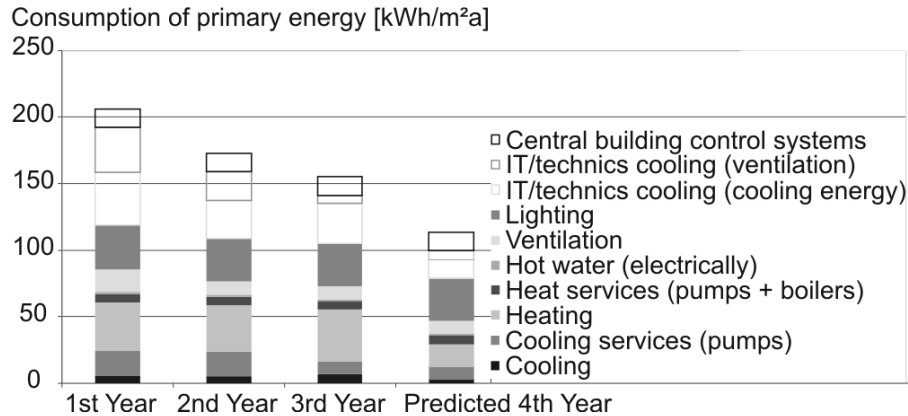


Figure 4. Primary energy consumption during the 3 years of monitoring including a prediction for the fourth year. Energy consumptions for the building control system and IT-cooling are marked differently as they were not considered in the funding programme's building evaluation. Biomass is evaluated with a primary energy factor of 0.2, electricity with 3.0.

design values. Finally, energy losses due to ventilation are higher than in a building with mechanical ventilation and heat recovery and therefore contribute more strongly to the heating energy consumption. In Figure 4 the potential of improvements in the heating system is shown by the predicted consumption in the fourth year.

Cooling of the IT systems and technical service rooms contributed to approximately 30% of the total primary energy consumption in the first year. In the beginning, set temperatures of 20°C in many of the IT rooms caused the cooling system to run 24 hours a day. Additionally, the compressor water chiller had a COP of only 2.6. The change of the operation scheme for cooling and raising the set temperatures in the rooms to 26°C helped to significantly reduce both electrical energy consumption and energy for cooling (see Figure 5).

Also the energy consumption for cooling the offices could be reduced in the last year by optimizing the system operation. A remarkably high energy consumption was recorded for the central building control system. As a result it can be stated that the higher total energy consumption of the building in the beginning was mainly due to failures in operation and not to conceptual reasons. The ongoing and thorough monitoring proved to be a very efficient approach to optimizing the building's energy performance. This was also found in all of the 23 investigated buildings.

3.2 Reducing External Heat Loads

In addition to the optimized glazing (size and quality) and reduced internal heat loads, a remote-controlled external shading system supports the passive cooling concept during summer days. For

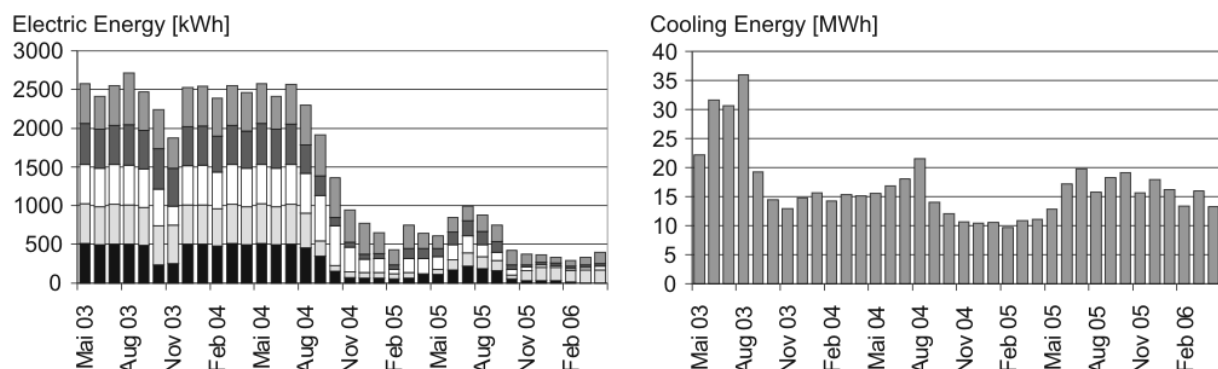


Figure 5. Monthly electrical energy consumption of five ventilators for air-conditioning the IT-rooms (left) and total cooling energy consumption for conditioning all technical service rooms (right).



Figure 6. The view on the east façade of the building shows that the shading systems are closed due to the insolation on the façade. The shading is not activated on the ground floor and only partly on the first floor except for rooms where the occupants decided differently. The picture also shows the gain of daylight in the upper part of the shading system due to the different blind angle (©ip5 ingenieurpartnerschaft).

every room an integrated shading calendar in the control system calculates whether the sun hits the window and therefore the blinds have to be closed (Figure 6). Obstructions of surrounding buildings and of the whole KfW building complex itself have been taken into account. The occupant has the possibility to overrule the automatic setting on the control panel in the room.

During the whole monitoring period the positions of blinds were recorded in 30 different rooms on all sides of the building. The average daily closing time of the blinds goes up to 6 hours a day during summer (Figure 7). The blinds are regarded as closed if more than 50% of the window is covered.

The examination was also undertaken with a covering fraction of 25% and 75%. From November until the end of February the average closing time is less than one hour a day.

In Figure 8 the recordings of all rooms are divided with respect to the different orientations. It can be seen that the blinds on the eastern façade move down first, followed by the ones on the southern and western façades, which means that the shading calendar is working properly. The blinds move up again due a time schedule which specifies the opening at a fixed time unless the occupants interfere earlier. During winter blinds are only closed on the southern façade.

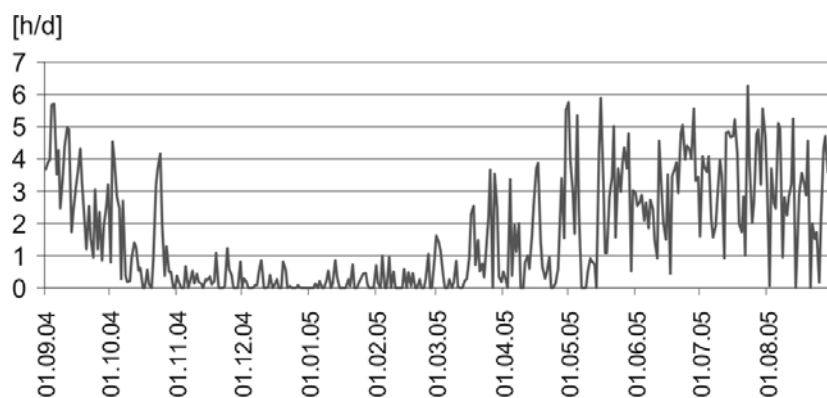


Figure 7. Average closing time of blinds during the day in all 30 monitored offices (hours/day).

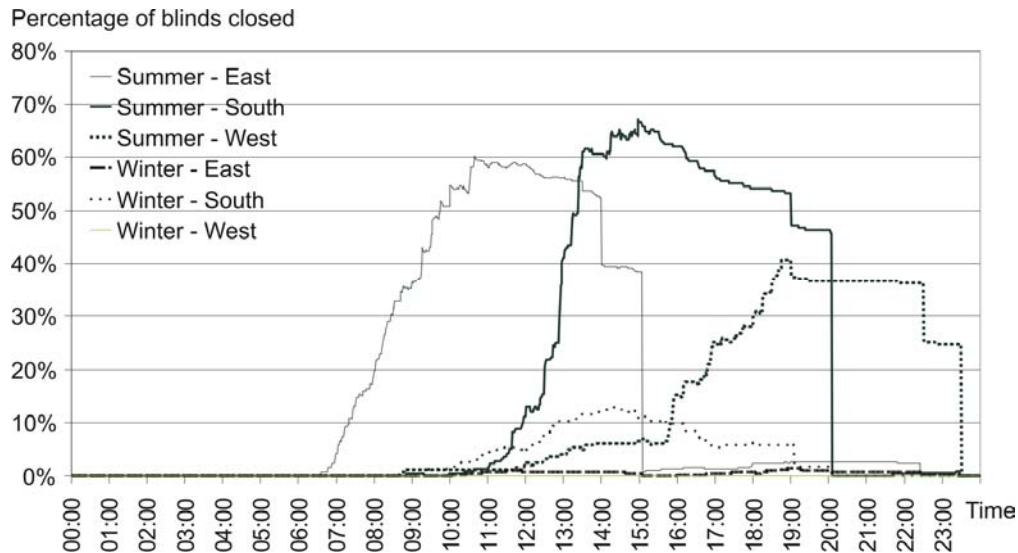


Figure 8. Percentage of rooms with the blinds closed during a typical day in summer and in winter.

3.3 Night Ventilation

Night ventilation takes advantage of natural thermal buoyancy forces in the building. During the night, when the indoor temperature is higher than the outdoor temperature, a negative pressure difference builds up at the bottom of the building and a positive pressure difference at the top. The level between the top and the bottom where the pressure difference between inside and outside is zero, is called the neutral pressure level (NPL). As shown in

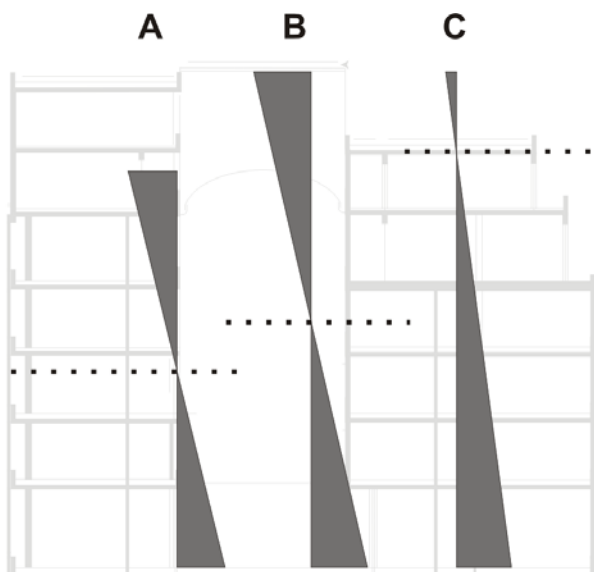


Figure 9. The normal neutral pressure level (NPL) without the additional stack (A) and with the additional stack (B). C is the targeted position of the NPL.

Figure 2, the night ventilation of the KfW building was designed in a way that cool air should enter the building through the skylights in the façade on all five floors and leave the building through the top of the atrium. This means that the NPL had to be above the fourth floor of the building.

Due to the two apartment floors above the offices a stack could be added on top of the atrium resulting in a higher NPL for the KfW bank (Figure 9, B). With equal pressure differences below and above the NPL there would have still been an airflow from the atrium into the offices of the fourth floor. Therefore the sizing of the air inlets on the different levels and the air outlet on top of the stack had to be optimized in a way that the NPL would be above the highest office level and all offices would profit from cool air entering from outside (Figure 9, C). Additionally, all opening angles of the skylights had to be defined to ensure an equal airflow rate on each floor and in each office room. As each room has two skylights – one in the façade and one towards the hallway / atrium – it was decided to open the latter to its maximum and to adjust the airflow rate by the opening angle of the skylight in the façade.

Depending on the number of skylights in a room and the length of the flow path on a specific floor, the opening angles rise from 10 to 17 degrees on the ground floor up to 20 to 38 degrees on the fourth floor. Measurements were performed in a laboratory to find out the effective inlet area of the skylights selected for the façade (Figure 10). In order to

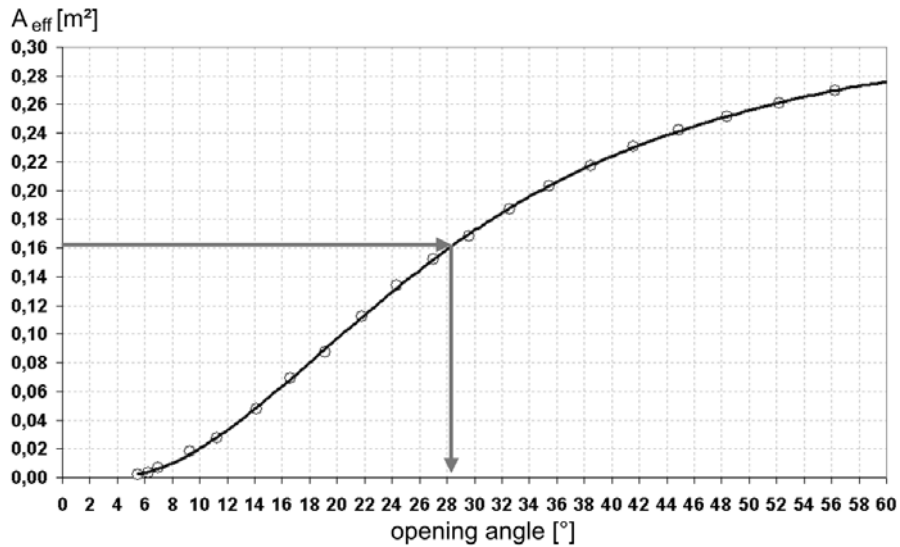


Figure 10. The effective inlet area depends on the opening angle of the skylight (©ip5 ingenieurpartnerschaft).

achieve the required opening angles the runtime of every electric motor (actuator) was calculated and stored in the control system of the building.

The following schedule for the night ventilation was then implemented in the building control system: Night ventilation is limited to a time period between 21:00 and 6:45 because employees start working at 7:00 in the morning. It is only activated when the indoor air temperature in an office is at least 1 Kelvin higher than the outdoor air temperature. However, night ventilation will be interrupted in cases when the indoor air temperature sinks below 18°C (20°C since 2005) to avoid uncomfortable conditions for the employees in the morning. The



Figure 11. View of the stack with the hood and the additional fans (© Architekten RKW Rhode Kellermann Wawrowsky).

skylights of an office open again within the specified period when the air temperature in this office exceeds 20°C (22°C). In cases that the atrium's hood on top of the stack has to be closed because of rain, wind or high outdoor temperatures, which would induce a reverse flow, additional ventilation fans in the stack are activated (Figure 11). Compared to the natural airflow the fans provide a much smaller airflow rate. The schematic of the complete control strategy is given in Figure 12.

Within the monitoring the actually implemented opening times for each skylight were derived from the control system and compared to the calculated times that the skylight should open. It was found that many opening times for the rooms on the third floor did not match the designed ones. The skylights opened wider than they were supposed to, which lowered the neutral pressure level. To examine this effect a simulation using CONTAM (2006) software was performed to examine the resulting average air exchange rate at each level of the building. For model validation the relevant data (10-minute intervals) like outdoor temperature, room temperatures, positions of skylights and windows were taken from the monitoring records.

Three weeks of data were taken for the simulation. July 18 to 24, 2006 was considered particularly interesting because data from the hood of the atrium were available along with it being an extremely hot week. In this week outdoor temperatures frequently reached 35 degrees and occasionally the temperature

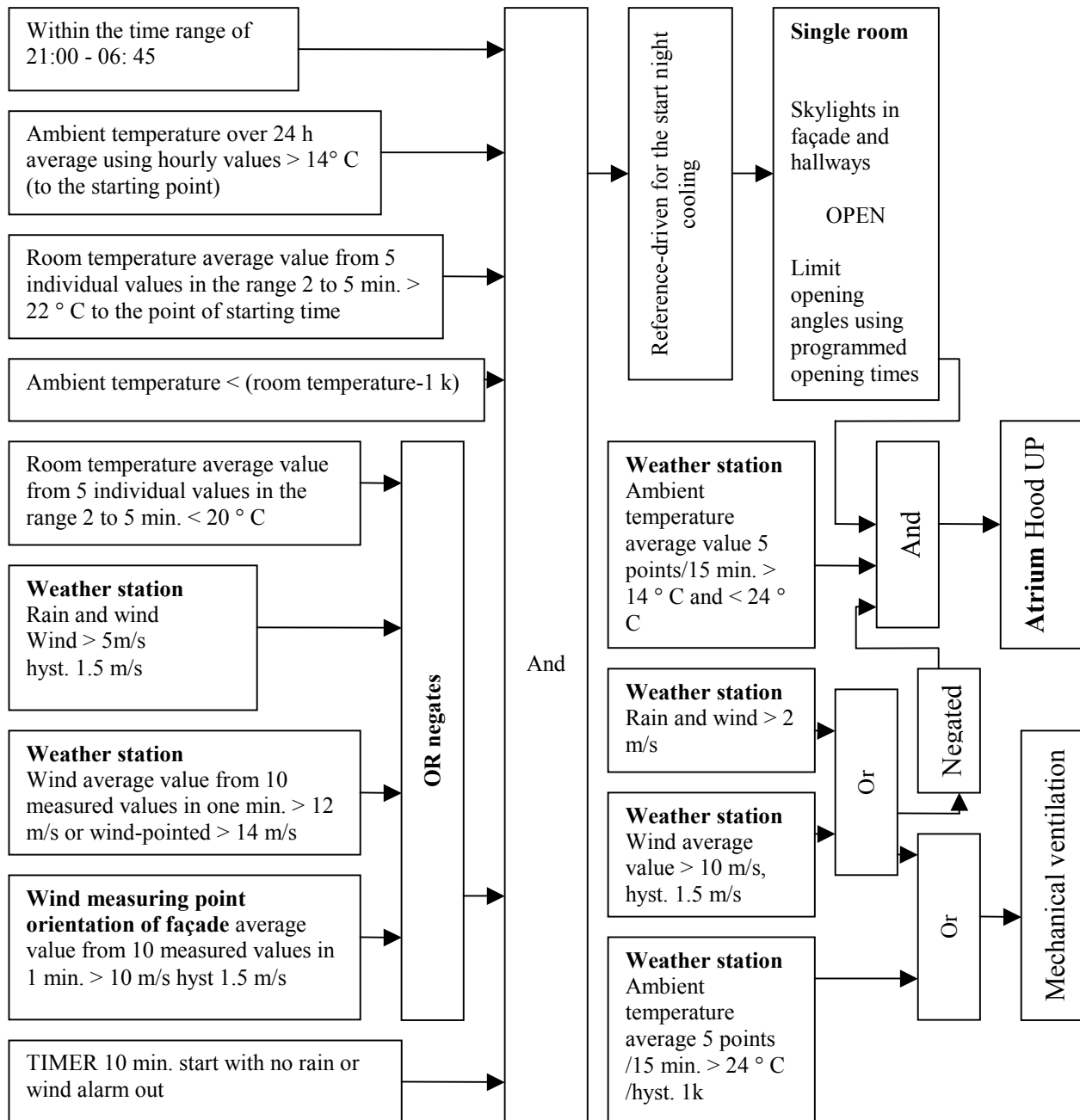


Figure 12. Schematic of the implemented control strategy for night ventilation in the KfW building (Parker 2006) (©ip5 ingenieurpartnerschaft).

outside did not go below the set temperature limit for the hood to open (see Figure 12). There was also one evening where it got significantly cooler creating a large temperature difference between the rooms and the outdoor air. Furthermore two other “normal” weeks were considered: June 29 to July 5, 2006 and July 13 to 19, 2005. First of all each case was simulated using the programmed actual opening angles. Then each room was again simulated using

the opening angles that should be in the system according to the design parameters.

When using the actual skylight opening angles it can be seen from Figure 13 that airflow rates are quite different. The ground floor and the third floor generally get the highest air exchange rates whereas the fourth floor gets a significantly smaller amount of airflow. The fourth floor gets a reduced airflow

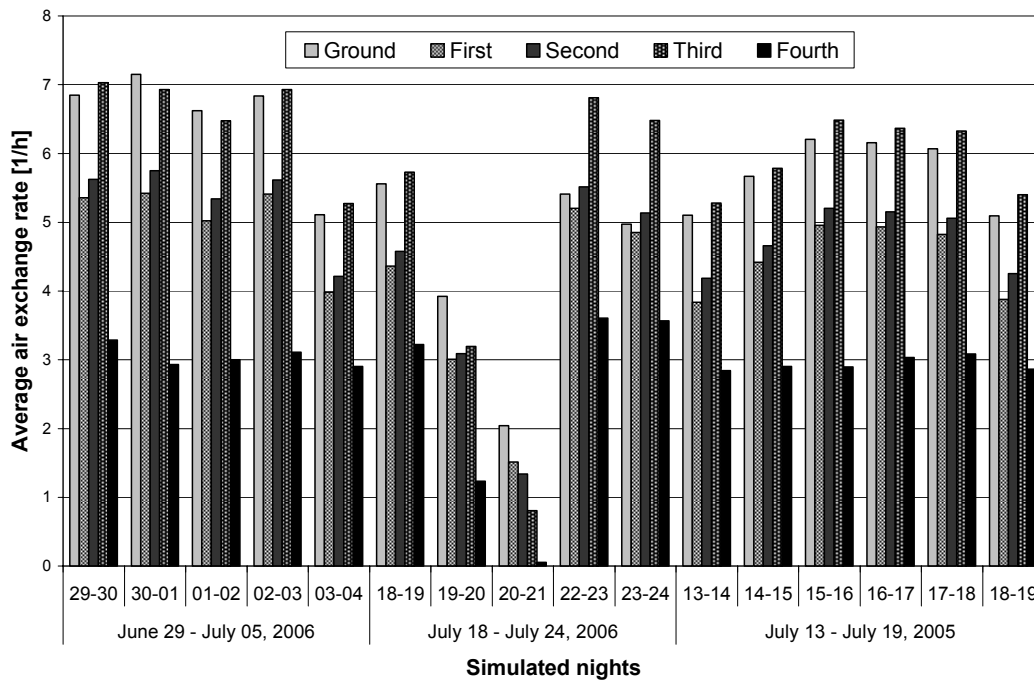


Figure 13. Average air change rates in the offices on the different levels of the building with current openings of the skylights for three simulated weeks.

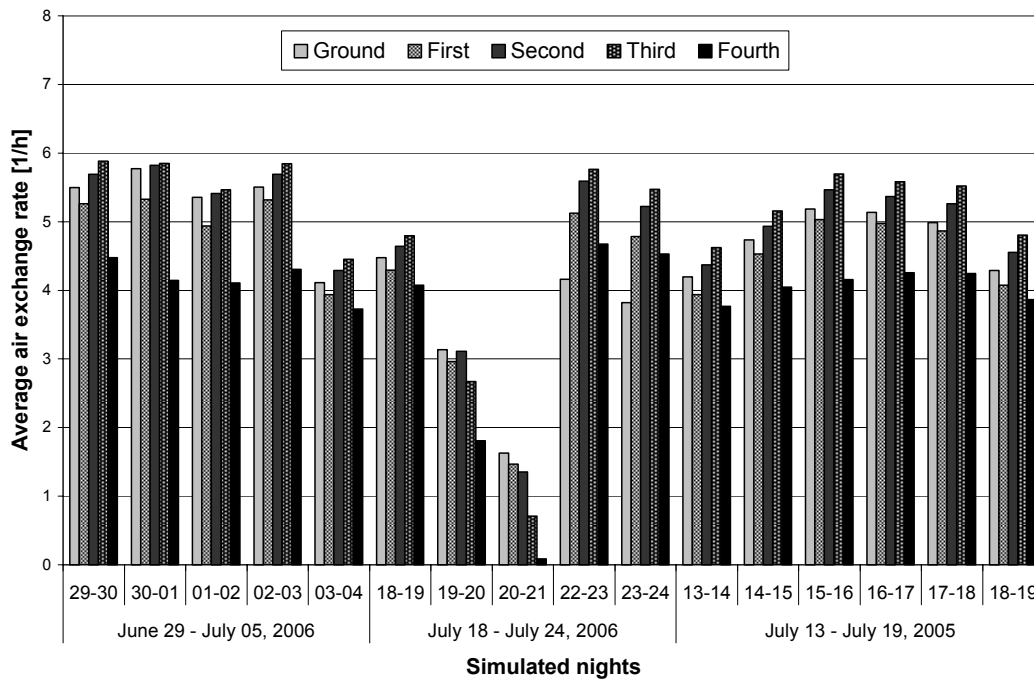


Figure 14. Average air change rates in the offices on the different levels of the building with design openings of the skylights for three simulated weeks.

because the skylights on the third floor are opened to a wider angle than designed causing a downward shift in the NPL. When the simulation is run using the designed opening angles, the results are quite

different. The average air exchange rates between the rooms are much closer to being equal as can be seen in Figure 14.

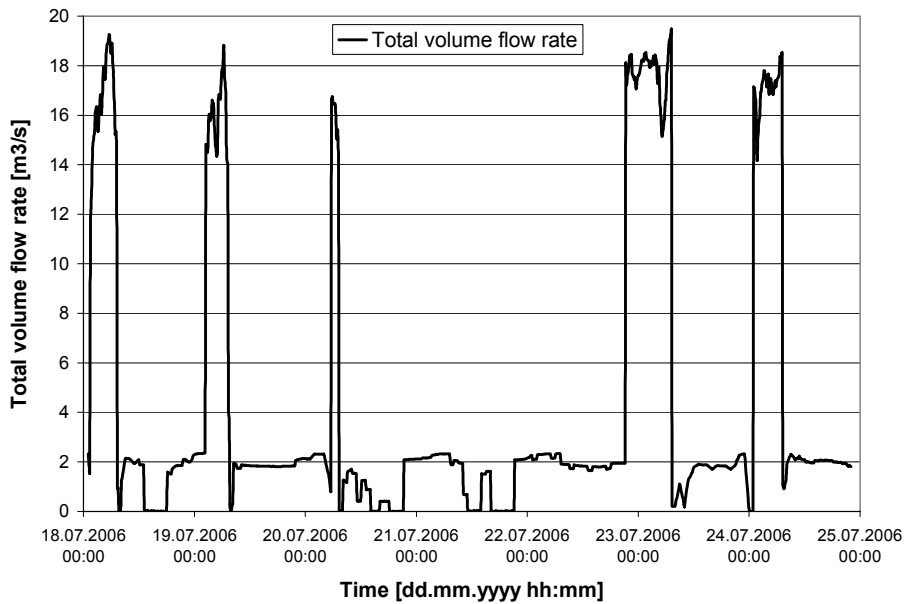


Figure 15. Total volumetric airflow rate at the top of the stack.

Although the fourth floor still receives a smaller airflow than any of the other floors it is now much closer to being uniform which was the design objective. When the overall airflows throughout the top of the stack were compared for both skylight opening cases it was found that wider opening produced about a 2% increase in flow rate. This small increase in airflow does not account for the large increase in airflow on the ground and third floors. Therefore it is seen that there is a reduction of flow for the other floors, specifically the fourth floor. Total airflows out of the top of the atrium can

be seen in Figure 15. Airflow rates generally range from 15 to 19 m³/s, which, compared to the ventilation fans which produce a flow of 2.5 m³/s, is about 7 times as much.

To check the effectiveness of night ventilation a thermal simulation was performed using TRNSYS (2006). As this was the software used during the design stages it was possible to use the same model with varying airflows. Only one room was modelled and typical climate data for the location were used for simplicity. Since only one room was simulated,

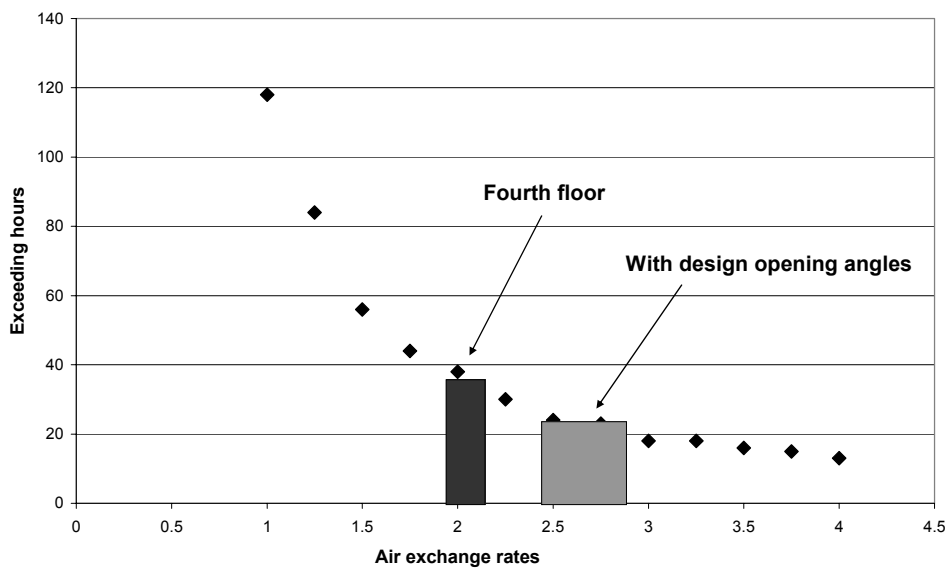


Figure 16. Hours exceeding the thermal comfort limit for varied air change rates in the KfW building.

pressure differentials between the room and the outdoor were unknown. However, the power-law model describing the airflow path between different zones of a building can be simplified with the calculated airflow rate from the CONTAM simulation to determine the constant in Equation 1.

$$Q = C_1 \cdot \sqrt{\Delta T} \tag{1}$$

From the CONTAM airflow simulations the range of values of C_1 was found to be between 2.4 and 2.8 most of the time. The TRNSYS simulations were performed for a varying airflow and giving an output of hours exceeding the thermal comfort limit (see Section 1). Since this simulation did not use outdoor conditions from any of the summers of monitoring it cannot be directly compared to any measured data. Its purpose was to see the effect of varying the airflow. A graph with varied values of air exchange rate from 1 to 4 can be seen in Figure 16.

From this graph it can be seen that the slope decreases significantly around 2.5 which means that the added benefit of increasing the airflow results in only little impact from that point. As seen from the simulations of the current skylight openings air exchange rates can vary as much as 1 h^{-1} or about 20 percent. For the TRNSYS simulation with an assumed value of $C_1 = 2.6$ a reduction in the air change rate of 20 percent results in about a 30

percent increase in exceeding hours. The light grey area in the figure represents normal air change rates seen when using the opening angles from the design. The dark grey area represents the air change rates in the fourth floor when the current opening angles are used.

In addition to the settings of the skylights the parameters of the control system were also analyzed. The control system for the hood and the skylights is quite complex since it depends on temperatures in- and outside, wind speed and state of rain (see Figure 12). After considering many of the parameters it was determined that the most important one is the limit that the outdoor temperature must be below a constant of 24°C before the hood is opened. The problem with this limit is that it does not account for varying weather conditions during the cooling season. During the hot days of the summer the atrium temperature will not drop below 26°C even with night ventilation. This means that there can be periods where there is a temperature difference of over 2 Kelvin but no ventilation.

To check the effect of increasing the limit of the maximum temperature, simulations were run for two week periods. Two types of days were considered: first a week with more normal temperatures and one extremely hot week. These

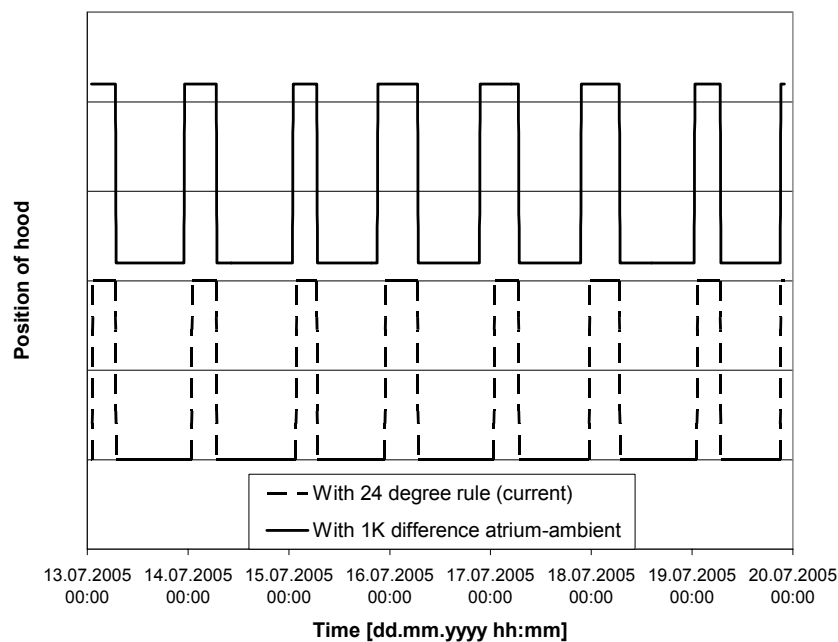


Figure 17. Hood opening times using both rules for the week of July 13-19, 2005.

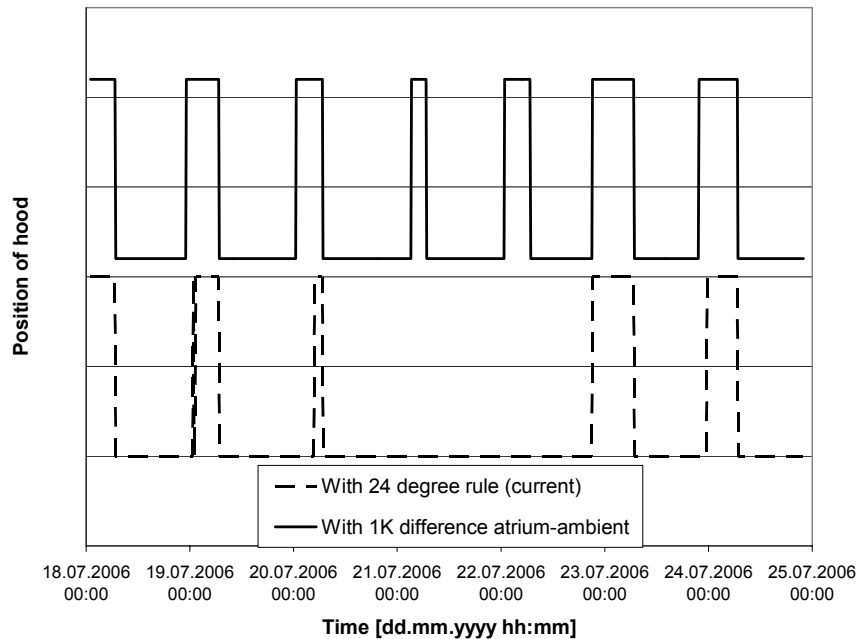


Figure 18: Hood opening times using both rules for the week of July 18-24, 2006.

weeks were July 13 to 19, 2005 and July 18 to 24, 2006. First a test was made to see if it was possible just to increase the set point of the minimum outdoor temperature which controls the hood. When applying 26°C instead of 24°C, flow rates above the limit of the fans' flow rate (9000 m³/h) were reached for all hours. However this did not work well for the cooler week - the hood opened too soon and induced a reversed flow in some of the rooms. The results of these simulations suggested that a constant set point of 24°C should not be used but instead a value that depends on the temperature in the atrium.

So a new rule in the control system was tested. The average of the four temperature measurements at the top of the atrium was compared to the outdoor temperature and a value of 1 Kelvin temperature difference was set for moving the hood. Results of this simulation showed that this rule worked well for both cooler and warmer periods. Airflow rates out of the top were above the flow rate of the fans and the hood opened earlier than before. A comparison of the opening time for both weeks can be seen in Figure 17 and Figure 18. Smaller temperature differences were also simulated but it was found that the airflow out of the top of the stack did not meet the required values for the opening times. Therefore a temperature difference of 1 Kelvin, both between the office and the outdoor temperature and also between the atrium and the outdoor temperature, was suggested to be implemented into the building

control system for opening the skylights and the hood of the atrium.

In ten rooms the temperatures of the ceiling (PT100 temperature sensors located at the surface and 40 mm into the concrete) were also recorded to obtain information about the influence of the room air temperature on the thermal behaviour of the concrete ceiling during night ventilation. In Figure 19 recordings of a room are shown for the first two weeks of August 2003. A long period of very hot days caused a permanent increase of the ceiling temperature as well as the room temperature. It can also be seen that night ventilation was not activated during three very warm nights at the beginning of the month. As soon as outdoor temperatures started to drop, the ceiling temperature decreased as well due to night cooling (Figure 20).

In rooms featuring exposed concrete ceilings there was a pronounced effect of the room air temperature on the ceiling temperature. Figure 21 shows how the cooler air temperature serves as a heat sink, decreasing the ceiling temperature during the night. With an average difference of 3 Kelvin between the ceiling and the room air temperature, the ceiling is cooled down by approximately 0.5 Kelvin within 9 hours. In rooms with suspended ceilings the measurements showed no correlation between the room air and the ceiling temperature.

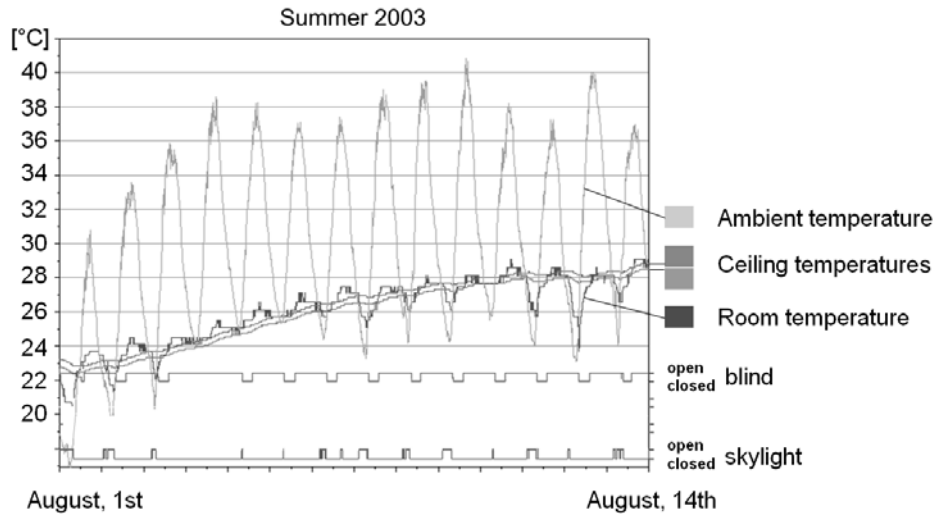


Figure 19. Temperature measurements in one standard office during the first two weeks in August 2003, together with the status of the blinds and the skylights.

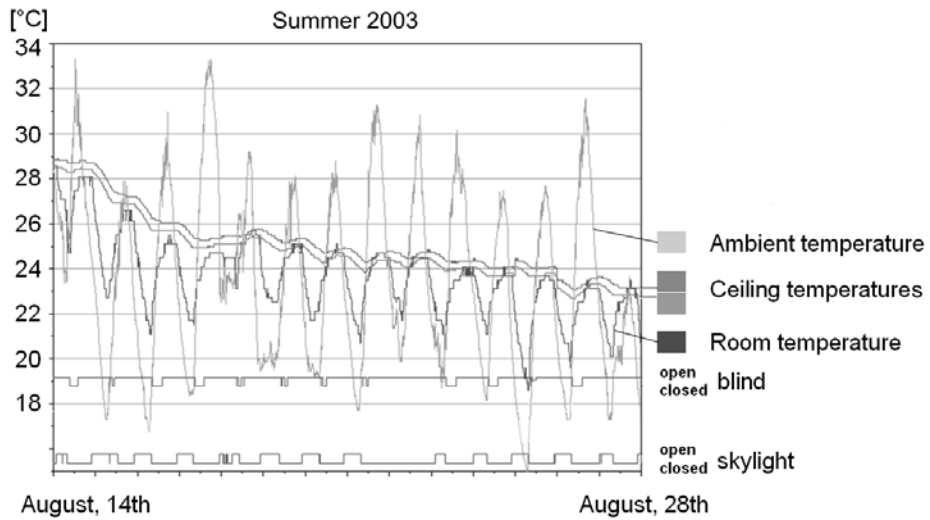


Figure 20. Temperature measurements in one standard office during the last two weeks in August 2003, together with the status of the blinds and the skylights.

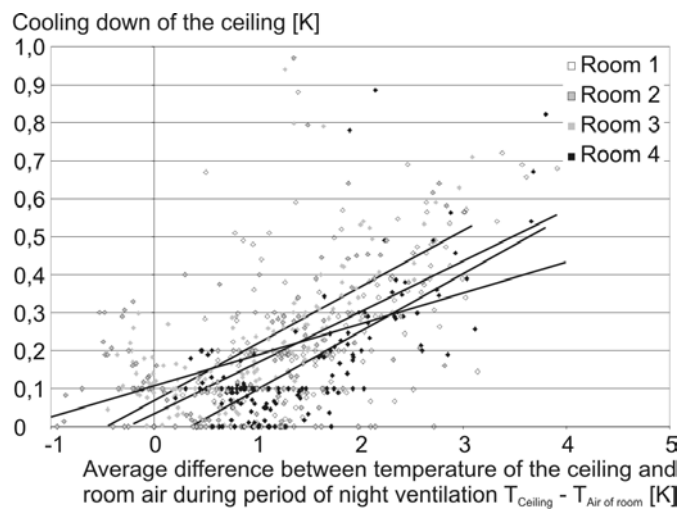


Figure 21. Cooling of the ceiling by night ventilation from 21:00 until 6:00 depending on the average difference between ceiling and room air temperature.

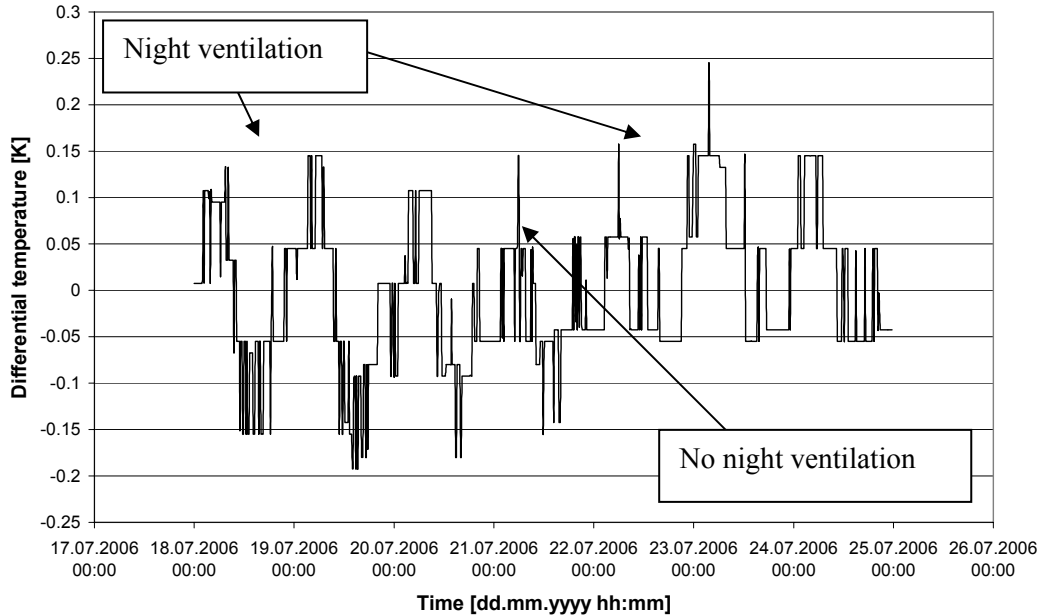


Figure 22. Differential temperature between the two measurement points in the concrete ceiling for one room in the KfW building. Heat is transferred out of the thermal mass when the temperature difference is positive.

As the concrete slab of the ceiling closely represents a one-dimensional conduction problem, with the bottom side exposed to the room and the other to an insulated false floor, the heat transfer into / outside the thermal mass can be calculated by Fourier's Law:

$$Q_h = \frac{-kA}{\Delta X} [T_{surface} - T_{40mm}] \quad (2)$$

where Q_h is the heat transfer in discrete form.

Due to the inaccuracy of the temperature data from building monitoring and uncertainties in the exact location of the sensors, a calculation of the heat transfer rates is not possible. However, when the temperature difference is graphed, time periods and relative magnitudes can be seen. A graph of the differential temperature for one room during the week of July 18 to 24, 2006 can be seen in Figure 22. During that week skylights opened every night; however, the atrium's hood did not open for two of the nights. These periods are seen in the middle of the week. During these days the temperature difference is significantly smaller than during periods when the hood of the atrium opens. This coincides with a higher heat transfer out of the ceiling when the hood is opened compared to periods when it does not open.

3.4 Thermal Comfort and Air Quality

In order to evaluate the thermal comfort conditions in the offices, indoor air temperatures and the attendance times of the occupants were recorded in 10 rooms out of 200 (since 2003) and in 20 further rooms from autumn 2004 onwards. A comparison with a globe temperature sensor showed that the measured (air) temperatures with the sensor being fixed on the interior walls of the offices were very close to the operative temperatures. The requirements defined by the building owner with regard to the room temperature are explained in section 1 and they are referred to as the 32/6-limit in Figure 23. Having gone into operation in the winter of 2002, the building had to face a first real challenge during the very hot summer of 2003. Hours with outdoor temperatures above 30°C occurred more than twice in 2003 compared to 2004, with maximum values exceeding 40°C. The measured room temperatures of four frequently used and passively cooled rooms exceeded the defined temperature limit on average by only 2.1% (32 hours) of the overall attendance time (Wagner et al, 2005). The maximum temperature in these offices reached 29.6°C (Figure 23).

In 2004 the room temperature in the same offices exceeded the temperature limit by only 0.4% (9 hours) and in 2005 by 2.1% (38 hours) of the total

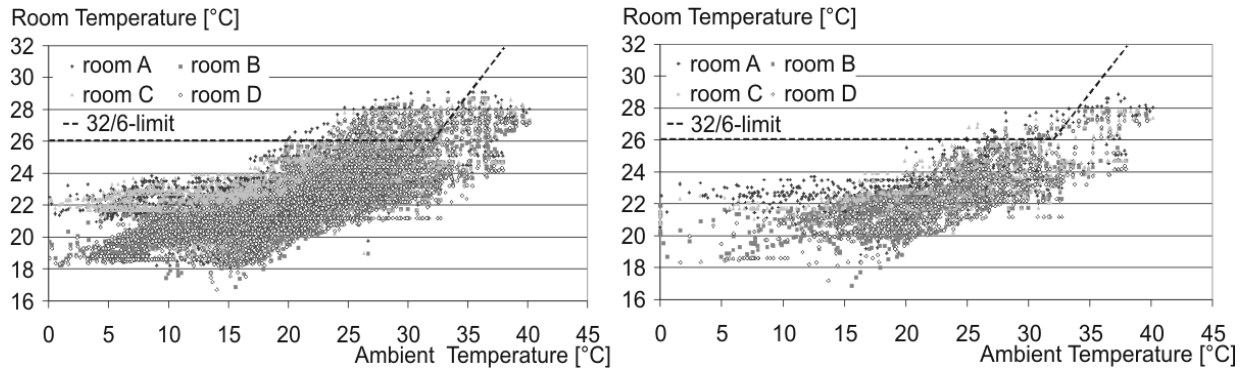


Figure 23. Average hourly room temperature of four passively cooled offices from May 2003 to October 2003 plotted over the actual outdoor air temperature. Data including all recorded hours (left) indicate a number of hours when the comfort limit was exceeded. When considering the attendance times (right) there were rarely any temperatures above the limit. The left picture also shows the lower limit of 18°C for the night cooling.

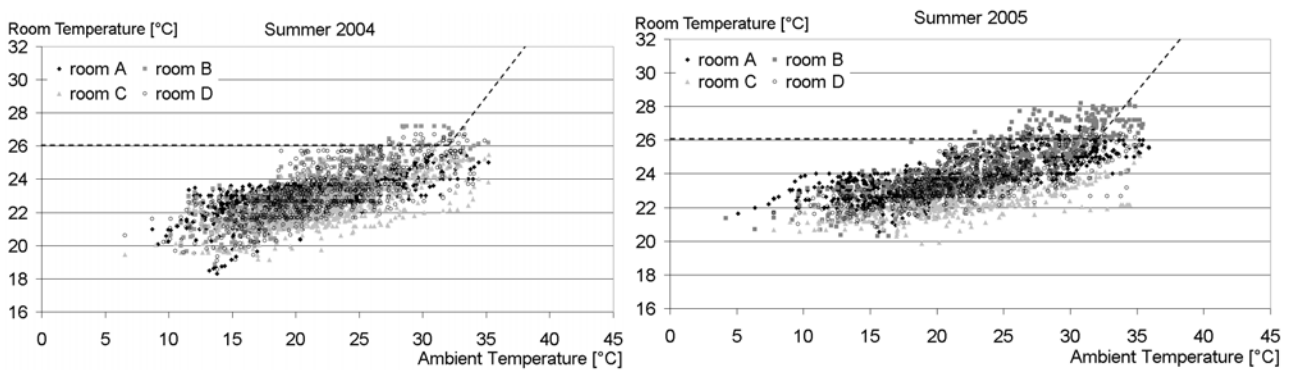


Figure 24. Average hourly room temperature during the attendance time of four passively cooled offices in summer 2004 and 2005 plotted over the actual outdoor air temperature. In 2005 the lower limit for the room temperature was raised from 18 to 20°C.

attendance time (Figure 24). The maximum temperature recorded in the offices was 27.2°C during the summer of 2004 and 28.2°C in the summer of 2005.

In summer 2006 the 60 hour limit was exceeded in different rooms. It was found that the atrium's hood did not open for most of the time and therefore night ventilation was not activated with its full capability. During the very warm nights during June 2006 there had been one week with room temperatures up to 30°C in the offices. This underlines the importance of proper operation of a passively cooled building, as there is no active cooling system as a backup.

Though being just a spot sample, the results of the four rooms show that the room temperature could be kept within the agreed limits by passive cooling even under extreme weather conditions (like in 2003). This was confirmed when all available data

of the rooms were evaluated. The results also revealed that the temperature and hour limits were exceeded in some of the air-conditioned offices as well. In addition to building operation, the exceeding hours strongly depend on the occupants' behaviour in terms of operating the shading systems and opening the windows during hot periods.

Recent results in comfort research show that thermal comfort in naturally ventilated and passively cooled buildings has to be evaluated differently in comparison to air-conditioned buildings. Occupants adapt to their thermal environment and accept higher indoor temperatures in non-conditioned buildings, particularly when they can control the climate conditions to some extent. Figure 25 shows the evaluation of comfort conditions in the KfW building according to two different adaptive comfort models (deDear and Brager 2002; Boerstra et al, 2002). A major difference between Figures 23 and

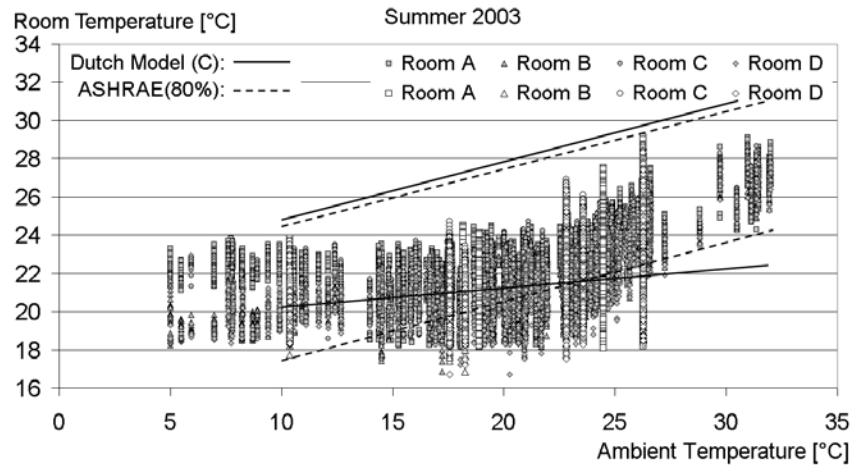


Figure 25. Average hourly room temperature of four passively cooled offices in summer 2003 plotted over the monthly mean outdoor air temperature according to the ASHRAE and the Dutch adaptive comfort models. All recorded data are used for this plot, explaining the data points below the lower temperature limits.

24 is that the room temperatures are plotted against monthly mean outdoor temperatures (ASHRAE model) or a weighted running mean outdoor temperature of the last four days respectively (Dutch model). It can be seen that all room temperature data are below the upper limit for thermal comfort.

With regard to indoor air quality, the CO₂-concentration was monitored in 5 rooms. Two of these offices were mechanically ventilated and the other three manually by the occupants. The results of more than two years monitoring showed that the limit of 1500 ppm was only exceeded for a few hours, independent of the type of ventilation (Kleber and Wagner, 2006). On average, the CO₂-concentration was below 1500 ppm for 99.8% and below 1000 ppm for 98.6% of the total attendance time. Figure 26 confirms that the concentration in

all the monitored offices was below 800 ppm for at least 90% of the attendance time. There was no significant difference between naturally and mechanically ventilated spaces.

Further analysis shows that the employees' manual use of the skylights did not depend on the outdoor temperature. For example, the average opening times of the skylights were almost identical in January 2005 and June 2005. In contrast, the manual opening of the windows correlates with the outdoor temperature. In June 2005 occupants used the windows more than three times as often for ventilation as in January 2005. With a decreasing frequency of opening the windows in winter, the CO₂-concentrations in the offices increased slightly (Figure 27).

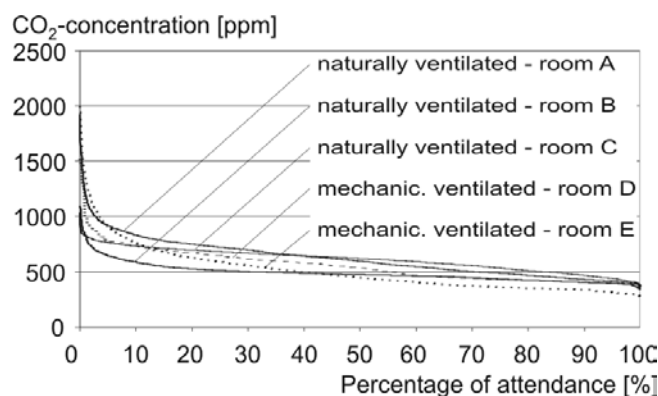


Figure 26. Cumulative frequency distributions for hourly averaged CO₂-concentration in 3 naturally and 2 mechanically ventilated offices plotted over the relative attendance time of the occupants (data of one year).

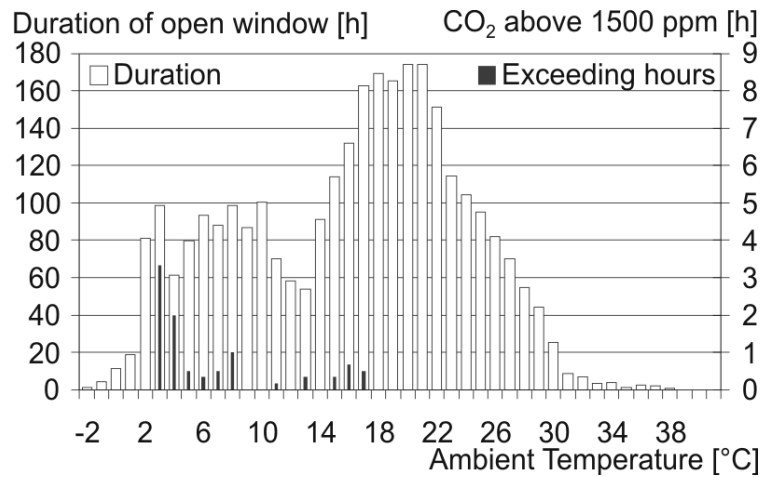


Figure 27. Total opening time of the window and with CO₂-concentrations exceeding 1500 ppm for one office over one year, classified in steps of outdoor temperature.

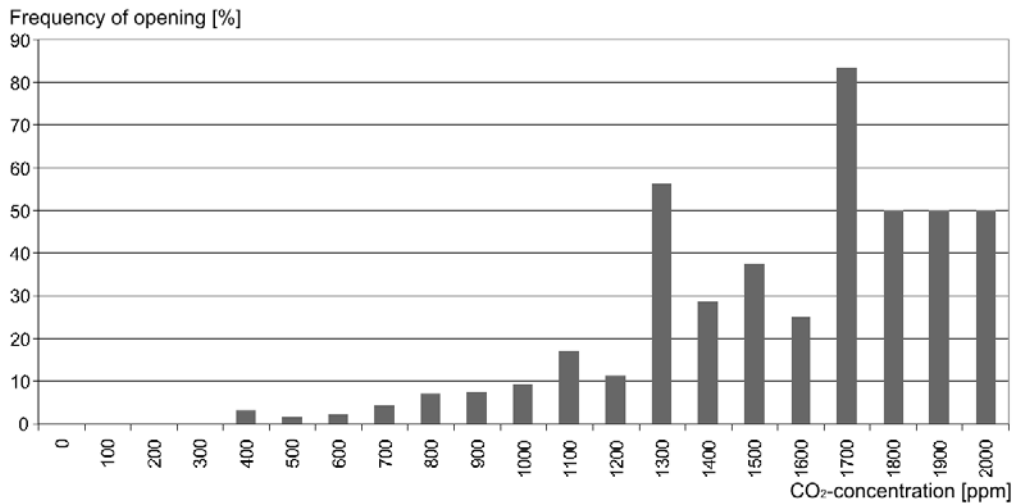


Figure 28. Frequency of the occupant opening a window as a function of CO₂ in one sample room.

In order to find out if occupants are sensitive to low indoor air quality and open the window in reaction, the CO₂-concentrations just before opening the window have been extracted and statistically analysed. The result for one room is displayed in Figure 28. The probability that the occupant opens the window rises with decreasing air quality (increasing measured CO₂-concentration) in the office. Only a few rooms have been examined so far.

4. Conclusions

As a demonstration building for the German funding programme EnBau the KfW bank building was

monitored for three years. The programme's ambitious target of a primary energy consumption of 100 kWh m⁻² a⁻¹ was almost reached after the third year, with a prediction to fall below this value in the future. In comparison with conventional office buildings in Germany the KfW building shows an outstanding energy performance.

The higher energy consumption at the beginning was mostly caused by failures in the operation of the technical building services systems. This is in accordance with the results of the other demonstration buildings of the programme and underlines the importance of continuous monitoring of a building. Important pre-requisites for this are

appropriate data management and visualisation as well as experienced facility managers who are familiar with energy performance issues.

It could also be shown that requirements in terms of thermal comfort could be met by the passive cooling concept. Even under extreme climate conditions, acceptable conditions could be reached with passive cooling and, on the other hand, comfort boundaries were exceeded in air-conditioned offices. Again an appropriate building operation is important to keep the room temperature within the required limits but also the occupants' behaviour with respect to operating shading systems and opening windows has a strong influence. European standards have to be revised with respect to adaptive comfort models which predict the occupant's acceptance of indoor climate much better for non-conditioned buildings. This is particularly important because building concepts like the one presented will be realized more frequently in the future under the new European "Energy Performance of Buildings Directive".

Special emphasis was given to the night ventilation design and control strategy. Measured room temperatures and ambient conditions were used to model the airflow throughout passively cooled sections of the building. Simulations showed that incorrect opening angles of the skylights caused lower air change rates and an uneven distribution over the different levels of the building. It became obvious that night ventilation is very sensitive to changing conditions and that it is not easy to ensure correct implementation of design parameters into the building management system. Further, it could be shown that the control strategy can be improved resulting in higher airflow rates and a better discharge of heat from the building mass.

Acknowledgements

The work was funded by the German Ministry of Economy and Technology (BMWi) under the reference number of 0335007F. The authors also acknowledge the support from the ministry's project coordinator PTJ in Jülich. Special thanks go to all partners of the project team for providing data and information for this paper.

References

Funding programme of the Federal Ministry of Economics and Technology (BMWi), <http://www.enob.info>

CONTAM: (2006) "CONTAM, multizone airflow and contaminant transport analysis software", <http://www.bfrl.nist.gov/IAQanalysis/CONTAM>

deDear RJ and Brager GS: (2002): "Thermal Comfort in Naturally Ventilated Buildings - Revisions to ASHRAE Standard 55", Energy and Buildings 34 (6).

Parker C: (2006): Passive cooling through night ventilation: KfW Ostarkade. Thesis submitted to University of Karlsruhe and Purdue University.

TRNSYS: (2006) "Transient System Simulation Program", www.trnsys.com

Voss K, Löhnert G, Herkel S, Wagner A and Wambganß M: (2006): Bürogebäude mit Zukunft (in German), Solarpraxis GmbH

Wagner A, Kleber M and Rohlfes K: (2005): "The passively cooled KfW building in Germany - monitoring results". *Proceedings of PALENC Conference, Santorini*

Flow Pattern Effects on Night Cooling Ventilation

Jose Manuel Salmerón Lissen¹, Juan Antonio Sanz Fernández¹, Francisco José Sánchez de la Flor², Servando Álvarez Domínguez¹ and Álvaro Ruiz Pardo¹

¹Universidad de Sevilla. Departamento de Ingeniería Energética. Grupo de Termotecnia, Escuela Superior de Ingenieros. Camino de los Descubrimientos s/n, 41092 Sevilla, Spain.

²Escuela Superior de Ingeniería. Departamento de Máquinas y Motores Térmicos. Universidad de Cádiz.C/ Chile 1, 11002 Cádiz, Spain.

Abstract

Passive cooling techniques such as night time cross ventilation can potentially provide substantial cooling energy savings in warm climates. The efficiency of night cooling ventilation is determined by three main factors: the external airflow rate in the room, the flow pattern and the thermal mass distribution. The aim of this paper is to analyse the effect of the enclosure shape and the situation of inlet/outlet openings on the total cooling energy stored in the structure. This analysis presents a comprehensive sample of typologies to generate guidelines which can help the designer with the distribution of the thermal mass and inlet/outlet openings in the enclosure. The approach combines a theoretical analysis which characterizes the enclosure charge/discharge time constants and storage efficiencies with simulation studies based on computational fluid dynamics software (CFD).

Key words: night cooling ventilation, computational fluid dynamics software (CFD), heat transfer coefficients.

1. Introduction

Night ventilation has been known since ancient times. Numerous authors have been involved in the developments of design guidelines in order to promote and to extend its use (Kimura, 1977; Lunardini, 1981; Santamouris et al, 1996; Allard et al, 1998; Mahone, 2003; Santamouris et al, 2003). The basic concept behind this strategy is to cool down the building structure overnight with the aim of providing a heat sink which is available during usual occupancy periods, i.e. the day-time (Artmann et al, 2007). In this paper a global approach is considered which incorporates an assessment of the reduction in energy consumption, based on a quantitative comparison between different solutions or strategies using computer fluid dynamic simulation software (CFD) (Sánchez et al, 2003; Sánchez et al, 2006).

In regard to the implementation of this approach, it has only been since the 1990's that designers have begun to take into consideration night ventilation as a cooling technique. This has aroused considerable interest among European building designers in recent years (Favarolo et al, 2005). In fact, during an architectural competition in Zephyr (1994), most of the projects included night ventilation for passive

cooling. Moreover, night ventilation or natural ventilation seemed to give an answer to problems associated with mechanical ventilation systems, in relation to the level of noise, health problems, the need for periodic maintenance works and energy consumption.

If the application of night ventilation as a cooling strategy has not grown as expected or desired, it is due to the lack of realistic and reliable design guidelines which take into account all the variables involved in this physical mechanism (Sánchez et al, 2004; Sánchez et al, 2005).

The main goal of this paper is to provide building designers with some quantitative results of the comparisons of different solutions in night cooling ventilation strategies. These results will enable the establishment of some design guidelines in order to make easier its application.

1.1 Thermal Sensation and Comfort

Thermal sensation takes an important role in comfort perception and, as with any comfort parameter, it is very subjective. The international standard ISO 7730 defines thermal comfort as: "That condition of mind which expresses

satisfaction with the thermal environment" and the ASHRAE Fundamentals Handbook (1993) revises exhaustively this concept. Thermal comfort is difficult to evaluate due to its dependency on several parameters which can be classified in the following groups:

- Physical parameters;
- Psychological parameters;
- External parameters.

Among these variables, dry bulb temperature, humidity and wind velocity are the most influential on thermal comfort. The level of human comfort can be modified in an enclosure by the air movement around a person because of the convective flux and mass exchange between the occupants and the air in contact with them. For instance, in summer, high air velocities would lead to an increase in the evaporation rate over the skin surface and, consequently, an improvement in the thermal comfort.

1.2 Ventilation Effect on Internal Heat Gains

The second direct effect of ventilation on comfort conditions is the reduction of internal heat gains through the removal of heat generated in the interior of buildings. In mild climates, buildings are usually well ventilated and achieve a small difference between the external and the internal temperature. This strategy is typically used in buildings with a low thermal inertia and has to be combined with the control of solar radiation in order to be more effective.

1.3 Ventilation and Structural Thermal Storage

Another strategy for improving thermal comfort is to cool down the structural components of the building when it is unoccupied, i.e. normally during the night. This technique is known as night cooling ventilation. In this situation the building behaves as a cold sink during the day and the objective is to take out all this stored energy in the structure thus changing its behaviour to hot sink during the night. This charge and discharge of energy in the building structure is made cyclically through the circulation of air. To achieve this it is essential to evaluate the energy offer and energy demand in order to properly close the cooling cycle. In a building, the energy offer is the storage heat capacity of the structure and the energy demand is the heat necessary to assure comfort conditions. Under this viewpoint, three situations can happen:

- Energy offer higher than energy demand;
- Energy offer equal to energy demand;
- Energy offer lower than energy demand.

In cooling, it can seem that, for the second and the third cases, the energy requirements of the building would be null. Nevertheless, by making a deeper analysis, it will be possible to understand that all the energy stored in the structure will not satisfy the demand. To explain this, the concept of effective stored heat can be introduced. This is defined as the fraction of stored energy that is used to reduce the energy demand of the building. The total stored energy is seldom used to fully reduce energy demand because a part of this energy escapes to the exterior.

To characterise night cooling it is necessary to understand the particularities of this technique.

Once the physical process is understood, there exist two situations which can be optimised:

- *The position of the inlet/outlet openings in the enclosure:*
These openings will determine the flow patterns whose influence on the stored energy in the building structure is crucial. In order to compare relatively different enclosures, the term storage efficiency (SE) will be defined. This is the ratio between the actual stored energy and the maximum theoretical energy that could be stored under ideal conditions.
- *The distribution of the thermal mass in the enclosure:*
All the mass contained in the building structure does not count equally in the calculation of the inertia, since the air which flows inside a room does not touch all the walls in the same way. In other words, the air velocity close to the walls changes depending on the flow pattern and, consequently, the heat transfer coefficients vary as well. Similar to the previous situation, an additional parameter called time constant (τ) will be used to evaluate different distributions of thermal mass. This variable will depend on the total mass of the enclosing walls as well as the air in contact with the surface of these walls. The higher the thermal inertia of the building, the higher the possibility to reduce the energy demand becomes.

In general, natural ventilation will depend on the air velocity in the entrance of the enclosure, the air movement inside the interior space, the construction typology, the climate and the set-point temperature. It is not necessary to incorporate the last two parameters when simulating different configurations by means of computational fluid dynamics software (CFD). Thus, the following graphs have been obtained which will help to characterise natural ventilation.

Figure 1 shows the streamlines of one enclosure corresponding to a configuration where element 1 is the floor, elements “2” and “4” are the walls and element “3” is the ceiling. It can be also appreciated that the inlet opening is located at floor level and the outlet opening at ceiling level.

The airflow pattern can be divided in two regions. The first region is where the air flows from the inlet to the outlet opening touching directly the floor and the wall. The second region is where the flow stands stagnant. As a consequence of this phenomenon, the heat transfer coefficients are different on each element due to the variation of the air velocity on the surfaces. The airflow pattern directly cools down elements “1” and “2” while the elements “3” and “4” are cooled down indirectly by the stagnant air. Figure 2 shows the superficial temperatures versus operation time of these elements.

Each element has its own evolution depending on the temperature of the air with which it is in contact, the convective heat transfer coefficients, and the thermal inertia.

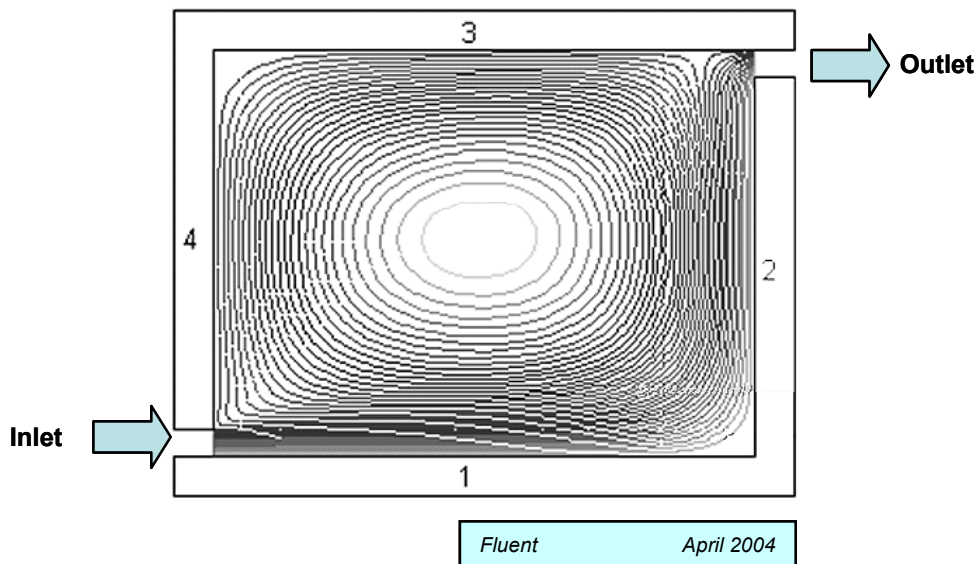


Figure 1. Streamlines in configuration 1.

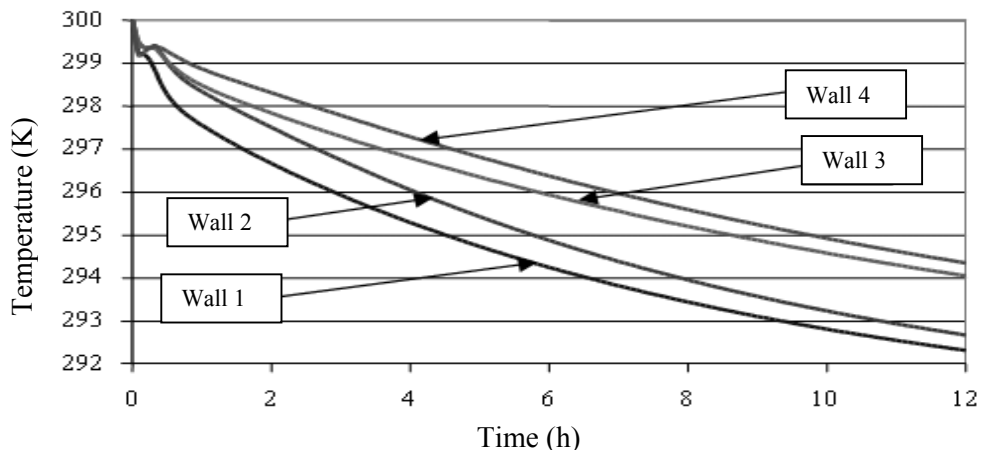


Figure 2. Hourly evolutions of temperatures for the elements in configuration 1.

2. Global Characterization of Zones

In this section, the influence of the airflow patterns on the capacity to store energy of the enclosures is studied. This study is based on the concept of storage efficiency (SE), as defined in the previous Section (Salmerón 2005). Mathematically, the previous definition can be expressed as:

$$SE = \frac{T_{storage}(0) - T_{storage}(t)}{T_{storage}(0) - T_{outdoor}} \quad (1)$$

On the other hand, the thermal inertia of each element in the studied zone determines the whole thermal inertia of the enclosure, and consequently the capacity to store energy and to release heat to the space. This effect has been studied traditionally with time constants (τ) and, for this reason, they appear in most of the publications where the concept of utilisation factor is studied both for heating and cooling (Roucoult et al, 1999; Lundin et al, 2005; Yam et al, 2003).

Both characterisation parameters permit studying the joint influence of the airflow patterns and thermal inertia of each element in the enclosure on natural ventilation. It has been shown that the higher storage capacity of a room, the higher the thermal inertia of the elements affected by the movement of air in the interior space. On the contrary, the augmentation of the storage capacity is negligible if there is an increase of the thermal inertia of the elements not touched by the main current of air. Thus, following the same deductions and keeping constant the total thermal inertia in the enclosure, the higher the distribution of thermal mass in the elements most affected by the airflow, the higher the capacity of storage.

2.1 Mathematical Definition of the Set of Characterization Parameters

In this section, the mathematical method of formulating the time constant (τ) and its relation with the previously defined storage efficiency (SE) are explained.

In an enclosure consisting of different elements with capacity of storing cool or, thermodynamically speaking, capacity of releasing heat, the cool stored from an initial instant of time to another instant t can be expressed by Equation 2:

$$Q_{0 \rightarrow t} = M_1 Cp_1 (T_1(0) - T_1(t)) + M_2 Cp_2 (T_2(0) - T_2(t)) + \dots + M_n Cp_n (T_n(0) - T_n(t)) \quad (2)$$

Similarly, the cool stored from an instant of time t to an instant long enough to ensure that the system temperature and external temperature are the same:

$$Q_{t \rightarrow \infty} = M_1 Cp_1 (T_1(t) - T_e) + M_2 Cp_2 (T_2(t) - T_e) + \dots + M_n Cp_n (T_n(t) - T_e) \quad (3)$$

Therefore, the maximum storing cool has the following expression:

$$Q_{0 \rightarrow \infty} = Q_{max} = M_1 Cp_1 (T_1(0) - T_e) + M_2 Cp_2 (T_2(0) - T_e) + \dots + M_n Cp_n (T_n(0) - T_e) \quad (4)$$

The stored cool can also be defined as a function of the storage efficiency:

$$SE \times Q_{max} = Q_{max} - Q_{t \rightarrow \infty} \quad (5)$$

Working out the value of the storage efficiency from the last equation, the following equation: is obtained

$$SE = 1 - \frac{Q_{t \rightarrow \infty}}{Q_{max}} \quad (6)$$

$$SE = 1 - \frac{M_1 Cp_1 (T_1(t) - T_e) + M_2 Cp_2 (T_2(t) - T_e) + \dots + M_n Cp_n (T_n(t) - T_e)}{M_1 Cp_1 (T_1(0) - T_e) + M_2 Cp_2 (T_2(0) - T_e) + \dots + M_n Cp_n (T_n(0) - T_e)} \quad (7)$$

If it is supposed that the initial temperature has the same value for all the elements of the system, the last expression can be simplified as follows:

$$SE = 1 - \frac{M_1 Cp_1 (T_1(t) - T_e) + M_2 Cp_2 (T_2(t) - T_e) + \dots + M_n Cp_n (T_n(t) - T_e)}{\sum_{i=1}^n M_i Cp_i (T(0) - T_e)} \quad (8)$$

$$SE = 1 - \frac{M_1 Cp_1 (T_1(t) - T_e)}{\sum_{i=1}^n M_i Cp_i (T(0) - T_e)} - \frac{M_2 Cp_2 (T_2(t) - T_e)}{\sum_{i=1}^n M_i Cp_i (T(0) - T_e)} - \dots - \frac{M_n Cp_n (T_n(t) - T_e)}{\sum_{i=1}^n M_i Cp_i (T(0) - T_e)} \quad (9)$$

By setting the differential equations for each element without taking into account the others and supposing a fraction of total airflow affecting the above mentioned element, the next sets of equations can be established:

$$\begin{cases} M_1 Cp_1 \frac{dT_1(t)}{dt} = h_1 A_1 (T_1(t) - T_s(t)) \\ h_1 A_1 (T_1(t) - T_e) = \dot{m}_1 cp (T_s(t) - T_e) \\ \\ M_2 Cp_2 \frac{dT_2(t)}{dt} = h_2 A_2 (T_2(t) - T_s) \\ h_2 A_2 (T_2(t) - T_e) = \dot{m}_2 cp (T_s(t) - T_e) \\ \\ \vdots \end{cases} \quad (10)$$

$$\begin{cases} M_n Cp_n \frac{dT_n(t)}{dt} = h_n A_n (T_n(t) - T_s) \\ h_n A_n (T_n(t) - T_e) = \dot{m}_n cp (T_s(t) - T_e) \end{cases}$$

If one generic equation is taken

$$\begin{cases} M_k Cp_k \frac{dT_k(t)}{dt} = h_k A_k (T_k(t) - T_s(t)) \\ h_k A_k (T_k(t) - T_e) = \dot{m}_k cp (T_s(t) - T_e) \end{cases} \quad (11)$$

and if the dependency of the outlet temperature on the first equation is eliminated by working out this value from the second equation, the next expression is obtained:

$$M_k Cp_k \frac{dT_k(t)}{dt} = \dot{m}_k cp (T_k - T_e) \frac{h_k A_k}{h_k A_k + \dot{m}_k cp} \quad (12)$$

The algebraic solution to Equation 12 is:

$$T_k(t) = C1 + C2 \exp\left(-\frac{\dot{m}_k cp}{M_k Cp_k} \frac{h_k A_k}{h_k A_k + \dot{m}_k cp} t\right) \quad (13)$$

where C1 and C2 are two constants which can be determined by the initial and the steady conditions:

$$\begin{cases} en \quad t = 0 \quad T(0) = C1 + C2 \\ en \quad t = \infty \quad T(\infty) = C1 \end{cases}$$

In the steady state, the last equation can be written as follows:

$$\dot{m}_k cp (T_k(t) - T_e) \frac{h_k A_k}{h_k A_k + \dot{m}_k cp} = 0 \quad (14)$$

and therefore

$$\begin{cases} C1 = T(\infty) = T_e \\ C2 = T(0) - T_e \end{cases}$$

By replacing the last constants in the algebraic solution for the temperature:

$$T_k(t) = T_e + (T_k(0) - T_e) \exp\left(-\frac{\dot{m}_k cp}{M_k Cp_k} \frac{h_k A_k}{h_k A_k + \dot{m}_k cp} t\right) \quad (15)$$

where

$$\tau = \frac{(h_k A_k + \dot{m}_k cp) M_k Cp_k}{h_k A_k \dot{m}_k cp}$$

is the time constant of the storage element.

The storage efficiency (SE) can be defined as the ratio between the stored energy and the maximum energy which could possibly be stored under ideal conditions.

$$SE_k = \frac{T_k(0) - T_k(t)}{T_k(0) - T_e} = 1 - \exp\left(-\frac{\dot{m}_k cp}{M_k Cp_k} \frac{h_k A_k}{h_k A_k + \dot{m}_k cp} t\right) \quad (16)$$

thus, the time constant can be expressed as:

$$\tau_k = \frac{(h_k A_k + \dot{m}_k cp) M_k Cp_k}{h_k A_k \dot{m}_k cp} \quad (17)$$

$$1 - SE = \frac{\left(M_1 Cp_1 \exp\left(-\frac{t}{\tau_1}\right) + M_2 Cp_2 \exp\left(-\frac{t}{\tau_2}\right) + \dots + M_n Cp_n \exp\left(-\frac{t}{\tau_n}\right)\right)}{\sum_{i=1}^n M_i Cp_i} \quad (18)$$

If the times are sufficiently small, the next simplification can be done:

$$1 - SE = \frac{\left(M_1 Cp_1 \left(1 - \frac{t}{\tau_1}\right) + M_2 Cp_2 \left(1 - \frac{t}{\tau_2}\right) + \dots + M_n Cp_n \left(1 - \frac{t}{\tau_n}\right)\right)}{\sum_{i=1}^n M_i Cp_i} \quad (19)$$

$$1 - SE = \exp\left\{\frac{1}{\sum_{i=1}^n M_i Cp_i} \left(-\frac{M_1 Cp_1 t}{\tau_1} - \frac{M_2 Cp_2 t}{\tau_2} - \dots - \frac{M_n Cp_n t}{\tau_n}\right)\right\} \quad (20)$$

that is, the time constant would have the following mathematical definition:

$$\frac{1}{\tau} = \frac{M_1 Cp_1}{\sum_{i=1}^n M_i Cp_i} \frac{1}{\tau_1} + \frac{M_2 Cp_2}{\sum_{i=1}^n M_i Cp_i} \frac{1}{\tau_2} + \dots + \frac{M_n Cp_n}{\sum_{i=1}^n M_i Cp_i} \frac{1}{\tau_n} \quad (21)$$

2.2 The Influence of Airflow Pattern on Storage Efficiency

The enclosure geometry affects the airflow pattern, and this, in its part, affects the storage efficiency. The designer normally establishes the layout of the various spaces within the building according to principles which do not usually consider the airflow pattern. However, he has a degree of freedom in the selection of the position of openings. In the case of natural ventilation, these openings can be windows and vents that allow the movement of air from and towards the interior of the room.

Figure 3 shows a summary of the usual typologies that can be found in many buildings. The typologies are two-dimensional; it is supposed that the third dimension does not substantially alter the flow pattern. In general, this supposition is true if the length of the third dimension is greater than the other two dimensions, or if there is no possibility of airflow in the third dimension. Under the previous assumptions, the figures must be understood as sections of the space in the horizontal or vertical

position. The lengths of elements 1 and 3 are four metres and of the elements 2 and 3 three metres.

The existence of a differential pressure between the inlet and the outlet openings has been assumed, and this constitutes the impelling force of the airflow.

Figure 4 shows the storage efficiency depending on the duration of the charge for all the typologies shown in Figure 3. In all the cases, the differential pressure between the outlet and the inlet pressure is the same.

Among the proposed configurations, number two is the one with most capability to store energy while number seven has the least capability.

If the charge period is eight hours, the storage efficiency in configuration two is 18 % while in configuration seven it is 3 % (Salmerón 2005). It must be stressed that, despite the geometry of the enclosure, initial interior temperature and thermal inertia being the same, it is possible to store six times more energy depending only on the position

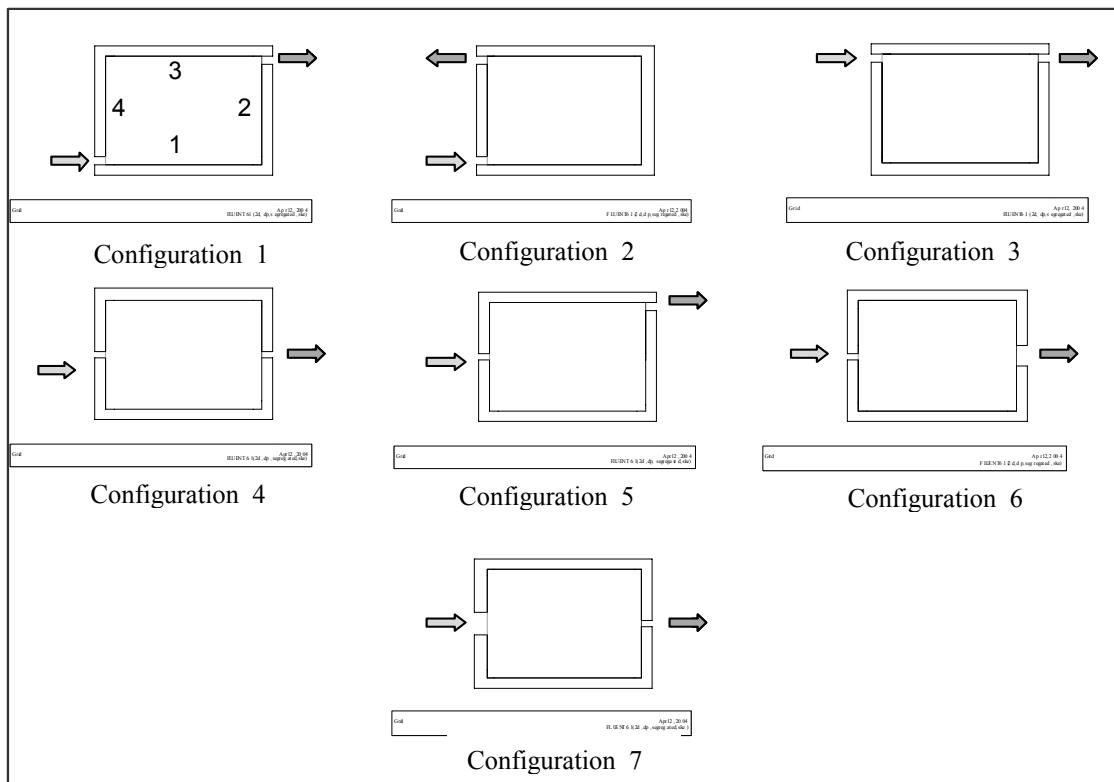


Figure 3. Usual typologies for natural ventilation in buildings.

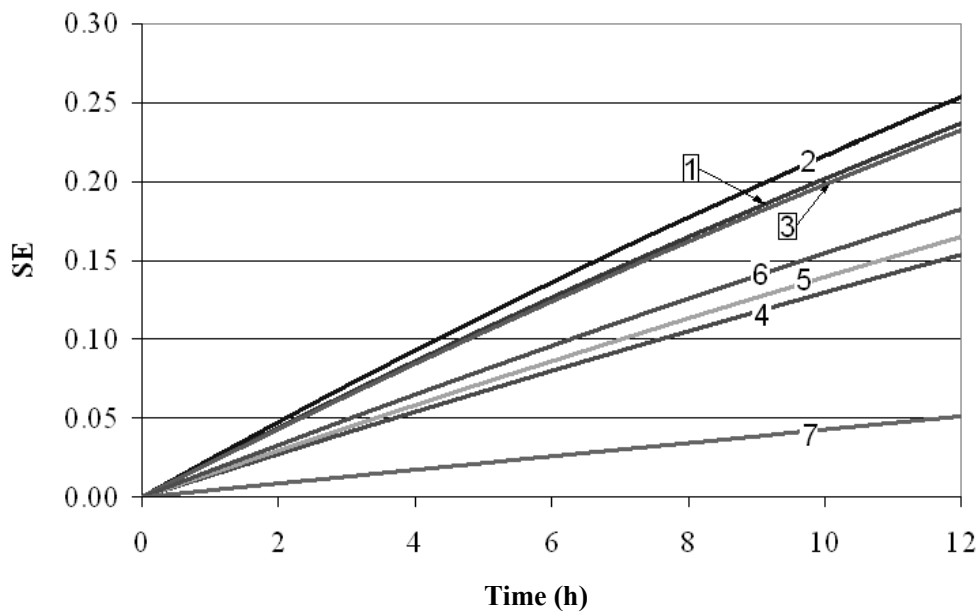


Figure 4. Storage efficiency based on the length of the period of charge for all the typologies.

of the inlet and outlet openings, and consequently on the airflow pattern.

An analysis of the different typologies reveals that the best configurations are those where the main airflow pattern touches directly more elements of the room. For example, in typology two, the main current of the airflow comes into contact with elements 1, 2 and 3 while there is a short circuit in typology seven. Typologies four and six present a short circuit too but they are not as inefficient as configuration seven. The reason for this effect is that the inlet is bigger than the outlet opening in configuration seven and this produces an acceleration of the airflow inside the room. In this way the airflow exits quickly without making contact with the room walls. In the other configurations of facing openings, the air flow does not experience an increase of velocity and therefore elements 3 and 1 are in contact with the airflow.

Some ventilation design guidelines recommend larger inlet than outlet openings in order to increase the air velocity in the room and improve the comfort sense of the occupants. This seems to be a correct consideration from the point of view of comfort but it could be interesting to take into consideration not having the openings directly facing each other.

In typology three, there is a short circuit too but in this case, the main airflow pattern is intensively in contact with element 3, thus allowing the removal of a large amount of heat from this wall.

2.3 Influence of Thermal Inertia in Each Enclosing Surface

As has been pointed out previously, an airflow pattern is much more effective in increasing the total energy storage capacity of the enclosure if the velocity of the air is higher on the elements with more thermal inertia. On the other hand, it is not very effective to increase equally the velocity of the air in all the elements of the building without taking into account the different thermal inertias.

In order to quantify the capacity to store energy as a function of the thermal inertia of each element which constitutes the room, the time constant (τ) is used. In this way, the equations of Section 2.1 can be solved to calculate the time constant of each element individually or of the whole enclosure. The latter time constant is more interesting for evaluating the potential of night cooling ventilation because it takes into account the interaction of the different elements in the room. These interactions are decisive if passive cooling is to work properly.

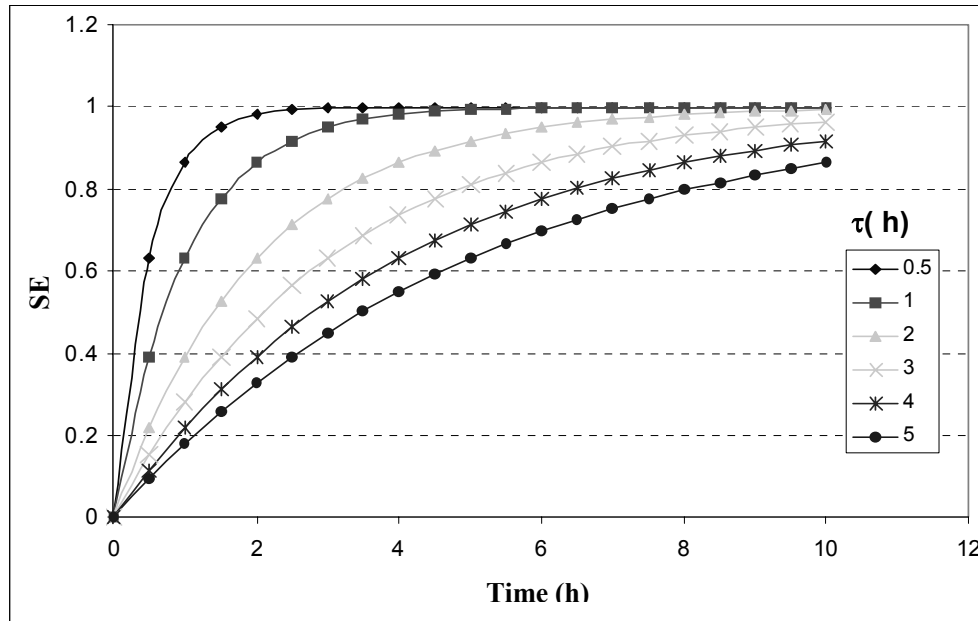


Figure 5. Influence of the time constant on the capacity to store energy.

As is well known, the time constant of a system is useful for quantifying its response time. The response speed of a system increases when its response time decreases. In this case, it is said that the system has low thermal inertia. On the other hand, a system has high thermal inertia when its time response increases and the response speed decreases.

The equations presented previously, in Section 2.1, permit the relationship between the capacity to store energy and the time constant of a room to be shown. To simplify and summarise the conclusions of this study, both parameters are presented graphically in Figure 5. This shows the capacity to store energy versus the storing time. Each curve has been calculated for a different thermal inertia and therefore for a different time constant (τ).

From Figure 5, it can be appreciated that as the time constants increase the storage efficiency increases more slowly. From this point, important conclusions can be inferred relating to the use of natural ventilation to reduce cooling demand. These conclusions, listed in the next section, will help the building designer in defining interior spaces, or more generally, in the design of the whole building with a passive cooling approach.

3. Conclusions

The results obtained in this paper can be summarized with the following statement: “The position of the inlet/outlet openings in the enclosure is important in reducing the cooling demand due to night ventilation”. Quantitatively, it has been shown that one configuration can store and release five times more energy than another configuration because of the existence of a short circuit of air between the inlet and the outlet openings.

Other conclusions or recommendations which can be drawn from the mathematical development of equations for the time constant and the storage efficiency are:

- The greater the time constant, the more time is needed to reach a fixed storage efficiency. This happens because a large time constant means that the system responds slowly to an excitation.
- On the other hand, for a specified time constant, the storage efficiency increases when the charge time increases.
- Finally, and most importantly, if the charge time is kept constant, the higher the storage efficiency the lower the time constant.

The third statement must be clarified because it can be contradictory if the interpretation is that the best way to have high storage efficiencies is to reduce the time constants in the enclosure and therefore the thermal inertia. It is clear that it is easier to fill a container fully when it is small. In this case, although the filling efficiency would be high, the content could be much less than in other cases in which larger containers are almost empty. In summary, the most favourable situation to meet cooling demand using natural ventilation would be to have high time constants (container) and high storage efficiencies (filling efficiency).

If the storage efficiency is high, there will be a high capability to store heat during the day in the building structure and to release it during the night. If the time constant is also high, the release of stored energy will be delayed until the time the night cooling ventilation starts. Vice versa, the storage of heat will begin some hours later at the end of the night ventilation. These delays and the planning of operational schedules is the basis of the strategy described in the article. The defined parameters (time constant and storage efficiency) help to achieve this objective.

In order to guarantee the good performance of night cooling ventilation, it is essential to combine high storage efficiencies with high thermal inertia or, in other words, ensure a high time constant for the enclosure. This can be achieved by:

- increasing the storage efficiency by establishing a suitable airflow pattern in the space. To make the correct choice, the positions of the inlet/outlet openings and the air velocity must be analysed.
- Increasing the time constant of the enclosure by ensuring that all elements are in direct contact with the airflow.

The design of the air flow pattern and the calculation of the thermal inertia in the enclosure must be performed together because of their joint influence on natural ventilation.

Nomenclature

Symbols

| | |
|----|--------------------|
| SE | Storage Efficiency |
| T | Temperature |
| t | Time |
| M | Mass |

| | |
|----------|---|
| Cp | Specific Heat of a solid element |
| Q | Stored cool or Heat released |
| h | Convective Heat Transfer Coefficient |
| <i>m</i> | Fraction of air flow in contact with a surface given by the subscript |
| cp | Air Specific Heat |
| A | Area of a surface given by the subscript |
| τ | Time Constant |

Subscripts

| | |
|----------|---|
| 1,2,...n | Surface indices |
| k | Generic surface index |
| 0→t | Period of time between 0 and instant "t" |
| t→∞ | Period of time between instant "t" and infinity |
| e | Outdoor |
| s | Outlet |

References

- Allard F, Santamouris M, Alvarez S, Guarraccino G and Maldonado E: (1998) "Natural ventilation in buildings", UK, James & James (Science publishers), London.
- ASHRAE: (1993) "ASHRAE Fundamentals", American Society of Heating, Refrigeration and Air Conditioning. Atlanta.
- Artmann N, Manz H and Heiselberg P: (2007), "Climatic potential for passive cooling of buildings by night-time ventilation in Europe" *Applied Energy*, **84**, pp187-201.
- Favarolo PA and Manz H: (2005) "Temperature-driven single-sided ventilation through a large rectangular opening", *Building and Environment*, **40**, pp689-699.
- Geros V, Santamouris M, Tsagrasoulis A and Guarracino G: (1999) "Experimental evaluation of night ventilation phenomena". *Energy and Buildings*, **29**, pp141-154.
- Kimura K: (1977) "Scientific basis of air conditioning", Applied Science Publishers Ltd, London.
- Lunardini VJ: (1981) "Heat transfer in cold climates", Van Nostrand Reinhold Company, New York.
- Lundin M, Andersson S and Östin R: (2005), "Further validation of a method aimed to estimate building performance parameters", *Energy and Buildings*, **37**, pp867-871.

Mahone D (2003) “Night ventilation cooling”, California building Energy Efficiency Standards, revisions for July 2003 Adoptions.

Roucoul JM, Douzane O and Langlet T: (1999). “Incorporation of thermal inertia in the aim of installing a natural night-time ventilation system in buildings” *Energy and Buildings*, **29**, pp129-133.

Salmerón JM: (2005) “Characterization of natural cooling techniques with structural storage. energy saving potential for building conditioning” PhD Thesis, University of Seville. “Caracterización de las Técnicas de Refrigeración Natural con Acumulación Estructural. Potencial de Ahorro Energético en el Acondicionamiento de Edificios”. Tesis Doctoral Universidad de Sevilla, ETSII. http://fondosdigitales.us.es/public_thesis/327/8095.pdf. ISBN 84-689-7782-9.

Sánchez F and Álvarez S: (2004) “Modelling microclimate in urban environments and assessing its influence on the performance of surrounding buildings”. *Energy and Buildings*, **36**, pp 403–413.

Sánchez F: (2003) “Modificaciones Microclimáticas Inducidas por el Entorno del Edificio y su Influencia sobre las Demandas Energéticas de Acondicionamiento”. Tesis Doctoral Universidad de Sevilla, ETSII.

Sánchez FJ, Ortiz R, Molina JL and Álvarez S: (2005) “Solar radiation calculation methodology for building exterior surfaces”. *Solar Energy*, **79**, pp513-522.

Sánchez FJ, Salmerón JM and Álvarez S: (2006) “A new methodology towards determining building performance under modified outdoor conditions”. *Building and Environment*, **41**, pp1231–1238.

Santamouris M and Asimakopoulos D: (1996) “Passive cooling of buildings”. James & James (Science publishers), London.

Santamouris M: (2003) “Solar thermal technologies for buildings”. James & James (Science publishers), London.

Yam J, Li Y and Zheng Z: (2003), “Nonlinear coupling between thermal mass and natural ventilation in buildings”, *International Journal of Heat and Mass Transfer*, **46**, pp1251-1264.

ZEPHYR. Architecture Competition. Energy Research Group, School of Architecture, University College Dublin.

Numerical Evaluation of Earth to Air Heat Exchangers and Heat Recovery Ventilation Systems

F. Chlela¹, A. Husaundee¹, P. Riederer¹ and C. Inard²

¹ Centre Scientifique et Technique du Bâtiment (CSTB), 84 avenue Jean Jaurès,
77421 Marne-la-Vallée, France

² LEPTAB, University of La Rochelle, Av. Michel Crépeau, 17042 La Rochelle, France

Abstract

In France there is an increasing demand for energy efficient and environmentally friendly buildings of high thermal comfort. Balanced ventilation systems with heat recovery on the exhaust air and earth to air heat exchangers (EAHEX) are interesting techniques which can reduce the heating and cooling demand of buildings, and improve internal thermal comfort. A numerical study was carried out to evaluate the impact of these two systems on the energy performance and internal thermal comfort of a dwelling, with respect to the French climate characteristics. The impact on CO₂ emission was also analyzed.

The results showed that a balanced ventilation system with heat recovery is a better preheating technique than the earth to air heat exchanger. The additional heating gain obtained from coupling an earth to air heat exchanger to a balanced ventilation system is rather marginal. However, earth to air heat exchangers present a significant potential for cooling. Regarded in this way, winter preheating becomes an additional free service, which can be coupled to other preheating techniques.

Key words: Energy consumption reduction, earth to air heat exchanger, passive cooling, mechanical ventilation systems, heat recovery, CO₂ emission.

1. Introduction

Heat recovery ventilation systems and earth to air exchangers are promising technologies widely used in low energy buildings. Balanced ventilation combines extract and supply systems as separately ducted networks. It uses two fans, one for air supply and one for extraction. Typically, air is supplied to occupied zones and extracted from polluted zones. The heat recovery unit is usually a flat plate heat exchanger which recovers heat from extracted air and transfers it to the supply air. This thus reduces the heat losses due to ventilation. An earth to air heat exchanger (EAHEX), sometimes called a buried pipe or ground coupled air heat exchanger, consists of a tube put into the ground, through which air is drawn. Because of the high thermal inertia of the soil, the temperature fluctuations at the ground surface exposed to the exterior climate are damped deeper in the ground. Further, a time lag occurs between the temperature fluctuations in the ground and at the surface. Therefore, at a sufficient depth, the ground temperature is lower than the outside air temperature in summer and higher in winter. When fresh ventilation air is drawn through the earth to air

heat exchanger, the air is cooled in summer and heated in winter. In combination with other passive systems and good thermal design of the building, the earth to air heat exchanger can be used to avoid air conditioning units in buildings.

There are many experimental and analytical reported studies on earth to air heat exchangers and balanced ventilation systems with heat recovery. However, the use of these two systems in buildings has not often been investigated for French climate characteristics.

Dorer et al (1998) checked the performance of mechanical ventilation systems in several innovative residential buildings in Switzerland. All these buildings were very airtight and equipped with mechanical ventilation systems consisting of balanced ventilation with heat recovery (efficiency over 85%) coupled to an EAHEX for outside air intake. The efficiency of the ventilation systems, defined as the ratio of heat gained from heat exchanger(s) and the electric energy use of fans, varied between 7.4 and 8.7. The detailed energy flow diagram (heat gains and losses) for only one project was presented. It showed a marginal contribution of

the EAHEX to the heat gain. The only advantage during the cold season was the protection of the heat recovery unit from freezing. Simulation work and monitoring of mechanical ventilation systems was also carried out by Hollmuller et al (2001) in Switzerland. This showed that a heat exchanger on the exhaust air was a better preheating technique than the buried pipe system. On the other hand, buried pipe inertial cooling turned out to be competitive with, and avoided the need for, an air conditioning system. Winter air preheating therefore becomes an additional free service, which can be coupled to other preheating techniques.

Al-Amji et al (2006) developed a theoretical model of EAHEX. The model was validated against other published works and showed good agreement. Simulation results for a dwelling in a desert climate showed that the EAHEX reduces cooling energy demand by 30% over the peak summer season. Ghosal et al (2004) developed an analytical model to evaluate the performance of an earth air heat exchanger coupled with a greenhouse located in Delhi, India. Temperatures of greenhouse air were found to be on average 6-7 °C more in winter and 3-4 °C less in summer than the same greenhouse when operating without an earth air heat exchanger. Predicted and measured values of greenhouse air temperatures exhibited fair agreement. Bojic et al (1997) evaluated the technical and economic performance of an EAHEX coupled to the system for heating or cooling a building that uses 100% fresh air as the heating or cooling medium during winter and summer. It was found that the use of the EAHEX covered a portion of the daily building energy needs. The system was more energy and cost efficient in summer than in winter. Gauthier et al (1997) presented a numerical model for the prediction of the thermal behaviour of an EAHEX. The model was validated with experimental data taken from an EAHEX installed in a commercial type greenhouse located in Quebec, Canada. The effects of several design and operating parameters on the heat transfer processes and on the performance of the system were examined. Results showed that EAHEX were very attractive for reducing the energy consumption of greenhouses as long as they were properly designed and operated.

This work consists of a numerical analysis to evaluate the thermal performance of EAHEX and balanced ventilation systems with a heat exchanger on the exhaust air, under the French climate. First, a description of the dwelling and the climate characteristics is given. Then the principles of the

studied ventilation systems and the models used to carry out the simulations are described. After a brief description of the simulated cases, the potential of the ventilation systems for heating and cooling and also for CO₂ emission reduction is outlined.

2. The Studied Cases

In order to evaluate the performance of each system separately and the performance of their coupling, four system configurations were simulated:

- The dwelling with a mechanical extract ventilation system without heat recovery (EV);
- The dwelling with a heat recovery balanced ventilation system (BV);
- The dwelling with a mechanical extract ventilation system coupled with an earth to air heat exchanger (EV + EAHEX);
- The dwelling with a heat recovery balanced ventilation system coupled with an earth to air heat exchanger (BV + EAHEX).

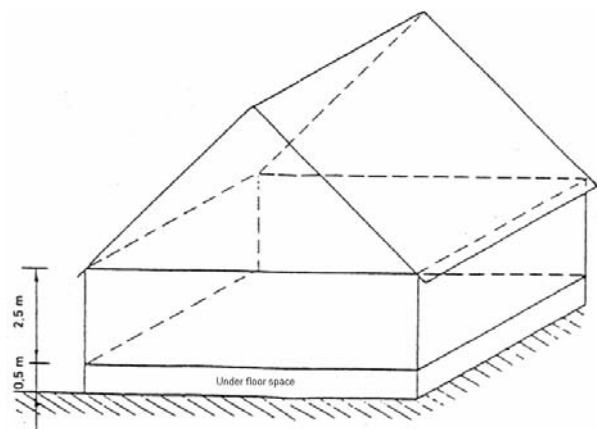


Figure 1. Global view of the Mozart house.

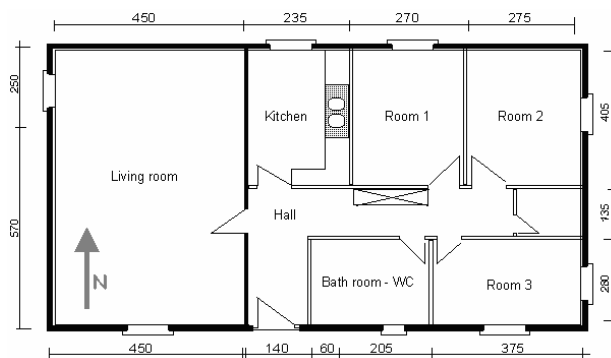


Figure 2. Top view of the Mozart house.

3. Building Description

The studied building is a dwelling called “Mozart” (see Figure 1 and Figure 2), which was taken from a typology on French buildings carried out by the CSTB (CSTB, 1995).

Mozart has a floor area of 101 m², a volume of 253 m³ and an average ventilation air change rate of 0.57 h⁻¹. The envelope average heat transfer coefficient value is equal to 0.4 W/m²K. These characteristics were chosen according to the French thermal regulation (RT, 2005). The house also contains 0.5 m of horizontal sunshades over all the windows.

4. Climate Characteristics

The simulations were carried out for three French cities: Nancy (cold climate), La Rochelle (moderate climate) and Nice (hot climate). Table 1 gives some

Table 1. Climate characteristics.

| | Nancy | La Rochelle | Nice |
|--|-------|-------------|-------|
| T _{min} [°C] | -11.9 | -4.9 | 1.9 |
| T _{max} [°C] | 33.0 | 30.7 | 28.9 |
| DH _(19 °C) [°C.h] | 86384 | 60626 | 44257 |
| DH _(26°C) [°C.h] | 257 | 169 | 207 |
| DH _(20-26°C) [°C.h] | 1748 | 1935 | 4873 |
| Φ _{solar} [kWh/m ²] | 1066 | 1293 | 1397 |

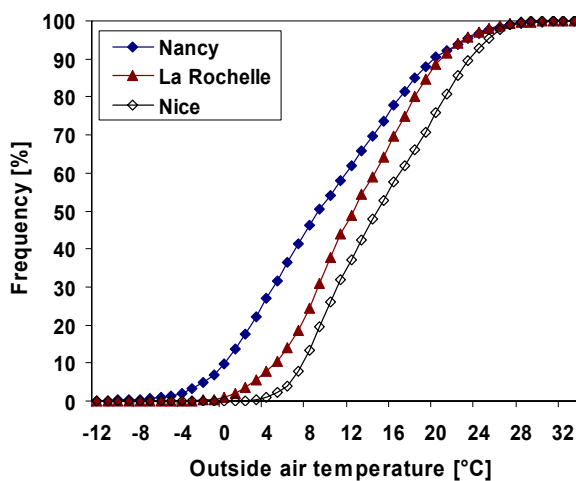


Figure 3. Cumulative frequency distribution for the outside air temperature.

key data of the three cities weather. Figure 3 shows the cumulative frequency distribution of the outside air temperature for the three climates.

5. Characteristics of Ventilation Systems

5.1 Mechanical Extract Ventilation System

The mechanical extract ventilation system consists of a single fan which removes air from the kitchen and the bathroom. This thus creates an internal negative pressure which promotes an equal mass of fresh air into the other zones through air inlets and the air leakage of the building. The fan power is equal to 27 W.

5.2 Balanced Ventilation System

For the balanced ventilation system, the air is extracted from the kitchen and the bathroom and supplied to the other zones. The thermal efficiency of the flat plate heat exchanger was chosen to be 75% according to the Passivhaus calculation method guidelines (PHPP, 2004). For negative outside air temperatures, an electrical resistance of 1 kW is activated for freezing protection. During the summer season, the heat exchanger is bypassed. The extract fan power is equal to 27 W and the supply fan power is equal to 33 W.

5.3 Earth to Air Heat Exchanger

The length and number of the buried pipes depends not only on the cooling and heating demand of the building, but also on the available space around the house. For a minimum available space, buried pipes could be positioned all around the house perimeter. For Mozart, a single buried pipe of 40 m length, corresponding to the perimeter of the house, was chosen. The diameter of the tube was 160 mm. The depth of the buried tube was 1.8 m, which is the maximum depth permitted without an obligatory special treatment for the ground in France. The soil is supposed to be clay (see Table 2).

Table 2. Clay soil thermal characteristics.

| λ [W/m ² K] | C _p [J/kgK] | ρ [m ³ /kg] |
|------------------------|------------------------|------------------------|
| 1.5 | 2085 | 1500 |

6. Models Used for the Simulations

Simulations were carried out using SIMBAD Toolbox (SIMBAD, 2005), developed by the CSTB in the Matlab/Simulink environment (SIMULINK, 2005).

6.1 The Building Model

The building thermal behaviour was simulated using the multizone building model of SIMBAD and was validated against experimental data and other building models (El Khoury et al, 2005).

6.1.1 Thermal Zone

The multizone building model in SIMBAD is a transient model with one air node per zone, representing the thermal capacity of the zone air volume. Each air zone is assumed to be homogeneous in temperature. The heat balance equation of an air node takes into account the convective heat exchange between the air and the walls, the convective gains due to ventilation; infiltration and air flow from other zones, and the internal convective gains (from people, equipment, etc.). It is expressed as follows:

$$\begin{aligned} \rho_a V_i \frac{dT_{a,i}}{dt} = & \sum_p h_{con,p} A_p (T_{w,p} - T_{a,i}) \\ & + \sum_j m_{vent,j} C_p a (T_{vent,j} - T_{a,i}) \\ & + \sum_j m_{ji} C_p a (T_{a,j} - T_{a,i}) + P_{gc} \end{aligned} \quad (1)$$

The radiation heat balance of each zone enables the evaluation of the mean radiant temperature:

$$\sum_p h_{rad,p} A_p (T_{w,p} - T_{mr,i}) = 0 \quad (2)$$

6.1.2 Walls Model

Multilayer walls are modelled using constant thermo-physical properties of each layer. The heat transfer process across the wall is considered to be one dimensional. It is described by the following one dimensional heat diffusion equation:

$$\rho C_p \cdot \frac{\partial T_w(x,t)}{\partial t} = \lambda \cdot \frac{\partial^2 T_w(x,t)}{\partial x^2} \quad (3)$$

The boundary conditions on the two surfaces of the wall are:

$$-\lambda \cdot \left. \frac{\partial T_w(x,t)}{\partial x} \right|_{x=0} = h_{c,1} (T_{a,1} - T_w(0,t)) + P_{rad,1} \quad (4)$$

$$-\lambda \cdot \left. \frac{\partial T_w(x,t)}{\partial x} \right|_{x=L} = h_{c,2} (T_{a,2} - T_w(L,t)) + P_{rad,2} \quad (5)$$

6.1.3 Windows Model

The window is described using a two-node model. It is thermally considered as an external wall with no thermal mass, partially transparent to solar radiation and opaque to long-wave radiation. The model takes into account the variation of solar optical properties such as solar transmissivity and absorptivity with respect to the incident angle of the solar radiation.

6.2 Air to Air Heat Exchanger Model

The heat exchanger model developed is based on the effectiveness-NTU method of analysis (Brandemuhel et al, 1993). This method calculates only sensible heat exchange. The effectiveness of the heat exchanger is defined as the ratio of the actual heat transfer rate to the maximum heat transfer rate for the given entering fluid conditions and flow rates. Since heat transfer rates can be expressed in terms of flow rates and entering and leaving fluid conditions, the outlet states of a heat exchanger can be determined from the inlet states, flow rates, and effectiveness. The following equations state these relationships:

$$\begin{cases} q = C_1 (T_{1,in} - T_{1,out}) = C_2 (T_{2,in} - T_{2,out}) \\ q_{max} = C_{min} (T_{max} - T_{min}) \\ q = \varepsilon \cdot q_{max} \end{cases} \quad (6)$$

For a given flow configuration, the effectiveness of a heat exchanger can be expressed as a function of two dimensionless variables: the number of transfer units, NTU, and the fluid capacity rate ratio, C.

$$\begin{cases} NTU = \frac{UA}{C_{min}} \\ C = \frac{C_{min}}{C_{max}} \end{cases} \quad (7)$$

For a counter flow configuration, the effectiveness is calculated by the following equation:

$$\varepsilon = \frac{1 - e^{-NTU(1-C)}}{1 - C \cdot e^{-NTU(1-C)}} \quad (8)$$

6.3 Earth to Air Heat Exchanger Model

Several calculation models for EAHEX were found in the literature. Tzaferis et al (1992) studied eight models which he classified in two groups:

1. An algorithm that first calculates the convective heat transfer from air to the pipe and then calculates the convective heat transfer from the pipe to the ground inside the ground mass.
2. An algorithm that only calculate the convective heat transfer from the circulating air to the pipe

Six of the models use a steady-state one-dimensional description of the pipe. The authors concluded that the different models give comparable results. This is mainly caused by the fact that the models offer different solution methods of the same equations. The compliance with measurements done by the authors is quite good. This shows that a steady-state one-dimensional model may characterize the behaviour of earth-air heat exchangers. This approach will be followed in this paper.

More complete and dynamic models are also reported such as Mihalakakou et al (1994), Bojic et al (1997), Gauthier et al (1997) and Hollmuller et al (2001). The models differ in the way the geometry is described (2D, 3D, polar coordinates) and in the way the effects of moisture in the ground and the air are accounted for. However these models are quite complex and time consuming.

The EAHEX model developed and integrated into SIMBAD is based on Al-Ajmi et al (2006). The latter was validated against one theoretical study (Mihalakakou et al, 1995), and two experimental studies (Dhaliwal et al, 1984; Shingari 1995). The validation process shows that the model does agree with all of the three models with respect to the input parameters.

The EAHEX system was modelled as three coupled heat transfer processes, the convection heat transfer between air flowing in the pipe and the pipe inner surface, the conduction heat transfer through the pipe, and between the pipe outer surface and the soil environment. In order to analyse the EAHEX system, the following assumptions were applied:

1. The soil surrounding the pipe is isotropic, with homogenous thermal conductivity in all ground strata.

2. The surface temperature of the ground can be approximated to the ambient air temperature, which equals the inlet air temperature.
3. The pipe is of uniform circular cross-section.
4. The pipe is embedded in a finite cylindrical soil layer with adiabatic boundary conditions.

6.3.1 Soil Temperature Model

Kusuda et al (1965) and Labs et al. (1989) have mathematically modelled the annual sub-surface soil temperature based on heat conduction theory applied to a semi-infinite homogenous solid. Predictions of soil temperature exhibit a sinusoidal pattern due to the annual temperature fluctuation above. The prediction accuracy of the undisturbed soil temperature is very sensitive to the values of the input parameters in the following equation:

$$T_{soil}(Z, t) = T_{mean} - T_{amp} \times e^{\left\{-Z \times \left(\frac{\pi}{365 \times \alpha_{soil}}\right)^{1/2}\right\}} \times \cos\left\{\frac{2\pi}{365} \left[J - J_{shift} - \frac{Z}{2} \left(\frac{365}{\pi \times \alpha_{soil}}\right)^{1/2} \right]\right\} \quad (9)$$

This equation has been validated against measured soil temperature values by Labs et al. (1989) and Al-Ajmi et al (2002). Good agreement between measured and predicted values to an accuracy of ± 1 °C has been found.

Figure 4 shows the soil temperature over a year at 1.8 m depth, for the three cities.

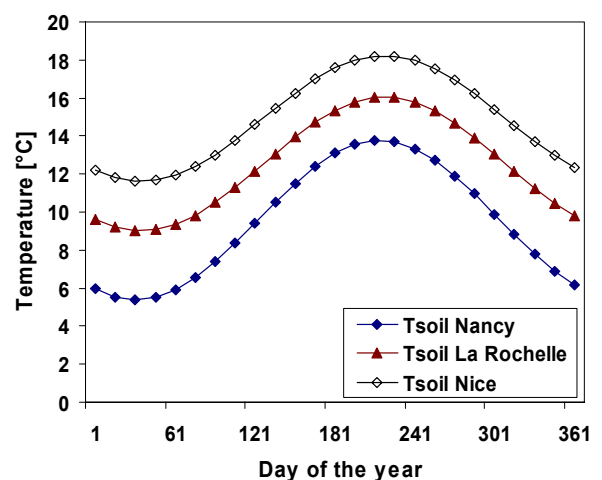


Figure 4. Soil temperature at 1.8m depth for the three cities.

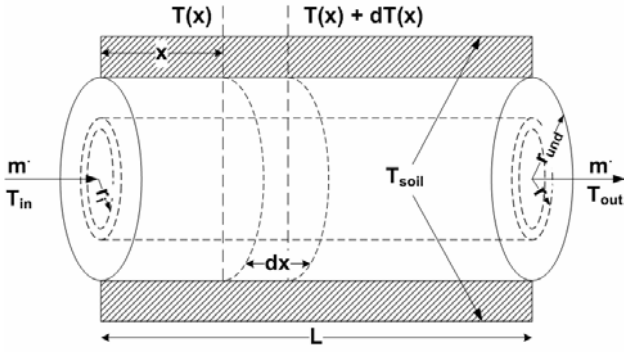


Figure 5. Energy exchange between ground and flowing air in the buried pipe.

6.3.2 EAHEX Model Development

An external thermal resistance was provided by a surrounding concentric cylinder of soil of arbitrary thickness, which was exposed to an undisturbed subsoil temperature as a boundary condition. In this work, the thickness of the annulus was taken as being equal to the radius of the pipe (Al-Ajmi et al, 2006).

Consider dx as the infinitesimal element of buried pipe in the direction of the air flow as shown in Figure 5. The energy balance in the elemental section becomes:

$$mC_{p_{air}}dT_{(x)} = \frac{dx}{R_{conv} + R_{pipe} + R_{soil}}(T_{soil} - T_{(x)}) \quad (10)$$

R_{conv} is the thermal resistance due to convective heat transfer between the air in the pipe and the pipe inner surface. R_{pipe} is the thermal resistance due to the conduction heat transfer through the pipe and R_{soil} is the thermal resistance due to the conduction heat transfer in the soil annulus:

$$\begin{cases} R_{conv} = \frac{1}{2\pi r_i h_{conv}} \\ R_{pipe} = \frac{1}{2\pi\lambda_{pipe}} \ln\left(\frac{r}{r_i}\right) \\ R_{soil} = \frac{1}{2\pi\lambda_{soil}} \ln\left(\frac{r_{und}}{r}\right) \end{cases} \quad (11)$$

The convective heat transfer coefficient h_{conv} is a function of the Reynolds number, Re , and the Nusselt number, Nu :

$$h_{conv} = \frac{Nu \cdot \lambda_{air}}{D} \quad (12)$$

A correlation for the Nusselt number for laminar and fully developed turbulent flow in a circular pipe for the Prandtl number ranges $0.5 \leq Pr \leq 2000$ is proposed by Gnielinski (1976):

$$Nu = \frac{(\xi/8)(Re-1000)Pr}{1 + 12.7\sqrt{\xi/8}(Pr^{2/3}-1)} \quad (13)$$

ξ is the friction coefficient for smooth pipes and is calculated as follows (Paepe et al, 2003):

$$\begin{cases} \xi = \frac{64}{Re}, & \text{if } Re < 2300 \\ \xi = (0.79 \times \ln(Re) - 1.64)^{-2}, & \text{if } Re \geq 2300 \end{cases} \quad (14)$$

The total thermal resistance between the air and the ground, R_{tot} , is expressed by the following equation:

$$R_{tot} = R_{conv} + R_{pipe} + R_{soil} \quad (15)$$

The overall coefficient of heat transfer is defined by:

$$U = \frac{1}{R_{tot}} \quad (16)$$

The solution of Equation (9) is:

$$T_{(x)} = T_{soil} + (T_{in} - T_{soil}) \cdot e^{\frac{-U}{mC_{p_{air}}}x} \quad (17)$$

The air outlet temperature is obtained for $x = L$:

$$T_{out} = T_{soil} + (T_{in} - T_{soil}) \cdot e^{\frac{-U \cdot L}{mC_{p_{air}}}} \quad (18)$$

The efficiency of the EAHEX is defined as follows:

$$\varepsilon = \frac{T_{out} - T_{in}}{T_{soil} - T_{in}} = 1 - e^{\frac{-U \cdot L}{mC_{p_{air}}}} \quad (19)$$

Hence, the outlet air temperature of the EAHEX is a function of the surrounding sub soil temperature T_{soil} , the inlet air temperature and the EAHEX efficiency:

$$T_{out} = T_{in} + \varepsilon \cdot (T_{soil} - T_{in}) \quad (20)$$

7. Simulation Results and Discussion

Yearly simulations were performed to assess the thermal performance of the EAHEX and the balanced ventilation system. The assessment criteria used were related to the heating, the auxiliary consumption, the thermal summer comfort and the CO₂ emission.

The heating season is the period corresponding to an outside air temperature below 15°C. During the hot season, the heat exchanger on the exhaust air was bypassed.

The operation of the earth to air heat exchanger was controlled in a way that avoided unwanted cooling during the cold season and unwanted heating during the hot season. Thus, the incoming outdoor air was passed through the earth to air heat exchanger only if the outside temperature was greater than 20°C or less than a threshold temperature value as given in Table 3. These limits were chosen according to the ground temperature given in Figure 4. For instance, the outside air in La Rochelle will bypass the EAHEX whenever its temperature is between 8°C and 20°C.

The results obtained are discussed in the following sections.

7.1 Heating Potential of the Ventilation Systems

Heating demands were computed for an internal temperature set point of 19°C. Figure 6 shows the heating demand of the Mozart house and the annual

Table 3. Temperature limit for the EAHEX operation during the cold season.

| Nancy | La Rochelle | Nice |
|-------|-------------|------|
| 5°C | 8°C | 10°C |

Table 4. Extract ventilation Vs Balanced ventilation.

| | Nancy | La Rochelle | Nice |
|--|-------|-------------|-------|
| Heat demand [kWh/m ² a] | -27.5 | -17.6 | -10.9 |
| Auxiliary consumption [kWh/m ² a] | +3.9 | +2.9 | +2.8 |

auxiliary consumption (fans and electrical resistance for frost protection), for the four cases previously mentioned and for the three cities. The auxiliary consumption presented here takes into account the operation of the system during the hot season.

Table 4 shows the heat demand and the annual auxiliary consumption difference between the extract ventilation configuration and the balanced ventilation configuration. The (-) sign indicates a decrease and (+) sign indicates an increase. Using balanced ventilation with a heat recovery unit of 75% efficiency, instead of mechanical extract ventilation, decreases considerably the heating demand for the three climates. The heat gain becomes less important when going from a cold climate to a moderate and a hot climate. The auxiliary consumption increases, but still by much less than the reduction in the heating demand.

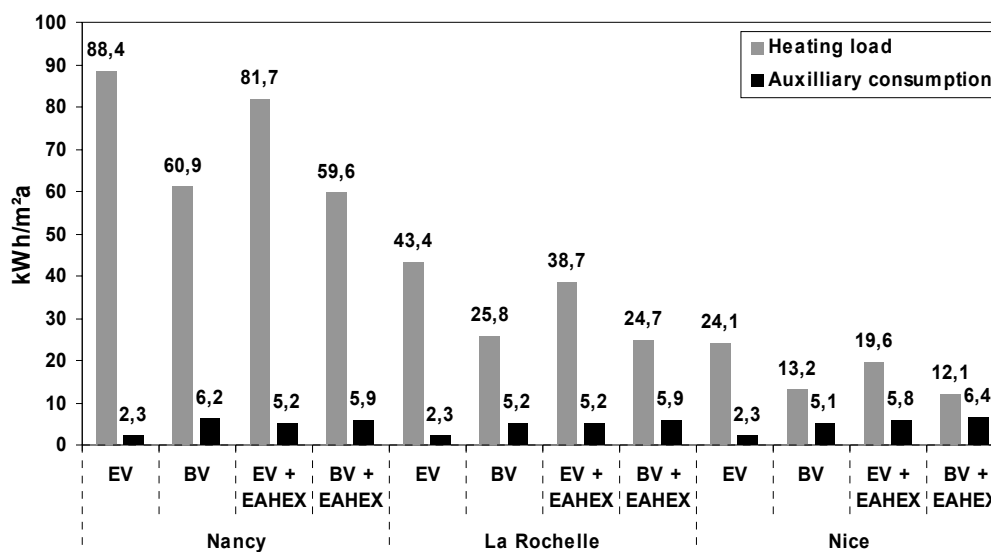


Figure 6. Annual heating demand and auxiliary consumption.

Table 5. Extract ventilation Vs Extract ventilation+EAHEX.

| | Nancy | La Rochelle | Nice |
|--|-------|-------------|------|
| Heat demand [kWh/m ² a] | -6.7 | -4.7 | -4.5 |
| Auxiliary consumption [kWh/m ² a] | +2.9 | +2.9 | +3.5 |

Table 6. Balanced ventilation Vs Balanced ventilation + EAHEX.

| | Nancy | La Rochelle | Nice |
|--|-------|-------------|------|
| Heat demand [kWh/m ² a] | -1.3 | -1.1 | -1.1 |
| Auxiliary consumption [kWh/m ² a] | -0.3 | +0.7 | +1.3 |

The results obtained for Nice are quite interesting. The heating demand of the Mozart house for the balanced ventilation system was 13.2 kWh/m²a. This value is below the target of 15 kWh/m² for the annual heating demand as fixed by the German standard for passive houses (PHPP, 2004).

Table 5 gives the heating demand and the annual auxiliary consumption difference between the extract ventilation configuration and the extract ventilation with the EAHEX configuration.

Using the earth to air heat exchanger and the mechanical extract ventilation decreases the heating demand for the three climates. However, the heat gain is less important than that obtained with the balanced ventilation with heat recovery, and it is of

the same order of magnitude as the increase in auxiliary energy consumption.

Table 6 gives the heating demand and the auxiliary consumption difference between the balanced ventilation configuration and the balanced ventilation with the EAHEX configuration.

The additional heat gain from the earth heat exchanger coupled with a balanced ventilation system is rather marginal. Further, the heat gain is of the same order as the increase in auxiliary energy consumption. However, even for negative outside temperatures, the air temperature at the outlet of the earth heat exchanger is always positive. Hence, it protects the heat recovery unit from freezing.

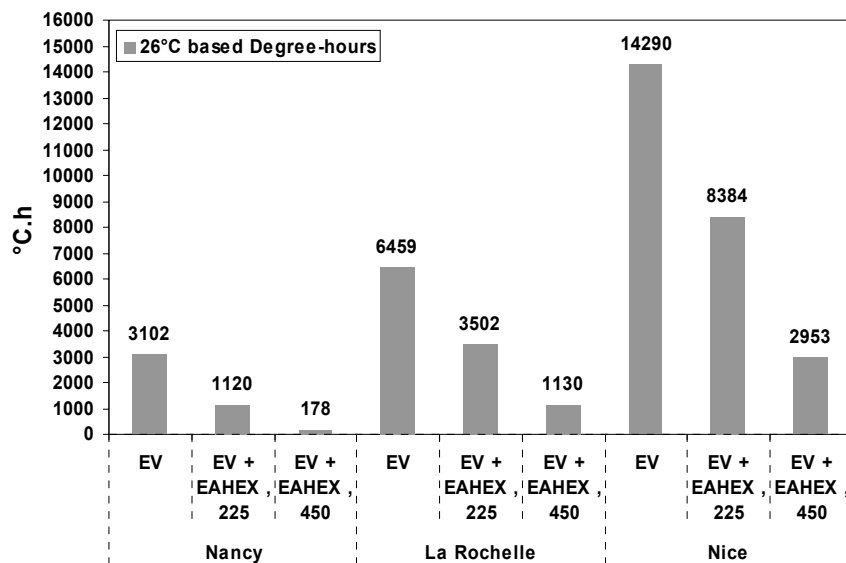


Figure 7. 26°C based degree-hours of the operative temperature.

The simulation results show that balanced ventilation with heat recovery on the exhaust air is a more efficient preheating technology than the earth to air heat exchanger, for the three climates. The major contribution of the earth heat exchanger coupled with a balanced ventilation system is the protection of the heat recovery unit from freezing.

7.2 Cooling Potential of the Earth to Air Heat Exchanger

During the summer season, the heat exchanger of the balanced ventilation system is bypassed.

The operative temperature is chosen as a thermal comfort indicator. It is given by the following equation:

$$T_{op} = \frac{h_{conv} T_{air} + h_{rad} T_{mr}}{h_{conv} + h_{rad}} \quad (21)$$

The optimal operative temperature in summer time, which depends on the metabolism and clothing resistance, is calculated following ISO 7730 (2006). A threshold temperature of 26°C is found.

For the three cities, Figure 7 gives the degree-hours of operative temperature which exceeds the threshold of 26°C computed for the following cases:

- Mozart with a mechanical extract ventilation system (EV).
- Mozart with a mechanical extract ventilation system, coupled with an earth to air heat exchanger. The air flow through the buried pipe during the summer is 225 m³/h (EV + EAHEX, 225)
- Mozart with a mechanical extract ventilation system, coupled with an earth to air heat exchanger. The air flow rate through the buried pipe is 450 m³/h (EV + EAHEX, 450)

The air flow rate of 450 m³/h corresponds to the maximum allowed air velocity in the ventilation ducts, which is 6 m/s according to the French regulation DTU68.1 (1995).

The results show that the earth to air heat exchanger has a large potential for improving thermal summer comfort inside the Mozart house. The number of degree-hours of operative temperature which exceeds 26°C is noticeably decreased for the three climates.

Table 7. Yearly cooling power of the earth to air heat exchanger.

| Cooling power [kWh/m ² a] | Nancy | La Rochelle | Nice |
|--------------------------------------|-------|-------------|------|
| Air flow = 225m ³ /h | 5.9 | 5.0 | 7.6 |
| Air flow = 450m ³ /h | 10.3 | 8.7 | 13.3 |

Table 8. Electrical primary energy conversion factors.

| | g of CO ₂ / kWh |
|-------------|----------------------------|
| Heating | 180 |
| Ventilation | 100 |

Table 7 shows the yearly cooling power of the earth to air heat exchanger obtained for the air flow of 225 m³/h and 450 m³/h. Air replacement, which has a negative energetic effect in winter and is, therefore, kept at minimum rates, turns out to have a positive function in summer when coupled to an inertial buffer like an earth to air heat exchanger. Flow rates as well as the number of buried pipes may in this case be increased, yielding increased cooling power.

Thus the earth to air heat exchanger presents a large potential for cooling. If looked at in this way, its contribution to winter air preheating could be regarded as an additional free service.

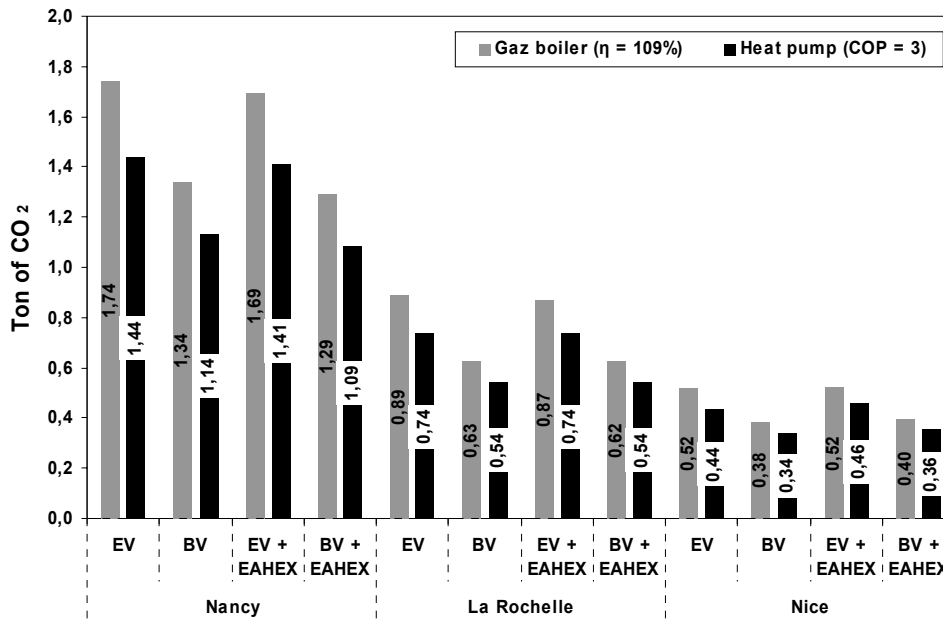
7.3 CO₂ Emission Reduction

To calculate the CO₂ emission, two types of heat production unit are considered: a condensing natural gas boiler with an annual efficiency of 109%, and an air to water heat pump with an annual COP of 3.

The CO₂ emissions are computed according to the Bilan Carbone (2005) method. This method uses conversion factors to convert the kWh of energy consumption to g of CO₂ emission.

The conversion factor of the natural gas as a combustible is 205.3 g of CO₂ per kWh. The conversion factors for the electricity consumption depend on the usage type (see Table 8).

Final energy consumptions were converted to primary energy consumptions using a conversion factor equal to 2.58 for electricity and 1 for natural gas according to the French thermal regulation (RT, 2005).

Figure 8. CO₂ emission.

The results obtained (see Figure 8) lead us to the same conclusions as those in Section 7.1. Balanced ventilation with heat recovery on the exhaust air is more efficient for air preheating than the earth to air heat exchanger. Hence, it has a greater impact on CO₂ emission.

A heat pump system is more efficient than a condensing gas boiler. It reduces the energy consumption used for heating and the CO₂ emission related to it.

8. Conclusions

Mechanical ventilation systems with heat recovery are an important element in the design of a low energy house. The aim of this work was to evaluate the impact of two mechanical ventilation systems on the thermal performance of a dwelling, under French climate characteristics. The mechanical ventilation systems consist of a balanced ventilation system with heat recovery unit on the exhaust air, and an earth to air heat exchanger for air cooling and preheating. The evaluation criteria were the heating demand, the auxiliary consumption, the thermal summer comfort and the CO₂ emission. Four system configurations were simulated in order to evaluate the performance of each system

separately and also the performance of their coupling.

Balanced ventilation with heat recovery on the exhaust air turns out to be a better preheating technology than the earth to air heat exchanger. The additional heat gain from the earth heat exchanger coupled with a balanced ventilation system is marginal. However, it protects the heat recovery unit from freezing.

The earth to air heat exchanger presents a substantial potential for cooling. The air preheating could be an additional free service and can be coupled to more efficient preheating techniques like a heat exchanger on the exhaust air.

These conclusions are in agreement with the findings of many other works. Dorer et al (1998) reported that, for the Swiss climate, the contribution of an earth to air heat exchanger to the heat gain when coupled with a balanced ventilation system with a heat recovery unit is rather marginal. Hollmuller et al (2001) found that, in Switzerland, an earth to air heat exchanger presented a high potential for cooling and was less efficient than heat exchangers on exhaust air for air preheating. Bojic et al (1997) reported that earth to an air heat exchanger is more energy and cost efficient in summer than in winter.

Nomenclature

| | |
|-------------|--|
| A | surface area (m ²) |
| C | fluid capacity (W/K) |
| C_p | specific heat capacity (J/kgK) |
| D | pipe diameter (m) |
| DH | number of degree-hours (°C.h) |
| h | heat transfer coefficient (W/m ² K) |
| J | Day of the year |
| J_{shift} | The time difference (in days) between the beginning of the calendar year and the occurrence of the minimum surface temperature |
| L | Length of the buried pipe (m) |
| m | mass flow rate (kg/s) |
| NTU | number of transfer unit (-) |
| Nu | Nusselt number (-) |
| P | power (W) or heat flux (W/m ²) |
| Pr | Prandtl number (-) |
| R | thermal resistance (mK/W) |
| Re | Reynolds number (-) |
| T | temperature (°C) |
| t | time (s) |
| UA | overall heat transfer coefficient (W/K) |
| V | volume (m ³) |
| x | co-ordinate (m) |
| Z | depth (m) |

Greek Symbols

| | |
|----------------|--|
| Φ_{solar} | global solar radiation on horizontal (kWh/m ²) |
| ρ | density (kg/m ³) |
| λ | thermal conductivity (W/mK) |
| ε | efficiency (-) |
| α | thermal diffusivity (m ² /s) |

Subscripts

| | |
|--------|-----------------------------------|
| gc | convective gain |
| und | undisturbed |
| a | air |
| amp | amplitude |
| con | convective |
| i | zone i |
| ji | from the zone j to the zone i |
| in | inlet |
| min | minimum |
| max | maximum |
| out | outlet |
| p | wall p |
| rad | radiative |
| $vent$ | ventilation air |
| w | wall |

References

- Al-Ajmi F, Loveday DL and Hanby VI: (2006) "The cooling potential of earth-air heat exchangers for domestic buildings in a desert climate", *Building and Environment*, **41**, pp235–244.
- Al-Ajmi F, Hanby VI and Loveday DL. (2002) "Thermal performance of the sub-soil environment in dry desert climate", *ASHRAE Transactions*, **108**, pt. 2.
- Brandemuhel M, Gabel S and Andersen I. (1993) "HVAC2 TOOLKIT, A Toolkit for secondary HVAC system energy calculations", *University of Colorado at Boulder, USA*.
- Bojic M, Trifunovic N, Papadakis G and Kyritsis S: (1997) "Numerical simulation, technical and economic evaluation of air-to-earth heat exchanger coupled to a building", *Energy*, **22**, pp1151-1158.
- Bilan Carbone : (2005) "Bilan Carbone - Calcul des facteurs d'émissions et sources bibliographiques utilisées (version 3.0)", *ADEME, France*.
- CSTB : (1995) "Résidences principales françaises - Typologies et Description de logements types", *CSTB, France*.
- Dorer V and Breer D: (1998) "Residential mechanical ventilation systems: performance criteria and evaluations", *Energy and Buildings*, **27**, pp247-255.
- DTU68.1 : (1995) "Installations de ventilation mécanique contrôlée - Règles de conception et de dimensionnement", *Norme Française XP P 50-410*.
- Dhaliwal AS and Goswami DY: (1984) "Heat transfer analysis environment control using an underground air tunnel", *ASME Solar Energy Div. Las Vegas* pp505–10.
- El Khoury Z, Riederer P, Couillaud N, Simon J and Raguin M: (2005) "A multizone building model for MATLAB/SIMULINK environment", *The 9th IBPSA Conference (Building Simulation 2005)*, Montréal, Canada.
- Ghosal MK, Tiwari GN and Srivastava NSL: (2004) "Thermal modelling of a greenhouse with an integrated earth to air heat exchanger: an experimental validation", *Energy and Buildings*, **36**, pp219–227.

- Gauthier C, Lacroix M and Bernier H: (1997) "Numerical simulation of soil heat exchanger-storage systems for greenhouses", *Solar Energy*, **60**, pp333-346.
- Gnielinski V: (1976) "New equation for heat and mass transfer in turbulent pipe and channel flow", *Int. Chem. Eng.*, **16**, pp359-68.
- Hollmuller P and Lachal B: (2001) "Cooling and preheating with buried pipe systems: monitoring, simulation and economic aspects", *Energy and Buildings*, **33**, pp509 – 518.
- Incropera F and David De W: (1996) "Introduction to heat transfer", 2nd ed. New York, NY: Wiley.
- Kusuda T and Archenbach PR: (1965) "Earth Temperature and Thermal Diffusivity at Selected Stations in the United States", *ASHRAE Transactions*, **71** part 1.
- Labs K and Cook J: (1989), "Passive cooling", *Cambridge Massachusetts*, London, England.
- Mihalakakou G, Santamouris M and Asimakopoulos D: (1994) "Modelling the thermal performance of Earth-to-air heat exchangers", *Solar Energy*, **53**, pp301-305.
- Mihalakakou G, Santamouris M, Asimakopoulos D. Tselepidaki: (1995) "Parametric prediction of the buried pipes cooling potential for passive cooling applications", *Solar Energy*, **55**, pp163-73.
- NF EN ISO 7730 : (2006) "Ergonomie des ambiances thermiques - Détermination analytique et interprétation du confort thermique par le calcul des indices PMV et PPD et par des critères de confort thermique local", *AFNOR*, France.
- Paepe MDE and Janssens A: (2003) "Thermo-hydraulic design of earth-air heat exchangers", *Energy and Building*, **35**, pp389-397.
- PHPP : (2004) "Passive House Planning Package 2004", *PassivHaus Institut*, Darmstadt, Germany.
- RT : (2005) "Réglementation thermique 2005 - Guide réglementaire", *CSTB*, France.
- SIMBAD: (2005). SIMBAD Building and HVAC Toolbox Version 4.0. CSTB, France.
Website: <http://kheops.champs.cstb.fr/Simbadvac/>.
- SIMULINK: (2005) "Dynamic System Simulation for MATLAB - Version 6.3", Mathworks Inc., USA
Site web: www.mathworks.com.
- Shingari BK: (1995) "Earth tube heat exchanger", *Poultry International*, **34**.
- Tzaferis A, Liparakis D, Santamouris M and Argiriou A: (1992) "Analysis of the accuracy and sensitivity of eight models to predict the performance of earth-to-air heat exchangers", *Energy and Buildings*, **18**, pp35-43.

Urban Canyon Influence on Building Natural Ventilation

K. Syrios and G. R. Hunt

Department of Civil and Environmental Engineering, Imperial College, London, U.K.

Abstract

The natural ventilation of a building, flanked by others forming urban canyons and driven by the combined forces of wind and thermal buoyancy, has been studied experimentally at small scale. The aim was to improve our understanding of the effect of the urban canyon geometry on passive building ventilation. The steady ventilation of an isolated building was observed to change dramatically, both in terms of the thermal stratification and airflow rate, when placed within the confines of urban canyons. The ventilation flows and internal stratifications observed at small scale are presented for a range of canyon widths (building densities) and wind speeds. Two typical opening arrangements are considered. Flanking an otherwise isolated building with others of similar geometry as in a typical urban canyon was shown to *reverse* the effect of wind on the thermally-driven ventilation. As a consequence, neglecting the surrounding geometry when designing naturally-ventilated buildings may result in poor ventilation. Further implications are discussed.

Key words: urban canyon, small-scale modelling, salt bath, natural ventilation, air flow, wind, buoyancy.

1. Introduction

Achieving the desired air flow rate and maintaining comfort levels using natural ventilation is not straightforward due to the variable nature of the driving forces, the often complex geometries involved and the turbulent nature of the flows. For urban settlements an additional challenge is to determine how the wind flow past the ventilated building is modified by the surrounding built environment. In cities the built environment is typically in the form of urban canyons.

Flows in urban canyons have been studied extensively, often with a focus on the dispersion of pollutants and air quality, see, for example, the review paper of Vardoulakis et al. (2003). Similarly, flows in naturally ventilated buildings have received considerable attention in the literature (e.g. Etheridge and Sandberg 1996; Linden 1999) as they offer a low-energy alternative to mechanical ventilation and air conditioning. However, the two families of flows, *i.e.* internal (building ventilation) and external (urban) flows have been studied in isolation. Despite this, for buildings in urban canyons where the ventilation openings (e.g. windows and doors) link to the canyon, the passive ventilation flow is expected to be coupled with and influenced by the canyon flow. Developing an understanding of how the two flows interact provides the motivation for the current study.

The naturally-ventilated enclosure we consider has low-level and high-level vents. These vent locations are often incorporated in the building design in order to harness the stack effect arising from internal and solar heat gains (Etheridge and Sandberg, 1996). The enclosure is flanked by streets and identical buildings, thus forming a typical urban canyon geometry. Figure 1 depicts the urban canyon geometry and the two opening combinations considered: Case 1, the windward façade bears the high-level vents and the leeward façade bears the low-level vents; Case 2, vice versa. The analytical and laboratory modelling of Hunt and Linden (2000, 2005) examined the effect of wind on the thermal stratification established by a localised heat source and showed that, in the absence of upstream and downstream buildings, Case 1 gives rise to an opposing wind flow – with increasing wind speeds yielding reduced ventilation flow rates when buoyancy effects dominate (displacement ventilation) and enhanced ventilation flow rates when wind effects dominate (mixing ventilation). In the absence of upstream and downstream buildings Hunt and Linden (2001) showed that Case 2 gives rise to an assisting wind and enhanced ventilation flow rates. Both assisting and opposing winds were modelled analytically in the absence of internal thermal stratification by Li and Delsante (2001).

The experimental approach employed to examine the ventilation established in Cases 1 and 2 is small-scale physical modelling. The specific technique

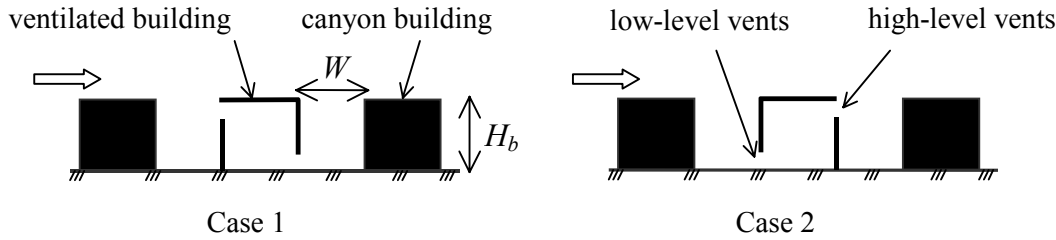


Figure 1. Schematics of the canyon geometry and opening combinations considered. Case 1: high-level vents on the windward façade and low-level vents on the leeward façade, Case 2: vice versa.

(see Section 2) has been used successfully to study solely thermally-driven flows (see for example Linden et al. 1990; Baker and Linden 1991) and was shown by Hunt and Linden (1997) to be appropriate to simulate the combined effects of wind and thermal buoyancy. Winds assisting and opposing the thermally-driven flow through an isolated enclosure were subsequently studied (Hunt and Linden 2001 and 2005, respectively). More recently, this technique for modelling wind- and thermally-induced flows was used to study single-sided ventilation of canyon buildings (Syrios and Hunt 2007a) and to provide insight on the appropriate positioning of ventilation openings for a building shielded from the wind on one, or both, sides by identical canyon buildings (Syrios and Hunt 2007b).

Our focus herein is on exploring the qualitative trends in the steady ventilation of the building as the wind speed and canyon aspect ratio are varied.

2. Methodology

The interaction of the building ventilation flow and the canyon flow was studied in the Hydrodynamics Laboratory by means of small-scale experiments with water, rather than air, as the fluid medium. A clear Perspex box (170 mmx170 mmx598 mm, internal height $H=150$ mm) with high-level and low-level rectangular vents represented the ventilated building.

Urban canyons were formed upstream and downstream by positioning two plastic boxes, of identical dimensions to the Perspex box, parallel to and on either side of the Perspex box. The canyon model was suspended in an 8.6 m long recirculating flume (0.6 m wide and 0.6 m deep). A pump-driven horizontal turbulent flow along the flume simulated a wind normal to the canyons' axis (Figure 2). The 'wind'-induced pressure drop Δ ($\text{gcm}^{-1}\text{s}^{-2}$) across

the vents was measured using oil/water U-tube manometers, see Syrios (2005) for details. The 'wind' speed (hence, Δ) was varied by regulating the pump speed by means of an inverter. No attempt was made to simulate the atmospheric boundary layer. The plastic boxes could be translated along and locked onto horizontal plastic boards which formed the streets between the buildings. The canyon aspect ratio H_b/W (building height/street width) could be varied within the range $1/5 \leq H_b/W \leq 2$. Ventilation of an isolated enclosure ($H_b/W=0$) was achieved simply by removing the two plastic boxes.

Convection from a localised heat source at floor level in the building was simulated by releasing salt solution in the Perspex box through a circular nozzle of diameter 5 mm in the lid. The buoyancy flux was kept constant at $B=133 \text{ cm}^4\text{s}^{-3}$ by supplying salt solution of density 1.071 gcm^{-3} at a rate of $1.9 \text{ cm}^3\text{s}^{-1}$. Conductive and radiative heat transfers were not reproduced and canyon surfaces were isothermal. The vertical inversion of the flow and model (Figure 2) does not affect the flow dynamics for the small density differences considered (Boussinesq flows). The technique adopted, often termed the 'salt-bath technique' provides approximate dynamical similarity with full-scale flows (Baker and Linden, 1991; Hunt and Linden, 1997). Density differences were measured using a density meter (Anton Paar DMA 35N, accuracy $\pm 5 \times 10^{-4} \text{ gcm}^{-3}$) and the internal stratification was visualised using a shadowgraph. Dye was added to the salt solution supplying the nozzle in order to mark regions of dense fluid within the box. The relatively large volume of water (of density ρ_a) in the flume ensured that changes in its density were negligible during the course of an experiment.

The area of the vents, as characterised by the effective opening area ($A^* = [(2C_{dlow}^2 A_{low}^2)^{-1} + (2C_{dhigh}^2 A_{high}^2)^{-1}]^{-1/2}$) according to the definition of

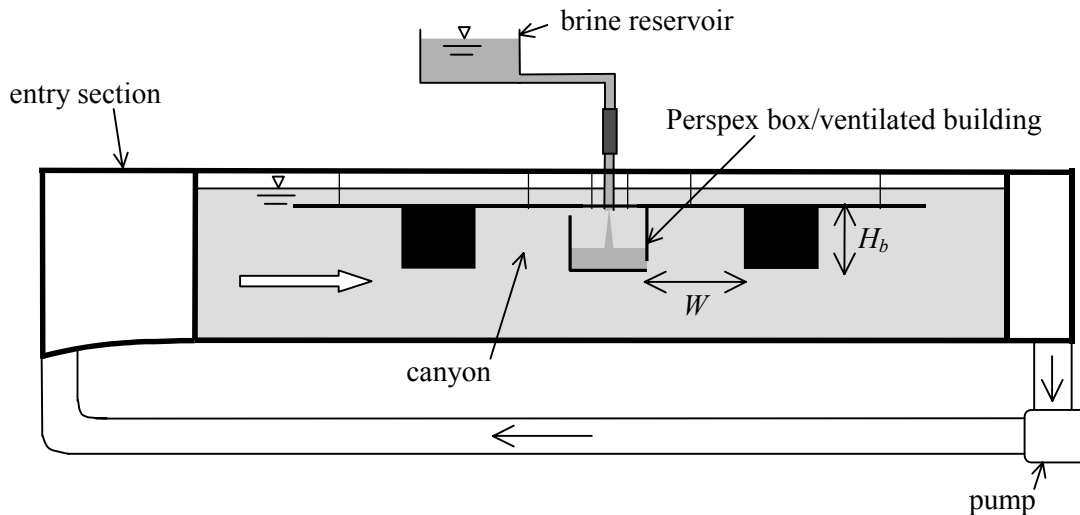


Figure 2. Schematic of flume in elevation and the canyon apparatus.

Linden 1999) was varied by removing (or adding) plugs from the vents in the box. The quantities A_{low} and A_{high} denote the low-level and high-level opening areas, respectively; C_{dlow} and C_{dhigh} are their respective discharge coefficients

3. Results

We focus solely on the effect of Δ and H_b/W on the ventilation. Vents giving a free open area of approximately 1% were chosen: opening areas were kept fixed at $A_{low}=6 \text{ cm}^2$ and $A_{high}=3 \text{ cm}^2$ giving $A^*=2.28 \text{ cm}^2$ (for $C_{dlow}=C_{dhigh}=0.6$). The total opening area (9 cm^2) was then approximately 1% of the floor area (924.8 cm^2). To study the effect of wind speed a square canyon was maintained.

Conservation of buoyancy flux gives the steady ventilation flow rate as $Q=B/g'$ (cm^3s^{-1}), where $g'=g(\rho_a-\rho)/\rho_a$ (cms^{-2}) is the reduced gravity of the outflow and ρ its density. The number of air changes per hour (ac/h) was deduced from the steady flow rate as $\text{ac/h}=3600Q/V$, where V is the internal volume of the box ($V=13872 \text{ cm}^3$). Ac/h estimates are given in Figures 3–6 of Sections 3.1 and 3.2. The relative magnitudes of a characteristic wind-induced velocity and a thermally-induced velocity for the ventilation flow, defined by the Froude number of Hunt and Linden (2001) as $Fr=(\Delta/\rho)^{1/2}/(B/H)^{1/3}$, are also presented.

The frame of reference for the discussion in the remainder of the paper is that of a full-scale building

with a plume of warm air rising from a heat source at floor level. The steady building ventilation flow established for Cases 1 and 2 (Figure 1) is now presented.

3.1 Case 1

The rising plume from the localised heat source established displacement flow and a distinct two-layer stratification with a steady interface at a height h (Figure 3a) above the floor. Inflow took place through the low-level vents and outflow through the high-level vents as shown in Figures 3 and 4. Mixing by the inflow was weak and this displacement flow was observed for the whole range of canyon aspect ratios examined and for wind speeds up to 20.1 cms^{-1} (for $0 \leq Fr \leq 8.4$, equivalently $0 \leq Fr(A^*/H^2)^{1/3} \leq 1.8$, cf. Hunt and Linden 2005).

3.1.1 Effect of Wind Speed

In the absence of upstream and downstream buildings, openings arranged as in Case 1 (Figure 1) resulted in the wind *opposing* the thermally-driven flow. However, for a square canyon ($H_b/W=1$) increasing the wind speed, and hence Δ , resulted in an increase in h , see Figure 3. The external flow drove an upward flow through the space, *i.e.* in the same sense as the thermally-driven flow. This *assisting* wind condition resulted in an increase in ac/h (with a small increase in h yielding a significant increase in ac/h), see Figures 3b and 3c. The upper layer cooled with increasing wind speed

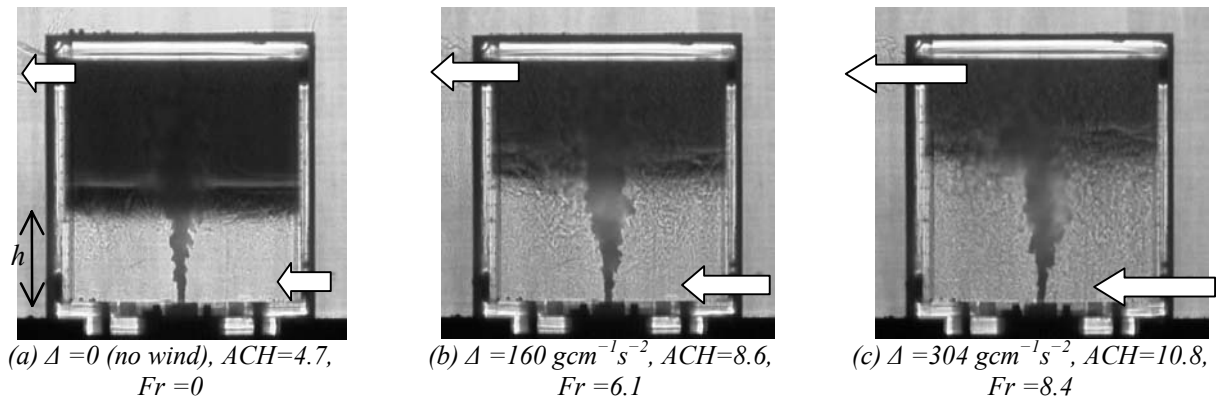


Figure 3. Case 1: Inverted shadowgraph images showing the effect of increasing wind speed ((a)-(c)) on the steady ventilation of a building in a square canyon ($H_b/W=1$). The arrows indicate the direction of flow and their relative size reflects the trends in the ventilation airflow rate.

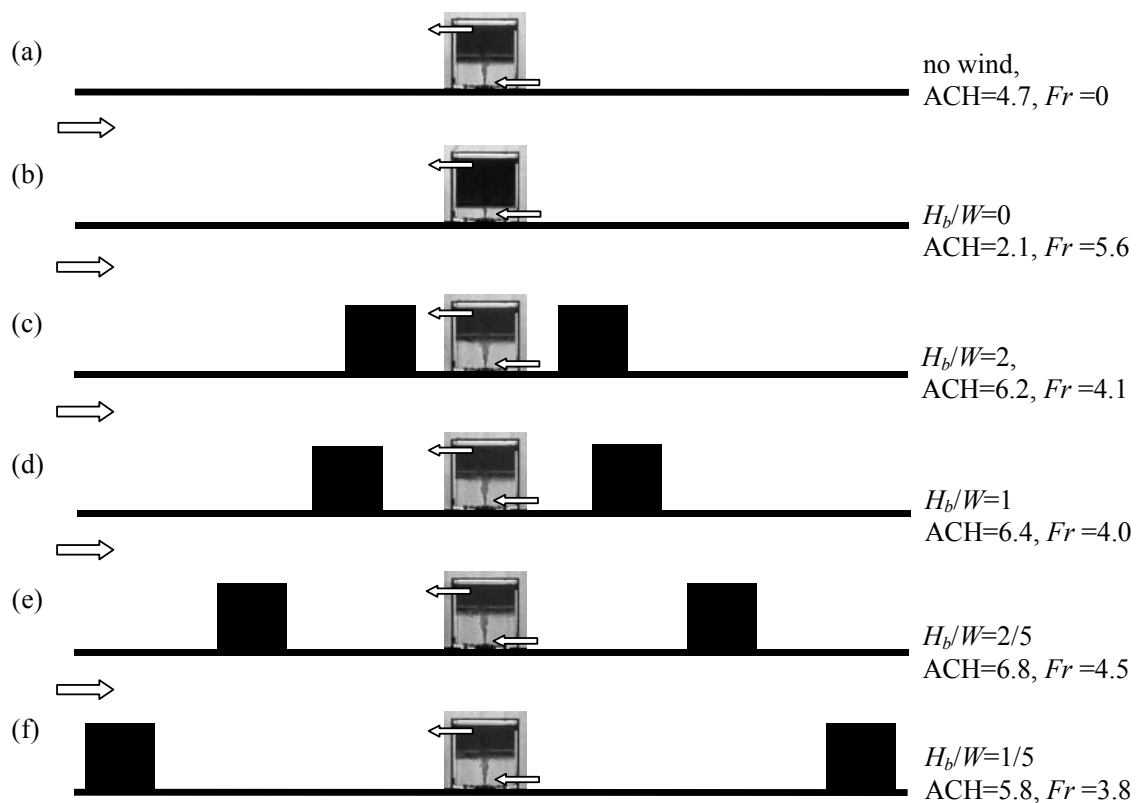


Figure 4. Case 1: Inverted shadowgraph images of the steady internal stratification are shown for $H_b/W=\{0, 2, 1, 2/5, 1/5\}$. The mean approaching 'wind' speed was constant at 9.9 cm s^{-1} .

as can be inferred by the increased dilution of the dye (compare the upper layer in Figures 3a and 3c) and was confirmed by density measurements.

3.1.2 Effect of Canyon Aspect Ratio

In the absence of canyons, successive increases in the wind speed (from zero) resulted in a decrease in

h and an increase in the upper-layer temperature, thereby, signifying an *opposing* wind condition (compare Figures 4a and 4b). However, introduction of the surrounding canyons (Figures 4c-f) resulted in *assisting* winds – the interface ascended indicating increased airflow rates and the upper layer cooled.

This reversal in the effect of the external flow on the building ventilation flow is attributed solely to the canyons, as the heat input, building geometry and wind speed remained unchanged. Note that maintaining a constant approach wind speed did not ensure a constant pressure drop Δ across the openings as the external flow pattern and, hence, pressure drop altered with the canyon geometry H_b/W . As a consequence, the relative magnitudes of the characteristic wind- and thermally- induced velocities, as indicated by the Froude numbers in Figure 4, varied with H_b/W .

3.2 Case 2

Displacement flow was observed for a range of wind speeds (Figures 5a and 5b). However, for sufficiently strong winds mixing flow was observed (Figure 5c), whereupon inflow took place through high-level vents, outflow through low-level vents and the interior was close to uniformly well-mixed (i.e. at a uniform temperature).

3.2.1 Effect of Wind Speed

For a square canyon ($H_b/W=1$) progressive increases in the wind speed, hence Δ , from zero resulted in a decrease in h for the displacement flow mode (compare Figures 5a and 5b), i.e. an *opposing* wind condition. Further increases in wind speed resulted in a break down of the stratification, turbulent mixing and a reversal in the direction of flow (Figure 5c). The wind then dominated and drove a mean downward flow through the space, i.e. against the thermally-driven flow.

Increasing wind speed resulted in decreasing ac/h for displacement flow and increasing ac/h for mixing flow. On comparison of Figures 5(b) and 5(c), the relatively sensitive nature of the ventilation to the wind speed is apparent: with over a five-fold increase in ac/h caused by a 30% increase in wind speed.

3.2.2 Effect of Canyon Aspect Ratio

In the absence of canyons, increasing the wind speed from zero resulted in an increase in h and a reduction in the upper-layer temperature, thereby signifying an *assisting* wind condition (compare Figures 6a and 6b). However, introduction of the canyons resulted in *opposing* wind conditions and either mixing flow (Figures 6c and 6d), or displacement flow with a deep and warm upper layer (Figures 6e and 6f: in each a shallow lower layer at ambient density can be seen). As in Case 1, introducing the canyons resulted in an interaction of the external flow and building ventilation flow which is opposite to what is expected for an isolated building.

4. Discussion and Conclusions

Canyons were shown to reverse the effect of the wind on the thermally-driven ventilation of an otherwise isolated building. Winds that, in general, enhance/oppose the thermally-driven passive ventilation flow through an isolated building were shown to oppose/enhance the thermally-driven flow through a canyon building. This reversal was

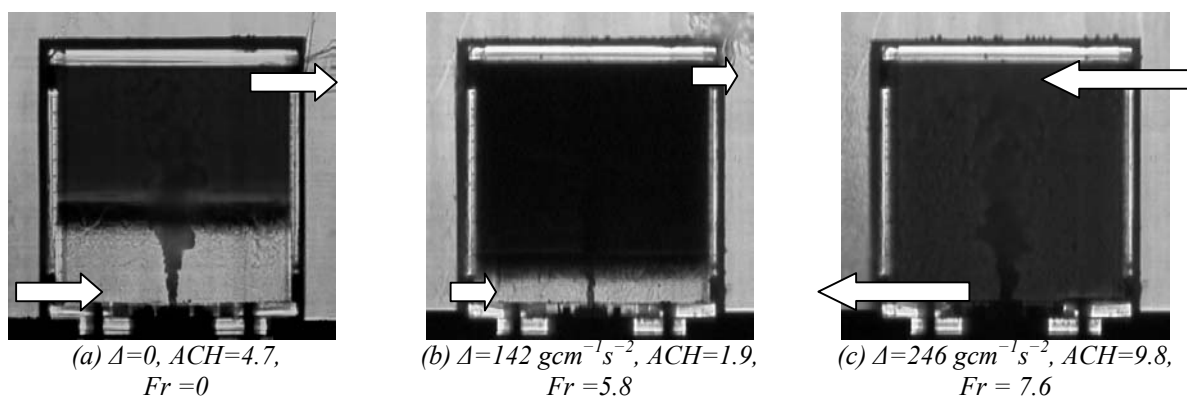


Figure 5. Case 2: Inverted shadowgraph images showing the effect of increasing wind speed ((a)-(c)) on the steady ventilation of a building in a square canyon ($H_b/W=1$). The arrows indicate the direction of flow and their relative size reflects the trends in the ventilation air flow rate.

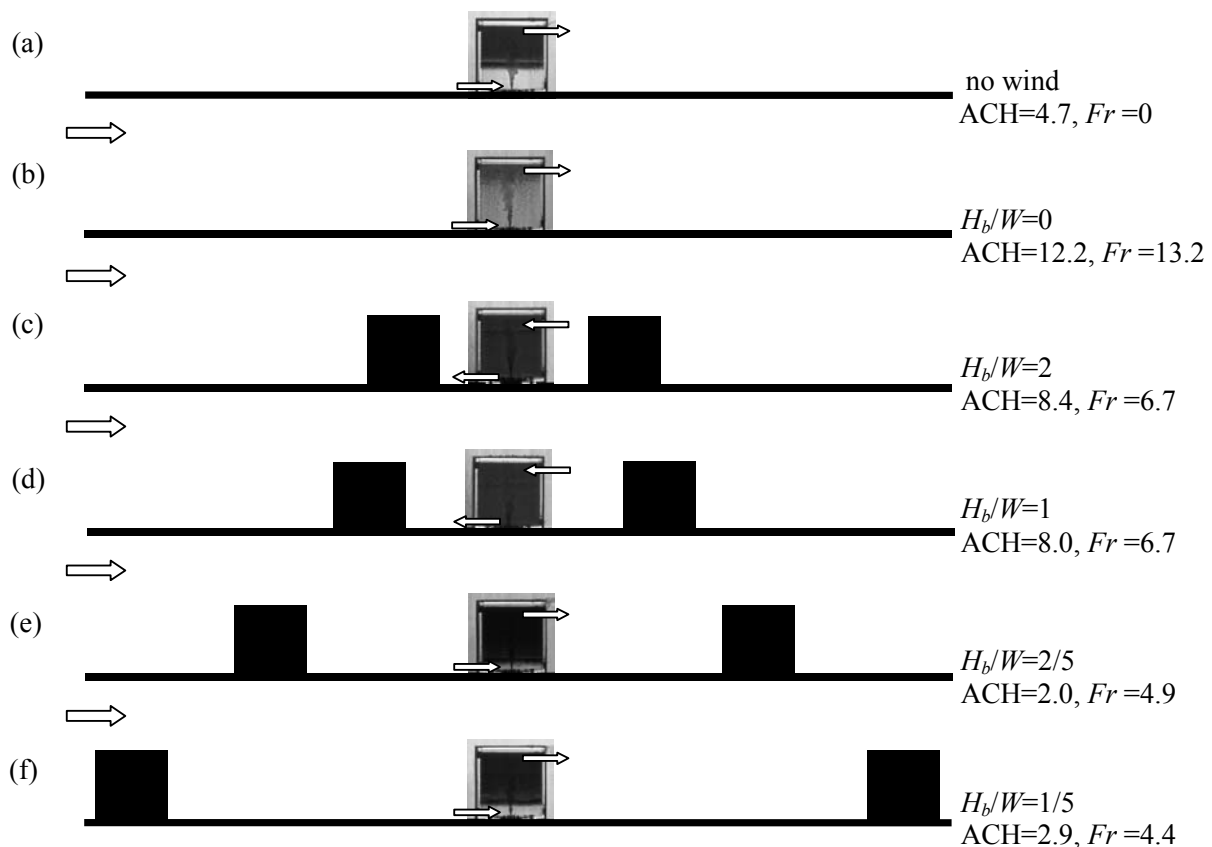


Figure 6. Case 2: Inverted shadowgraph images of the steady internal stratification are shown for $H_b/W = \{0, 2, 1, 2/5, 1/5\}$. The mean approaching 'wind' speed was constant at 20.1 cm s^{-1} .

evident for canyons as wide as five times the building height (compare Figure 4b with 4f and Figure 6b with 6f). A design implication is that ventilation openings may have to be positioned somewhat counter-intuitively. For example, wind-enhanced ventilation for canyon buildings can be obtained by positioning high-level vents on the windward façade (directly facing the oncoming wind) and with low-level vents on the leeward façade, *i.e.* as in Case 1.

In contrast, positioning low-level vents on the windward façade and high-level vents on the leeward façade results in wind and thermal forces that oppose. Furthermore, the variable degree of shielding offered by canyons of different widths (shielding increasing with decreasing width) may result in different ventilation modes (mixing or displacement flow) for the same building geometry and forcing (*i.e.* heat load and wind speed). These modes produce extremes of ventilation effectiveness

(*cf.* Linden et al. 1990, Gladstone and Woods 2001, Coffey and Hunt 2007a, b) and flows in opposite directions.

The reversal of the effect of wind on the thermally-driven flow when canyons are introduced may be explained in terms of the surface pressure on the leeward façade exceeding the surface pressure on the windward façade of the ventilated building. This pressure imbalance arises from the different flow patterns in the upstream and downstream canyons as verified by the dye injection experiments of Syrios (2005). For the isolated building, surface pressures on the windward façade exceed those in the lee.

Transitions between mixing ventilation and displacement ventilation triggered by changing the canyon aspect ratio, or indeed wind speed, were consistent with the Froude number condition established by Hunt and Linden (2005) for an isolated building.

The outcomes of this study highlight the need for information transfer between the architect, ventilation engineer and urban planner: if a passive ventilation technique is to be applied successfully, an awareness of the surrounding structures is necessary as these were shown herein to influence dramatically the natural ventilation flow. Building designs need to be flexible regarding the positioning of vents. The latter may have to be repositioned to accommodate changes in the surrounding built environment so that enhanced ventilation, as achieved by assisting winds, can be maintained.

Acknowledgements

The authors gratefully acknowledge the financial support of the BP Advanced Energy Programme in Buildings at Imperial College London. KS is also grateful to the Alexander S. Onassis Public Benefit Foundation and the Eugenides Foundation. We would like to thank Professor J.M.R. Graham of the Department of Aeronautics, Imperial College London for providing access to the Hydrodynamics Laboratory.

References

- Baker N and Linden PF: (1991) "Physical modelling of airflows – a new design tool", in *Atrium Buildings Architecture and Engineering* (ed. F. Mills), pp13-22.
- Coffey CJ and Hunt GR: (2007a) "Ventilation effectiveness measures based on heat removal: Part 1. Definitions", accepted for publication in *Build. Environ.* doi:10.1016/j.buildenv.2006.03.016.
- Coffey CJ and Hunt GR: (2007b) "Ventilation effectiveness measures based on heat removal: Part 2. Application to natural ventilation flows", accepted for publication in *Build. Environ.* doi:10.1016/j.buildenv.2006.03.015.
- Etheridge DW and Sandberg M: (1996) "Building ventilation: theory and measurement". John Wiley and Sons, Chichester.
- Gladstone C and Woods AW: (2001) "On buoyancy-driven natural ventilation of a room with a heated floor", *J. Fluid. Mech.* **441**, pp293-314.
- Hunt GR and Linden PF: (1997) "Laboratory modelling of natural ventilation flows driven by the combined forces of buoyancy and wind", in *Proc. CIBSE National Conference, October 1997, London, UK*, **1**, pp101-107.
- Hunt GR and Linden PF: (2000) "Multiple steady airflows and hysteresis when wind opposes buoyancy", *Air Infiltration Review*, **21**, No 2.
- Hunt GR and Linden PF: (2001) "Steady-state flows in an enclosure ventilated by buoyancy forces assisted by wind", *J. Fluid Mech.* **426**, pp355-386.
- Hunt GR and Linden PF (2005) "Displacement and mixing ventilation driven by opposing wind and buoyancy", *J. Fluid Mech.*, **527**, pp27-55.
- Li Y and Delsante A: (2001) "Natural ventilation by combined wind and thermal forces", *Build. Environ.*, **36**, pp59-71.
- Linden PF: (1999) "The fluid mechanics of natural ventilation", *Annu. Rev. Fluid Mech.*, **31**, pp201-238.
- Linden PF, Lane-Serff GF and Smeed DA: (1990) "Emptying filling boxes: the fluid mechanics of natural ventilation", *J. Fluid Mech.*, **212**, pp309-335.
- Syrios K: (2005) "Natural ventilation of buildings in urban canyons", PhD thesis, Imperial College London.
- Syrios K and Hunt GR: (2007a) "Passive air exchanges between building and urban canyon via openings in a single façade", submitted to *Int. J. Heat Fluid Fl.*
- Syrios K and Hunt GR: (2007b) "The influence of upstream and downstream shielding on displacement ventilation", submitted to *Atmos. Environ.*
- Vardoulakis S, Fisher BEA, Pericleous K and Gonzalez-Flesca N: (2003) "Modelling air quality in street canyons: a review", *Atmos. Environ.*, **37**, pp155-182.

Study of the Airflow Structure in Cross-Ventilated Rooms based on a Full-Scale Model Experiment

Shigeeki Nishizawa¹, Takao Sawachi¹, Ken-ichi. Narita², Nobuyoshi Kiyota³, Hironao Seto⁴

¹ National Institute for Land and Infrastructure Management, Japan

² Nippon Institute of Technology, Japan

³ Hiroshima Institute of Technology, Japan

⁴ Building Research Institute, Japan

Abstract

Cross ventilation to reduce cooling energy is one of the most important techniques for maintaining a comfortable indoor environment in hot and mild seasons. However, at present, it is difficult to design the indoor environment under cross ventilation because there is insufficient knowledge to evaluate the effect of cross ventilation quantitatively. To develop an understanding of the flow characteristics a full-scale model experiment was performed in a large wind tunnel to examine airflow properties in a cross-ventilated space. The purpose of this paper is to clarify the airflow structure in the cross-ventilated room in relation to wind direction.

The key factors determining the airflow structure in the space were found to be: the main current region, rebounding and changing flow direction, deflected flow, surface flow and circulating flow. It was observed that the main air current tends to travel in a straight line until it collides with obstacles. On collision, the flow changes direction and deflected flows are formed over and/or under the main current. When there is enough space alongside the main current region, a circulating flow is formed in each room. The room mean velocity was found to be dependent on the path of the air current. When the main current is well defined, a relatively low value of mean velocity is observed. When the main current is divided, the room containing the inflow opening has a relatively high velocity.

Keywords: cross ventilation, wind tunnel experiment, full-scale model, airflow structure, natural ventilation

1. Introduction

Cross ventilation to reduce cooling energy is one of the most important techniques for maintaining a comfortable indoor environment in hot and mild seasons. However, at present, it is difficult to design the indoor environment under cross ventilation because there is insufficient knowledge to evaluate the effect of cross ventilation quantitatively. Indoor airflow is particularly important in exhausting the heat from buildings and for the thermal comfort of occupants. The property of indoor airflow has been examined by visualization (McCutchan et al., 1952) and by velocity measurements in scale models and buildings. However an understanding of the detail of airflow distribution remains an issue because of measurement limitations. Thus, to improve understanding, a full-scale model experiment was undertaken in a large wind tunnel to examine the airflow properties in a cross-ventilated space. The purpose of this paper is to clarify the airflow structure in the cross-ventilated rooms. The airflow

velocity field was measured in detail in the model and the airflow structure was examined by three-dimensional mean velocity and turbulence characteristics.

2. Experimental Method

The plan and section of the wind tunnel used in this study are shown in Figure 1. The wind tunnel was constructed to examine the property of airflow in and around a full-scale building model. The wind tunnel has six fans (1.5 m in diameter, the maximum output of each fan is 37 kW) and a cooling coil to keep the air temperature below 25 °C. The range of wind speed in the working section is 1.0-5.0 m/s and its distribution was checked to be close to uniform before the construction of the building model (Sawachi et al., 1999). In the experiment described in this paper, the average wind speed was set to 3 m/s on the inlet side.

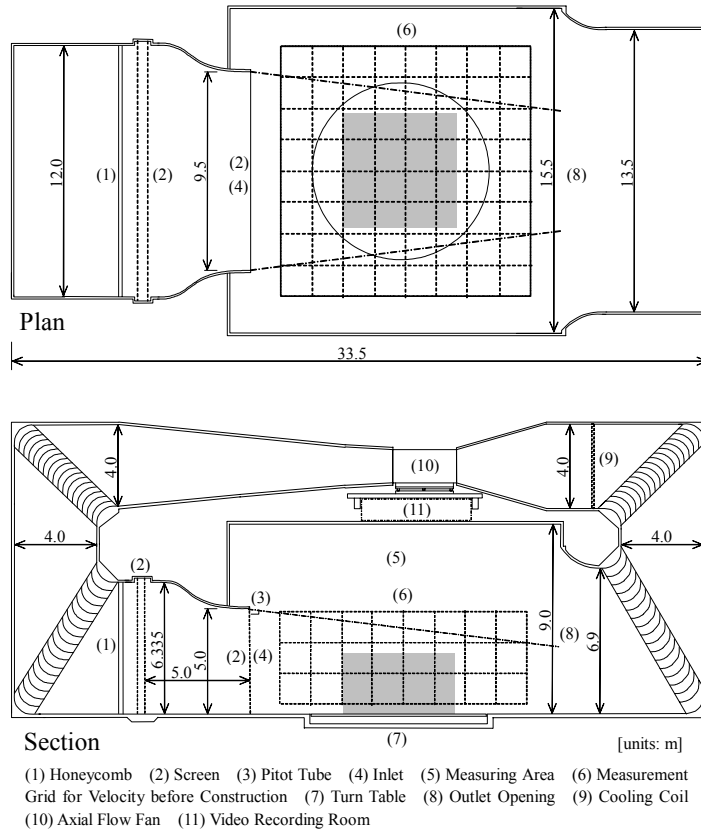


Figure 1. Plan and section of the wind tunnel.

Wind velocity is measured on indoor grid at 420mm intervals, at height of 50mm, 230mm, 710mm, 1,190mm and 1,670mm above room floor. And the grid near the building model is set at 463mm intervals (the nearest points from wall is 50mm away from the wall surface), and outside points near the model are set at 500mm, 1,000mm, 1,500mm, 2,000mm and 3,000mm height above floor of wind tunnel.

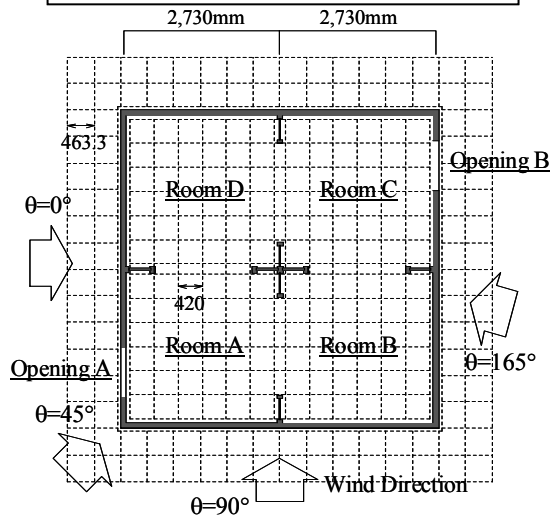


Figure 2. Building model and measurement points.

The plan of the building model is shown in Figure 2. It has four rooms and dimensions $W=D=5560$ mm and $H=3000$ mm. Diagonally opposite each other are two large openings of size $W=860$ mm, $H=1740$ mm. The wind direction was set at 15 degree intervals between 0° and 165° by rotating the building model on a turntable. The air velocity measurement points were set on a grid inside and near the building model. Measurements were made at six different heights i.e: 50 mm, 230 mm, 710 mm, 1190 mm, 1670 mm and 2100 mm above the floor. The velocity was measured using two types of KAIJO three-dimensional ultrasonic

anemometers, WA-390 (response time 0.5 seconds) and DA-600 (response time 0.05 seconds).

3. Results

3.1 Velocity Vector on the Horizontal Plane at a Height of 1190 mm above the Floor

Figure 3 shows the vector diagrams for wind directions between 0 and 165° on a horizontal plane. Measurements inside the building were at 1190 mm height above the floor (= 1690 mm above the floor

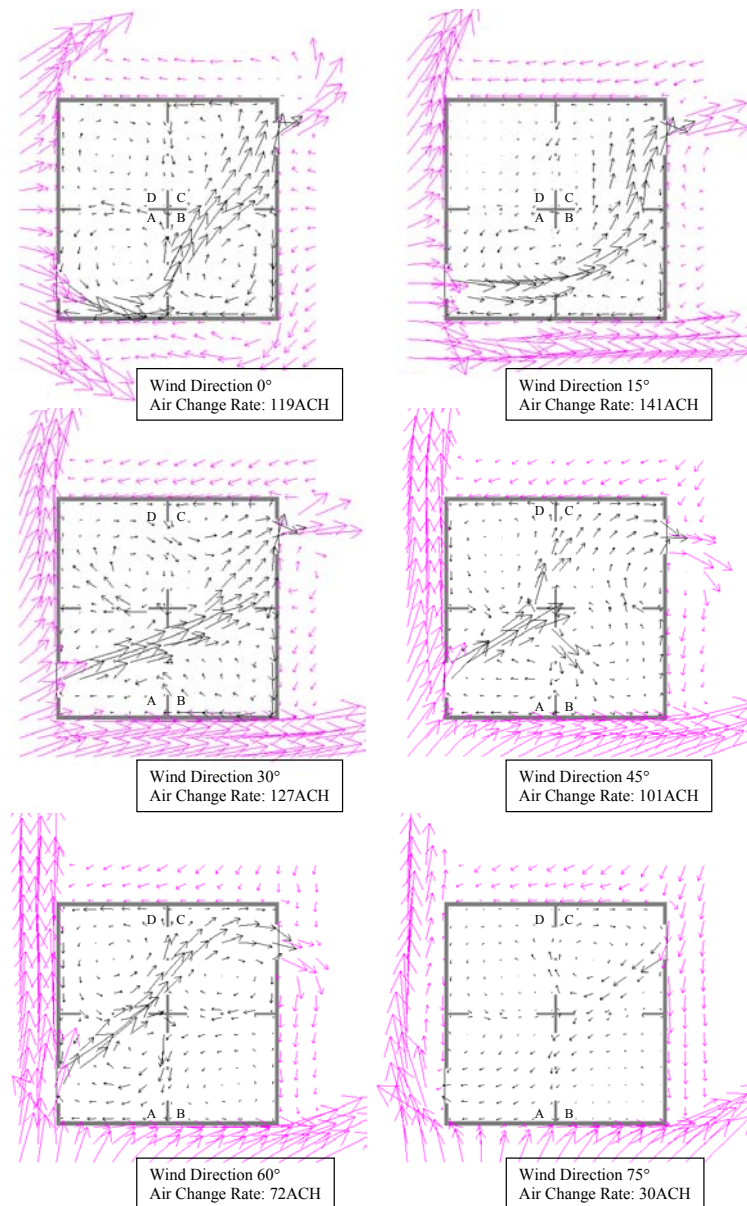


Figure 3 (part 1). Airflow distribution on horizontal plane at 1190 mm height.

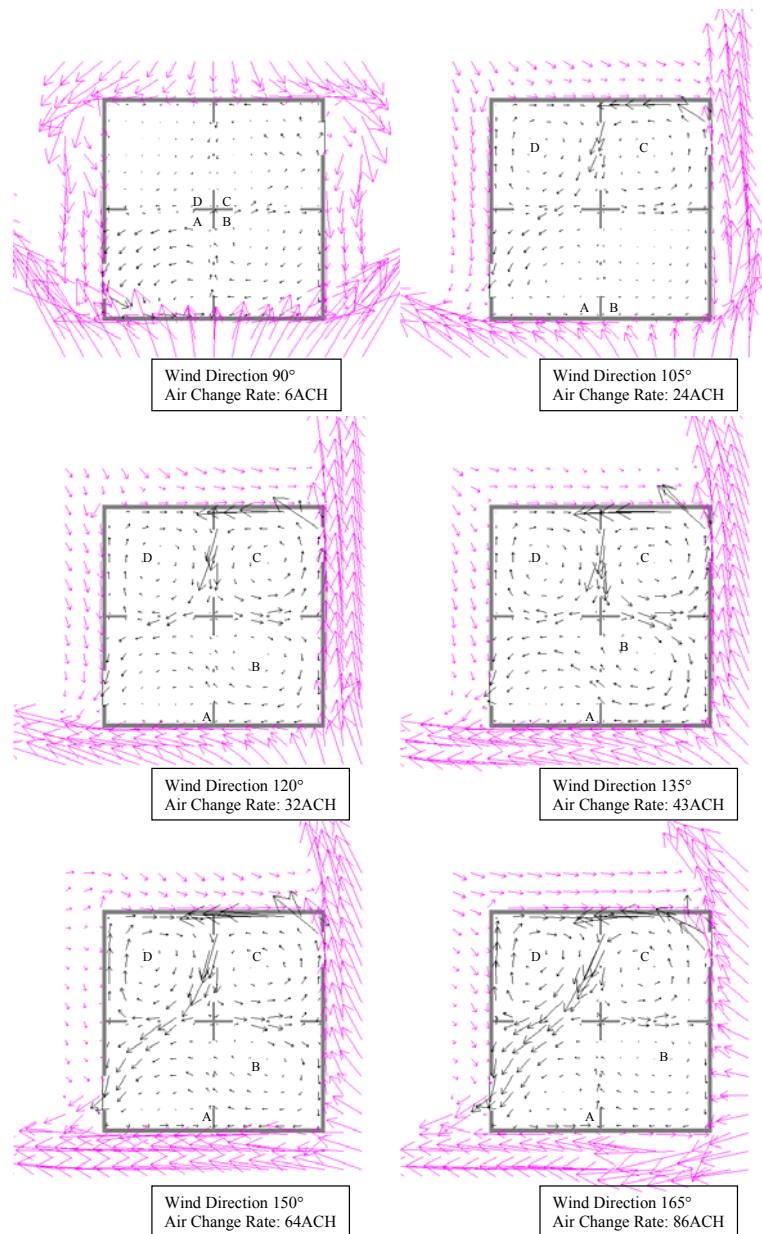


Figure 3 (continued). Airflow Distribution on Horizontal Plane at 1,190mm height.

of the wind tunnel). Measurements around the model were made at 1500 mm height above the floor of the wind tunnel. Opening A (Room A) is on the windward side for wind directions of 0-60° and 90°, and Opening B (Room C) is on the windward side for wind directions 75° and 105-165°.

At 15° wind direction the main current was found to flow at high air change rate through room B and up into room C. At 45°, the current collides with the pillar and walls at the centre of the model, and diverges into two separate flow paths giving moderate air change. In the case of 75° and 90°, the ventilation rate is relatively low, but there is still a

defined airflow pattern. In the case of 105-165°, the main current in room C flows along the surface, due to the Coanda effect, and there are circulating flows in Rooms B, C and D.

3.2 Velocity Vector on Horizontal Plane at the Six Measurement Heights

The airflow structure was examined in detail for each measurement height. Figure 4 shows the vector diagram for two cases (wind direction: 15° (left) and 165° (right)) for the horizontal planes at 50 mm, 230 mm, 710 mm, 1190 mm, 1670 mm and 2100 mm height above the floor.

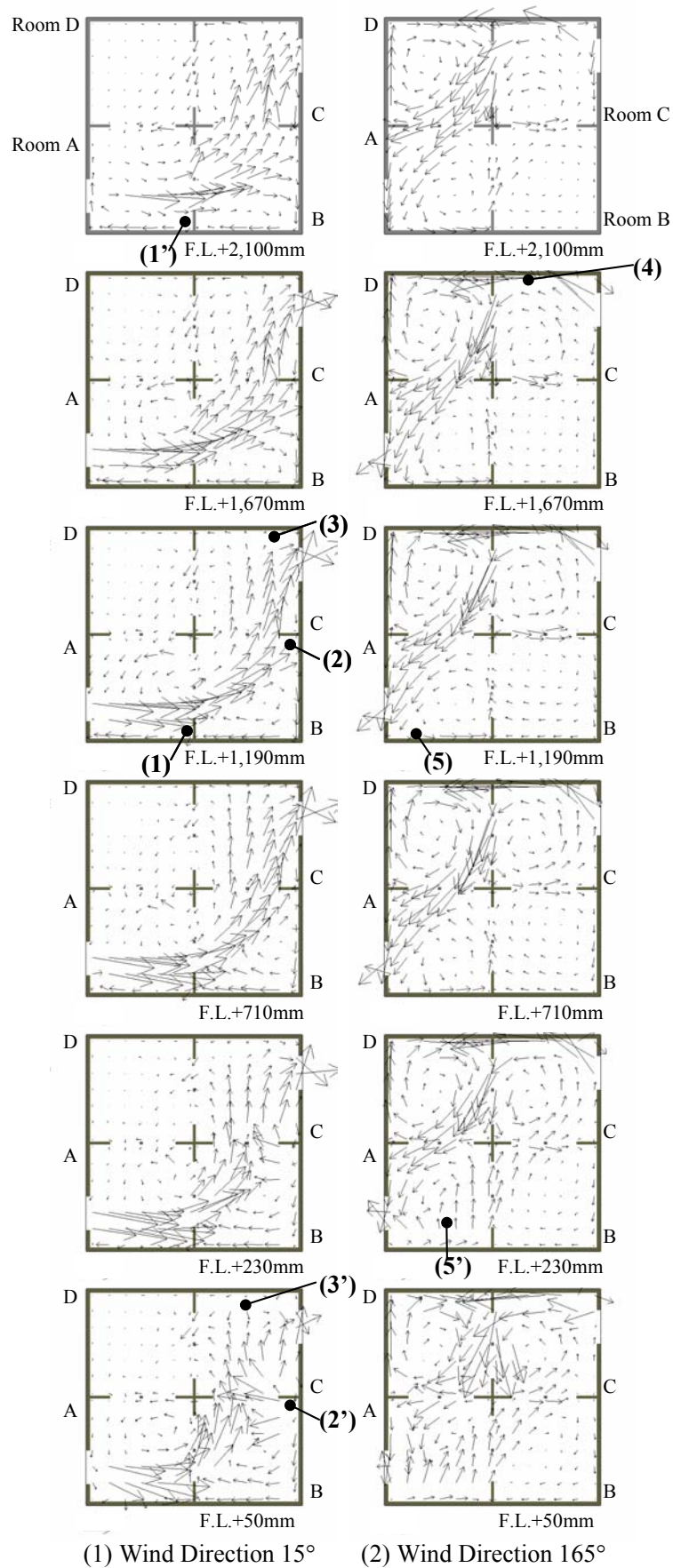


Figure 4. Horizontal indoor airflow distribution at the six measurement heights.

The main current path was through Room A→B→C for wind direction 15° and changes direction i.e. Room C→D→A for wind at 165°. After colliding with the obstacles (walls and sidewalls) and changing direction, the main current continues straight ahead because of inertia.

There are deflected flows near the wall and the sidewall (around the points 1-3 for a 15° wind and point 5 for a 165° wind). The deflected flows go over and/or under the main current after colliding with the walls at a large angle (around point 1', 3' for the 15° wind direction and 5' for the 165° wind

direction). In the case of wind at 165°, the rebounding flow at point 5' forms a returned flow in the top and bottom layer in the direction Room A→B→C. A return flow also appears slightly through Rooms C→D→A at a wind angle of 15°.

When the main current collides with walls at a small angle (relatively parallel to the surface), the air flows along the surface due to the Coanda effect (point 4 (165°)). Here circulating flows are formed next to the main current if there is sufficient space (Room A, C, D for wind at 165°).

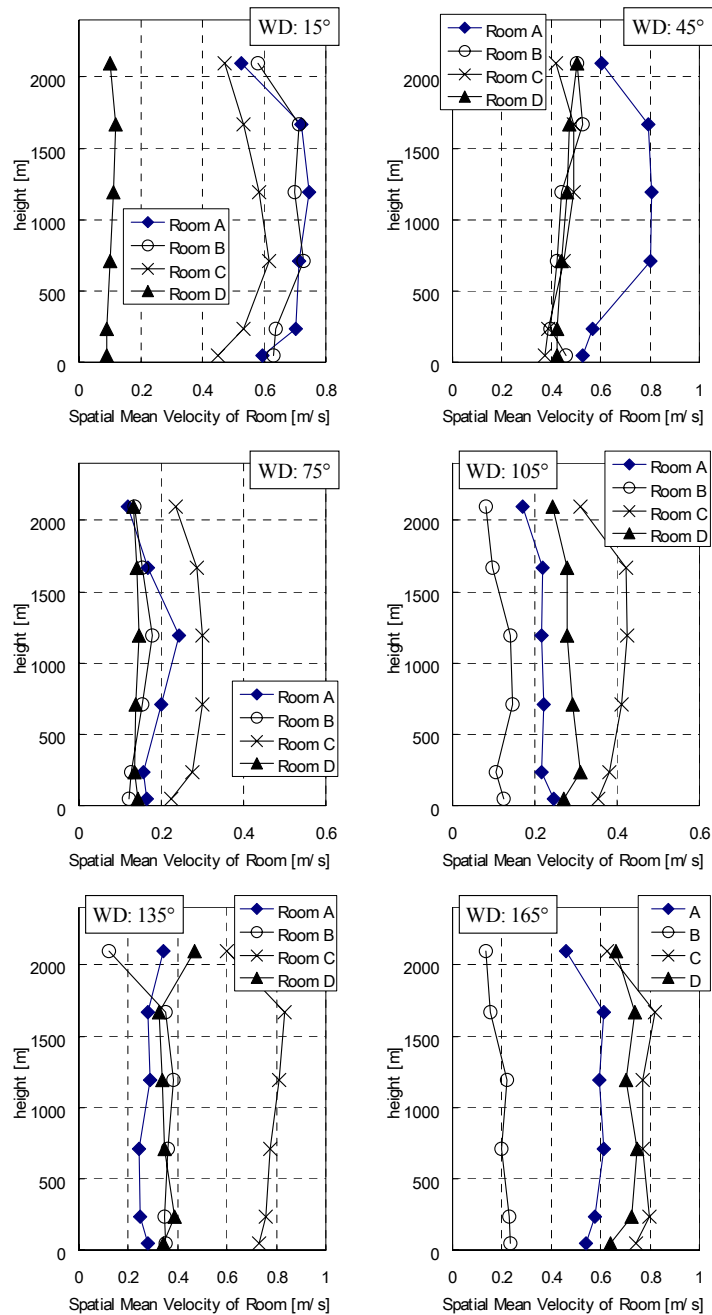


Figure 5. Spatial mean velocity of Room A-D at each height.

Hence these results show that the key factors for determining the airflow structure in cross-ventilated rooms are the main current region, changing direction, deflected flow, rebounding flow, surface flow and circulating flow.

3.3 Mean Velocity Profile at Each Height

The differences in vertical airflow profile for different wind directions are illustrated in Figure 5. These results are averaged for 49 points at each height in each room. There is no remarkable difference in the mean velocity profile in each room except at 2100 mm height which is higher than at the top opening. When the airflow velocity is compared for the four rooms the following three patterns were observed:

Pattern A:

At 15° and 165° wind directions one room (D and B respectively) has a much lower mean velocity than the remaining three.

Pattern B:

At 45°, 75° and 135° wind directions, one room has a higher value of the mean velocity than the remaining rooms (rooms A, C and C respectively).

Pattern C:

At 105° wind direction, each of the four rooms have different mean velocity profiles.

Similar results to pattern A were also observed for 0, 30, and 60° wind directions. For Pattern B the room with the inflow opening had the highest velocity and the main current was divided into small currents by striking pillars and walls. Similar results were found for the 120° wind direction. In the case of pattern C, the airflow mainly passed through one room after colliding with the pillars and walls.

3.4 Frequency Distribution of Mean Velocity

Figure 6 shows the frequency of the normalized mean velocity in each room. The normalized mean velocity was obtained from normalizing the average

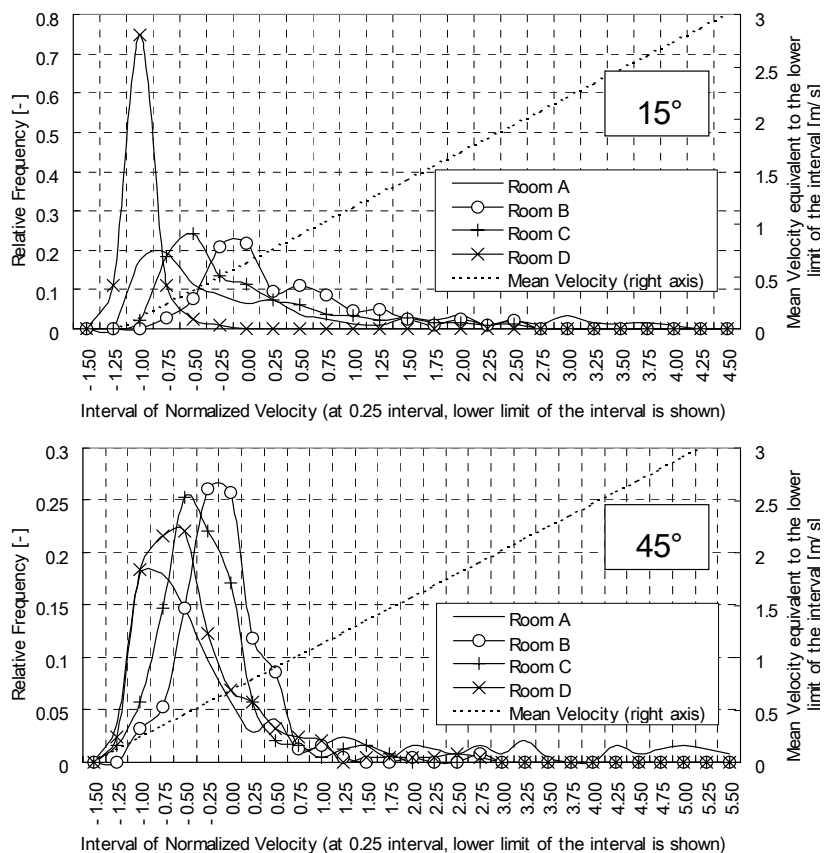


Figure 6 (part 1). Frequency of normalized mean velocity of Room A-D.

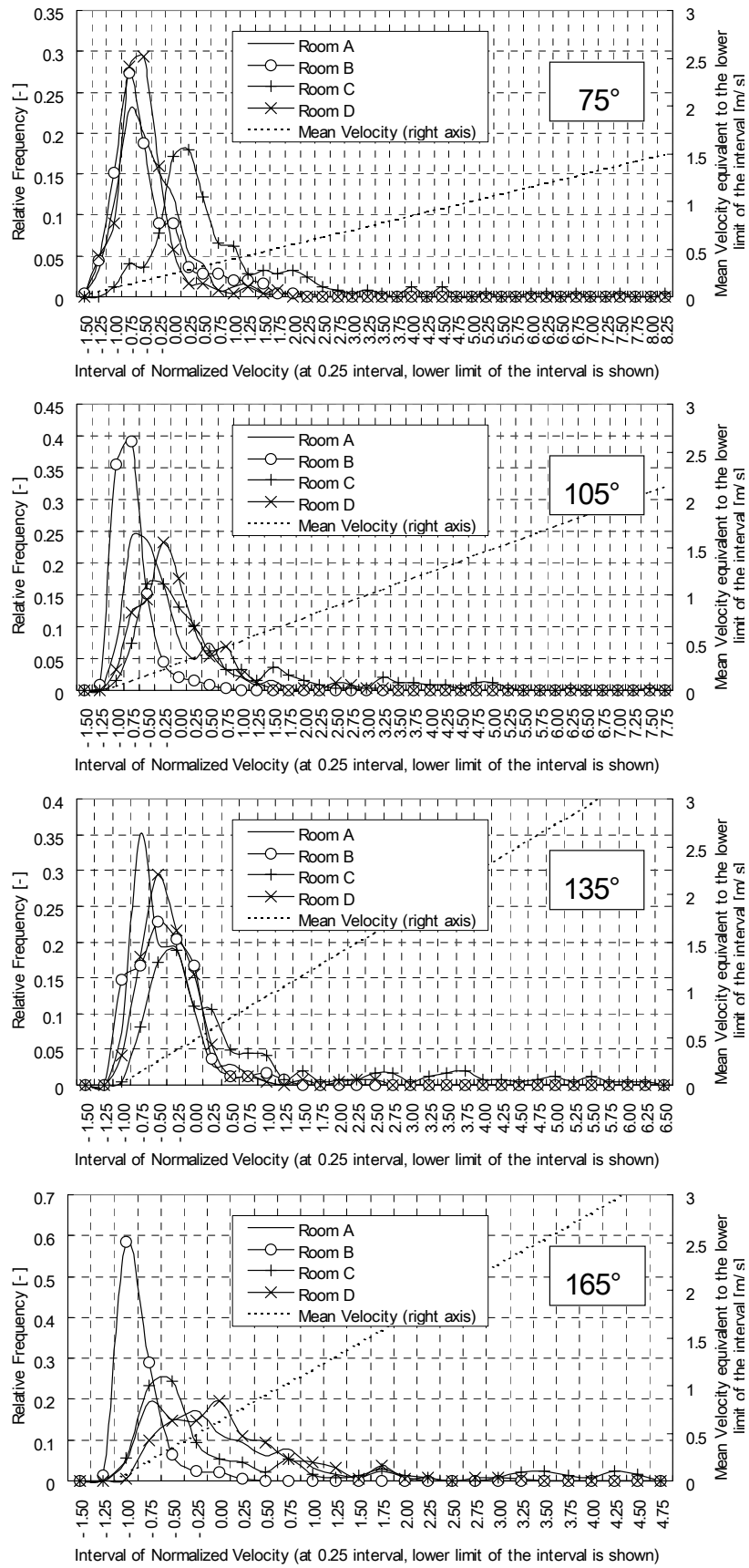


Figure 6 (continued). Frequency of normalized mean velocity of Room A-D.

value and the standard deviation of 980 measurement points at five heights (i.e. excluding the measurements at 50 mm height above the floor).

The highest air change rate was for a wind direction of 15°. For this wind direction the main current appears clearly and the room mean velocity is highest in Room A (i.e. the room with the inflow opening). However, the mode of the normalized velocity in Room A is smaller than in Rooms B and C. Room A has some low peaks in the high velocity class (in the velocity range between 1.5 - 3.0 m/s) and the peaks show high velocity points in the main current. In Room B, the mode is in the range of 0.5 - 0.6 m/s. This room has a larger area in the middle velocity range than observed for Room A, and has only a small area in the high velocity range. A similar tendency was also noted for Rooms C and D for the 165° wind direction.

In the case of the 45° wind direction, Room A had the smallest mode, but had some peaks in the high velocity range. Room B and C had a larger mode than Room A.

In the case of the 75° wind direction, the room mean velocity in the room with the inflow opening (Room C) was larger than the other three rooms and the mode of the velocity was also larger than in the other rooms. This trend was different from the cases of the 15° and 45° wind directions which had a relatively high ventilation rate.

In the case of wind directions giving low ventilation rates, the upstream room offered the greatest potential for achieving the sensation of cooling.

4. Conclusions

The airflow velocity field was measured in detail using a full-scale building model in a wind tunnel. The building model incorporated two openings positioned diagonally apart and the building was rotated in 15° increments between 0 and 165° to represent different wind directions. Conclusion are as follows:

- 1) Key factors in determining the airflow structure in a cross ventilated space are: the main current region, rebounding and changing direction, deflected flow, surface flow and circulating flow. The air current tends to continue in a straight line until it collides with obstacles. The flow then changes direction, and deflected flows

are formed over and/or under the main current. When there is sufficient space next to the main current region, circulating flow is formed in each room.

- 2) The room mean velocity is determined by the path of the air current. In rooms in which the main current appears clearly, the mean velocity is relatively low. When the main current is divided, the room containing the inflow opening has a relatively high velocity.
- 3) The mode of the mean velocity in the room with the inflow opening is lower than downstream rooms but has a higher velocity region in the main current.

The characteristics of ventilation in a cross-ventilated space are complex. This is because changes in outdoor wind direction and wind speed will considerably affect the flow pattern and air change rate in the space. Thus it is important to examine the properties of a cross ventilated space by wind tunnel experiments and making measurement in actual buildings.

References

- McCutchan G and Gaudill WW: (1952). "An experiment in architectural education through research", *Texas Engineering Experiment Station Research Report 32*.
- Sawachi T, Kiyota N and Kodama Y: (1999). "Airflow and wind pressure around a full-size cubical building model in a wind tunnel", *Proc. of the PLEA '99 conference*, 2, pp899-904.
- Sawachi T, Narita K, Kiyota N, Seto H, Nishizawa S and Ishikawa Y: (2004). "Wind pressure and air flow in a full-scale building model under cross ventilation". *The International Journal of Ventilation*, 2, (4), pp343-358.
- Nishizawa S, Sawachi T, Narita K, Seto H and Ishikawa Y: (2004). "Examination of the space with cross ventilation by tracer gas technique and zoning concept of the space with unevenness". *Roomvent 2004 Proceedings CD*.
- Nishizawa S, Sawachi T, Narita K, Seto H, Ishikawa Y and Goto T: (2005). "Experiment of the mixing property and the heat exhaust effect under cross ventilation in a full-scale building model". *26th AIVC Conference*, pp123-128.

Vent DisCourse: Development of Educational Material on Energy Efficient Ventilation of Buildings

M Kolokotroni¹, J Shilliday¹, M Liddament², M Santamouris³, I Farrou³, O Seppanen⁴,
R Brown⁵, J Parker⁵ and G Guarracino⁶

¹ Mechanical Engineering, School of Engineering and Design, Brunel University, UK

² VEETECH Ltd, 7a Barclays Venture Centre, Sir William Lyons Road, Coventry, UK

³ University of Athens, Building of Physics – 5, Applied Physics, Athens, Greece

⁴ Helsinki University of Technology, Finland

⁵ BSRIA, Bracknell, UK

⁶ ENTPE, LASH-DGCB, 69518 Vaulx en Velin, Cedex, France

Abstract

This paper is not a technical paper but, instead, focuses on the methods by which information on recent advances in ventilation technology and systems may be transferred to engineers. This is important because it enables the application of these innovations in the design and maintenance of buildings. In this context, the paper describes the educational material developed by the European project Vent DisCourse. It consists of material specifically written to facilitate distance learning postgraduate study in the area of energy efficient ventilation for buildings. Vent Discourse is mainly aimed at European building professionals to facilitate the implementation of the energy performance in buildings directive (EPBD). The method of development was based on a review and evaluation of educational distance learning methods for the target audience and their application to building ventilation. The contents were based on a study concerning the collection, evaluation and classification of existing information; available sources were identified and classified according to their usefulness for the education material. The paper then continues with a description of the methods used for developing the material and its contents. It was found that there is a great demand for distance learning training material suitable for industrial and educational training in relation to emerging issues in energy and buildings and the methods followed in this project might be useful for other areas.

Key words: ventilation, energy, training, distance learning, education, intelligent energy Europe programme, IEEA.

1. Introduction

The European Energy Performance of Buildings Directive (EPBD, 2007) is a legislative framework agreed by member states of the European Union concerning the overall energy performance of all types of buildings during design, major refurbishment and operation. It has been agreed that some parts of the EPBD must be implemented in national regulations by 2006 and implementation must continue until all elements are included. A core issue for an effective implementation is the training of building professionals on the design and operation of building systems for integral energy performance and also on energy sub-systems such as ventilation.

This paper describes such an initiative carried out by the project Vent DisCourse. This project addressed non-technological educational and cultural barriers

to the implementation of energy efficient ventilation in buildings. Efficient ventilation can increase comfort and quality of life in buildings in addition to a reduction of energy intensity and energy consumption. The degree of energy use can be determined to a large extent during the design (or major refurbishment) of a building. To this end, the market actors are not the actual users but the designers and operators of buildings. These actors are usually reluctant (mainly due to financial and job demand reasons) to devote a large percentage of their professional time to undertake additional training. However, they could always find some time to refresh their knowledge, especially if such knowledge would have a direct benefit in the carrying out of their job.

For this purpose distance learning methods, used extensively by educational establishments, could be used as opposed to whole day(s) seminars. Distance

learning methods could range from carefully structured textbooks to 3 to 4 dedicated pages that could appear in professional journals. This paper first describes the market requirements in the four participating countries in the project (Greece, UK, Finland and France), the availability of source material, and its classification for the purpose of this study. It continues with a description of the educational material developed.

2. Requirements, Market and Availability of Source Material

A review and evaluation of educational distance learning methods for the target audience and their application to building ventilation training material was carried out. It concluded that there is a need to improve the skills, competence and knowledge of professional engineers but time pressure and professional responsibilities comprise a barrier to continuing training. Distant learning material provides flexibility, independent studies, individualization, globalisation of the market, easy exchange of experience and adaptation to the new technology and legislation. A market study carried out indicated that the potential trainees are building designers (architects) and building services engineers. A study of all applicable distance learning methodologies was carried out and concluded that the following media are appropriate for the dissemination of knowledge on ventilation and its relevance to EPBD:

- *Textbook*. This is in the format of distance learning education delivery. The format is described in more detail in the following section and could be provided in the form of a hard copy or a CD-ROM.
- *Internet-based modules*. This was based on the WebCT platform for pilot training. However, it can be adapted to any teaching internet platform suitable for distance learning. The contents are based on the developed textbook and features of the platform are utilised to facilitate interaction between trainee and tutor and between trainees.
- *Continuing Professional Education articles (CPD)* These are suitable for publication in professional journals and include self assessment questions with solutions provided.

It was also observed that trainees would require the material in their national language for better understanding. It was therefore decided to translate

the developed material, which was written in English, into another language to investigate how this could be done in an accurate and time-efficient way.

In formulating this course a study concerning the collection, evaluation and classification of the necessary information to develop the distance learning training material was undertaken. Available sources were identified. Since this study was aimed at European engineers, a number of recently completed research and dissemination projects funded by the EU were identified including NatVent, STEVE, TipVent, AIOLOS, DUCT, URBVENT, SolVent and ECA. These describe new technological and legislative developments, industrial information, testing methods, predictive software and existing applications in buildings. Conclusions from international collaborative projects and recent developments in countries outside the EU were also investigated (such as IEA - ECBCS Annexes 35 and 27). Material published by the Air Infiltration and Ventilation Centre (AIVC) was consulted extensively. All this source information was evaluated and classified according to its usefulness for the education material. The resultant content was classified into the following nine categories:

1. Technological developments;
2. Industrial information;
3. Testing methods;
4. Predictive software;
5. Existing applications in buildings;
6. Case studies;
7. Developments linked to ventilation requirements e.g.:
 - 7.1 Protection of buildings (fire security, terrorism attacks),
 - 7.2 Air quality and health,
 - 7.3 Materials.
8. Critical barriers vs. ventilation systems;
9. Impact of double skin façade on ventilation system design.

Using the above classification, the educational material was developed and this is described in the following section.

3. Structure of the Developed Educational Material

The structure of the material was discussed and agreed by the authors during a two-day workshop. A number of educational and technical approaches were discussed and, based on the nature of the trainees (distance learning working building

professionals), the expertise of the project team and the source material available, it was decided to divide training into four main sections (called modules), plus two assisting modules as follows.

3.1 Foundation Module: Principles of Energy Efficient Building Ventilation

The foundation module is an introductory module to the distance learning material. It covers the basic engineering principles of ventilation necessary to complete the other modules. It would therefore be necessary only for trainees not familiar with ventilation theory and/or systems and components. The module covers the basic principles of ventilation including:

- The role of ventilation systems in the control of the indoor environment, air quality and thermal comfort;
- The influence of climate on the selection and operation of the ventilation system;
- Criteria that affect the selection of the ventilation flow rate including control parameters, the impact of human occupancy, indoor air pollutants and the heating and cooling load;
- The energy impact of ventilation;
- Psychrometry considering the properties of moist air and typical psychrometric processes used for mechanically cooling a building;
- Other aspects of the energy use of a mechanical or hybrid ventilation system including fan energy and duct losses.

3.2 Module 1: Natural and Hybrid Ventilation

This module outlines the development of natural and hybrid ventilation systems for buildings and introduces the basic definitions and equations. This is intended to enable the trainee to understand the concepts of natural and hybrid ventilation and the conditions under which natural and hybrid ventilation are applicable. Topics cover:

- Natural and hybrid ventilation configurations;
- The various components that are used to construct a natural and hybrid ventilation system including a discussion on the advantages and disadvantages of each component and identification of the most suitable components according to need;
- A mathematical description of the pressure and flow mechanisms;
- The incorporation of hybrid ventilation fans;
- Control systems.

Particular emphasis is given to basic calculation techniques and principles. This starts with the development of wind driven pressure across a building opening and how this pressure is influenced by shelter. The application of equations and data to approximate the value of wind pressure acting at an opening on the surface of a building is presented. The equation for buoyancy or stack driven flow pressure is then introduced. This shows how temperature difference creates a driving pressure across a building opening and how the pressure is influenced by the height difference between openings. Simple examples of how the buoyancy equation can be used to approximate the value of stack pressure acting at an opening on the surface of a building are presented.

The airflow induced by wind and stack action cannot be directly added together. Instead the pressures induced by each mechanism must be combined. This module describes the process in detail and then explains how the pressure across openings is altered by the inclusion of a hybrid ventilation fan.

Next, the method by which the overall pressure equations are formulated into an airflow equation is introduced. The trainee is provided with sufficient information to be able to undertake basic single-zone calculations and is provided with a background to multi-zone methods.

Finally the concept and significance of the variability of natural ventilation rate, as driving forces vary, is introduced. This is assessed in terms of resultant energy impact, cooling potential and ventilation needs. From this, decisions can be made about the need for the addition of mechanical systems or hybrid ventilation.

The outcome of this module is to present students with sufficient detail to perform basic natural and hybrid ventilation design solutions including assessing ventilation need, sizing openings, planning simple ventilation configurations and incorporating a hybrid fan.

3.3 Module 2: Ventilation for Urban Buildings

This module outlines the principles of natural and hybrid ventilation as it applies to urban buildings. Fundamental aspects include:

- Functions and control strategies of hybrid ventilation;
- The impact of the urban environment on natural and hybrid ventilation;

- Conditions under which the urban environment presents constraints on the use of natural and hybrid ventilation.

Particular guidance is given on developing strategies that enhance the use of natural and hybrid ventilation in urban buildings. This includes the application of pressure and flow equations to calculate airflows for different ventilation strategies when increasing the buoyancy stack pressure. Emphasis is also given to the evaluation of the natural and hybrid ventilation potential in urban environments. This covers assessing the impact of natural ventilation on IAQ according to the concentration of external pollutants, and determining the potential of night ventilation for cooling urban buildings. The role of hybrid ventilation systems for urban areas is also presented.

Calculation techniques are developed that assist in optimising opening sizes for naturally ventilated buildings located in urban canyons. Particular use is made of guidelines drawn from experimental data. The module concludes with recommendations for the use of natural and hybrid ventilation systems in urban buildings and the trainee should be able to suggest design solutions for the use of natural or hybrid ventilation systems in urban canyons considering different ventilation parameters.

3.4 Module 3: Energy Efficient Mechanical Ventilation

This module introduces the principles of mechanical ventilation. Primary topics include:

- Setting targets for indoor air quality;
- Improving air quality and energy efficiency by optimising airflows and flow directions;
- Direct and recirculation systems;
- Heat recovery;
- Room air distribution;
- Displacement vs mixed mode systems;
- Air cleaning (filtration);
- Mechanical ventilation controls.

Particular emphasis is devoted to system types and the methods needed to achieve good air quality and energy efficient control. An assessment is made of source strength and ventilation dilution principles. The application of pressure differences created by mechanical ventilation to control the pollution transfer into building and also between different indoor spaces is presented.

The roles of mechanical ventilation in dwellings and in non residential buildings are separately discussed. In the case of dwellings aspects include achieving optimum ventilation, demand control, avoiding the spread of pollutants from contaminating areas to living areas, heat recovery ventilation and the importance of airtightness to minimise air infiltration and resultant uncontrolled air change. Consideration is also given to using ventilation to avoid moisture and condensation problems. Particular design solutions for single family and multi-family residential buildings are described.

In the case of non-residential buildings the determination of ventilation rates according to actual pollution load is introduced. Calculation methods for determining energy use for heating and cooling depending on airflow and temperature (enthalpy) differences are presented. Other processes described include large scale demand control, controlling pollutant spread and minimising ventilation need by using the concepts of ventilation efficiency. The integration of mechanical ventilation with air-conditioning is also described. This covers techniques for minimising cooling energy and applying heat recovery.

Comprehensive design details are given covering fans, ducts, air handling units, heat recovery units and filters. This provides information on pressure losses, leakages and achieving optimum solutions. The importance of commissioning, including the balancing of flows, is described. Other aspects cover duct cleanliness, the insulation of ducts, and methods to minimise duct losses through sizing and component design.

By studying this module the trainee should be able to understand mechanical systems and be able to: calculate the system power and energy demands; identify the factors affecting the pressure requirements; select a fan for a specific purpose; understand the differences between static and dynamic pressure and conversion from one to the other; calculate the energy use and control of air flow (speed control vs. throttling control); calculate the specific power of a fan and identify its maximum allowable values; understand proper installation principles; identify the factors affecting energy efficiency; understand the principles for locating the air intakes to reduce cooling needs and pollutant concentrations in the ventilation air; and finally to understand filtration systems and select filters according to need.

3.5 Module 4: Assessment of Building Ventilation

This module considers the need for measurements in assessing building ventilation and methods for measuring ventilation parameters. Aspects include:

- Instrument types;
- Techniques;
- Factors influencing accuracy and uncertainty.

Of particular importance is the assessment of ventilation rate and comfort. This begins by looking at the reasons for airtight buildings and ductwork. It also presents details on the measurement of air change rate and ventilation effectiveness using tracer gas methods, pressurisation and pollutant monitoring methods.

A significant section of the module is devoted to the methods used to commission and balance ventilation systems. This includes the commissioning and testing of all components including air handling units, diffusers, controls and sensors. The importance of the appropriate positioning of measurement sensors is also described.

This is followed by details of ongoing operation and maintenance needs covering procedures to ensure that the system is regularly maintained and continues to operate at optimum efficiency. Issues cover the regular replacement of components (e.g. filters) and the detection of faults.

The module concludes with a chapter on design and construction issues. This is important because any ventilation system must be integrated within the overall structure of the building. With this chapter the trainee should be aware of some of the practical issues associated with the design and construction of ventilation systems including fire safety, mechanical support, noise attenuation, weather rejection and corrosion.

3.6 Common Resource Module

A resource module completes the course. This includes chapters on computerised tools and case studies for use as support material to illustrate points studied in the preceding modules. Information in this module covers a description of the inputs, applications and limitations of ventilation models. It also includes two worked examples of computerised tools to illustrate the development of a working ventilation model. The case studies are drawn from the projects NatVent and HybVent.

4. Method of Developing and Testing the Training Material

In order to address the needs of distance learning students the following principles were followed in developing each module.

Each module is divided into sections that the students can absorb in one session (for example 2-3 hours of study). Therefore each chapter is approximately 10-12 pages long to include the following elements:

1. Chapter objectives – so students are aware of the goals to be achieved by studying this specific section.
2. Introduction to the section.
3. 4 to 5 sub-sections, each with some illustrations in the form of pictures or graphs and with a number of self-assessment questions.
4. The self-assessment questions, which the students should attempt, are designed to revise the material learnt in the sub-section. Solutions to the personal feedback questions should be provided separately so that the students can instantly check their workings.
5. More complicated sub-sections, which contain key or difficult to understand principles, include worked examples so that the students have a similar solution before they attempt the corresponding personal feedback question.
6. Each section includes a summary at the end to highlight the key elements learnt while studying it.

Two assessment exercises were developed. The first tests knowledge of modules 1 and 2 and comprises a design exercise for a notional building to follow natural and hybrid ventilation strategies. The notional building could be placed in a rural or urban site and trainees are asked to recommend suitable solutions. Material from the common resource module can be used to carry out this assignment. The second assignment tests knowledge of modules 3 and 4 and takes the form of an open book examination where trainees are asked to solve problems similar to the ones contained in the material. They are also asked to write a report for a building owner who would like to investigate some ventilation problems in his building.

The first version of the educational material was developed by the authors as described above. A

number of European experts on ventilation commented on this first draft of the material and their comments were incorporated in a second version. This version was tested by students in six universities (Brunel, Helsinki, Athens, LaRochelle, ENTPE, Prague) using distance learning principles and utilising the WebCT platform to facilitate delivery. Comments from students were implemented in the final version of the material. The material was translated into another European language (Finnish) to further training opportunities. This translation was carried out by ventilation experts and can be used as a demonstration on how it could be achieved so that translation into other languages can be achieved more easily.

5. Contents of Short Educational Articles

In addition to the material developed for postgraduate professionals, four short articles were developed on specific topics for wider dissemination. The topics were chosen because there were indications that they would be of interest to engineers or because they cover the results of recent research activities. The articles were firstly written in English and published in the REHVA journal and they are also being translated into another three languages (French, Greek and Italian) to provide further opportunities for dissemination in national professional journals. The articles cover the topics described below.

5.1 Displacement Ventilation in Non-industrial Premises

This article (Skistad, 2006) gives a brief description of displacement ventilation as used in non-industrial premises. The main advantage of displacement ventilation is that it can provide better air quality in the occupied zones than mixing ventilation. The system is best suited for meeting rooms and other premises where air quality is the main objective. When the main objective is cooling and temperature control, as in most office spaces, other systems may be more advantageous. The article is based on REHVA Guidebook no.1: "Displacement Ventilation in Non-industrial Premises" (Skistad et al, 2002).

5.2 Performance of Natural Ventilation in the Urban Environment

This article (Farrou and Santamouris, 2006) focuses on the performance of natural ventilation in the urban environment as this can be seriously reduced by urban-specific characteristics. The main

constraints to natural ventilation in the urban context are reduced wind speeds, high ambient temperatures due to the heat loads from the buildings and traffic (island effect), increased external pollutants and increased noise levels. This article evaluates the potential application of natural ventilation in urban buildings based on the results of theoretical and experimental research that was carried out in real urban environments. Additionally, alternative ventilation strategies are described that can be used to enhance airflows in naturally ventilated buildings in urban areas.

5.3 Energy Impact of Ventilation

This article (Liddament, 2006) focuses on the energy impact of ventilation. In energy efficient buildings the energy impact of ventilation can account for 50% of total energy dissipation. Therefore understanding this energy impact is vital for proper resource management. This article provides simple guidance on calculating ventilation related energy losses for both heating and cooling conditions. The method is based on a technique developed by Colliver (1995).

5.4 Assessment of Ventilation and Comfort

This article (Brown, 2006) briefly discusses the relationship between design, commissioning and control of building ventilation systems to achieve an optimal balance of comfort and energy performance. It then describes the practical measurement of ventilation and comfort parameters that will assist in "tuning" the building systems to meet the needs and expectations of the occupants.

6. Conclusions and Lessons Learnt

This paper has described the method of developing distance learning educational material dedicated to energy efficient ventilation. The material has been produced in formats suitable for Masters level training (distance learning textbook and implementation to an education internet platform) and distance learning continuing professional education (CPD articles in professional journals).

The educational material was tested by European experts, evaluation workshops, and pilot distance learning courses. The feasibility of translating this material into other languages was demonstrated by translating both the distance learning textbook and the CPD articles.

During the development of the material the following were concluded:

- There is a great demand for distance learning training material suitable for industrial and educational training in relation to emerging issues in energy and buildings.
- The benefits of an international group of authors preparing the text are great – this is an important way to promote good technologies between European and other countries.
- The format should be flexible to leave a certain amount of freedom to training providers to suit the needs of target trainees.
- Textbook (print version) is the preferred method of learning for university students and industrial trainees alike. The web-based facility is preferred for selective release items such as question answers or assignments and for interactive contact with other students and/or trainer.
- Harmonisation of typically used terms and symbols in different countries and regions should be addressed early on in the development of any training material.

The main contribution of Vent DisCourse is targeted knowledge transfer to appropriate actors supported by employers and professional institutions. This has been achieved during the project through the publication of short training articles in the REHVA journal and the up-take of the pilot training by six universities. By the completion of the project and the availability of translated material, it is believed that thousands of engineers can be trained in the next few years. The project indicated a methodology of how recent research advances in a building services related topic could be developed into educational material so that rapid market penetration can be achieved through the education of recent graduates and more experienced professionals.

More information about the project and results can be found in: <http://dea.brunel.ac.uk/ventdiscourse>.

Acknowledgements

We are grateful to Johnny Anderson, Peter Warren, Jorma Railio and Nick Cullen for reading and commenting on the material. Also, to K Kabele and F Allard for their willingness to test the material within their universities and comments received. This project was co-financed by the Intelligent Energy – Europe Programme (IEEA). The sole responsibility for the content of this article lies with the authors. It does not represent the opinion of the Community. The European Commission is not responsible for any use that may be made of the information contained therein.

References

- Brown R: (2006) “Assessment of Ventilation and Comfort”, *REHVA Journal*, (www.rehva.com).
- Colliver D: (1995) “Energy requirements for the conditioning of ventilation air”. *AIVC Tech Note 47*.
- EPBD, Buildings Platform: Information resource on the Energy Performance of Buildings Directive <http://www.buildingsplatform.org/cms/>.
- Farrou I and Santamouris M: (2006), “Performance of Natural Ventilation in the Urban Environment”, *REHVA Journal*, (www.rehva.com).
- HybVent, Hybrid Ventilation, IEA - ECBCS Annex 35 <http://hybvent.civil.auc.dk>.
- Liddament M: (2006), “Energy Impact of Ventilation”, *REHVA Journal*, (www.rehva.com).
- NatVent, “Overcoming technical barriers to low-energy natural ventilation in office type buildings in moderate and cold climates” <http://projects.bre.co.uk/natvent/index.html>.
- Skistad H: (2006), “Displacement ventilation in non-industrial premises” *REHVA Journal*, (www.rehva.com).
- Skistad H (Ed), Mundt E, Nielsen PV, Hagstrom K and Railio J: (2002), “Displacement Ventilation in Non-industrial Premise”, Guidebook 1, REHVA, (www.rehva.com).

Application of the PHACES Tool in the Design of Natural Ventilation for Passive Cooling

M. El Mankibi and P. Michel

ENTPE DGCB LASH, 3 rue Maurice Audin, 69518 Vaulx en Velin Cedex, France

Abstract

Natural ventilation associated with shading techniques is an alternative way to reduce the use of expensive and environmentally harmful active systems, while providing summer thermal comfort and good indoor air quality. However, there is still a lack of knowledge concerning the design of such systems. The tool presented in this paper provides guidelines on natural ventilation and shading control strategies.

This tool (called PHACES) has been developed under the MATLAB/SIMULINK environment by modelling an experimental device (HYBCELL) designed at the LASH/ENTPE laboratory. The thermal model used is based on finite difference methods and the airflow model is based on pressure analysis. Several control strategies for shading and ventilating based on temperature, CO₂, occupancy, outdoor solar radiation and time have been implemented in PHACES. Simulations carried out using this tool revealed the key role of the tuning process in order to adapt control parameters such as set points and dead bands to the building and climate.

Key words: education, training, comfort, energy efficiency, control, natural ventilation, passive cooling.

1. Introduction

Widely held studies on natural ventilation and passive cooling systems design have been focussed on architectural and climatic elements of success such as the identification of prevailing wind, strategic orientation, size and position of opening on the building etc. Critical barriers to the application of natural ventilation have also been hugely investigated in order to ensure an efficient use of passive ventilation (Allard 1998).

However there is still a lack of knowledge concerning the design and the tuning of control strategies for natural ventilation. Indeed, studies held in this field of research are usually confronted with the problem of the control strategy implementation while the complexity of such a system depends on the purpose of the installed natural ventilation system (Michel and El Mankibi 2000). Thus, other constraints and parameters have to be taken into account as soon as possible in the design of the building. These include: indoor air quality, noise, occupancy, physical phenomena, climate, ventilation configuration, maintenance, control parameters, sensors and actuators.

This study presents a design tool for passive cooling developed at the LASH/ENTPE laboratory. The aim of this tool, called PHACES, is to offer valuable information for a better knowledge of passive cooling and natural ventilation. This tool has been largely used to familiarize ENTPE students with control techniques and allows users to perform simulations in order to tune control strategies for passive cooling.

2. The PHACES Tool

PHACES (Figure 1) was developed at the laboratory of building sciences ENTPE/DGCB/LASH in the framework of the PHACES project. This tool is described in detail by Michel and El Mankibi (2005). The purpose of this project was to carry out a comparative analysis of control strategies in different configurations and to underline and quantify the relative impact of the various parameters influencing passive cooling efficiency. The PHACES tool allows comparative analysis of control strategies in order to:

- Identify optimal control architecture for passive cooling;

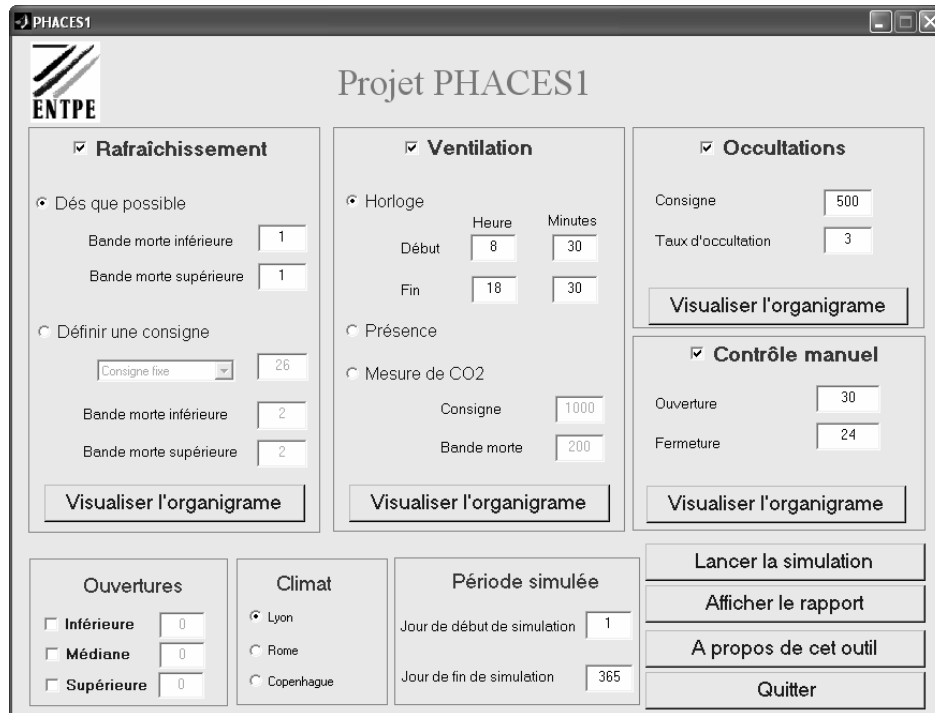


Figure 1. The main window of PHACES.

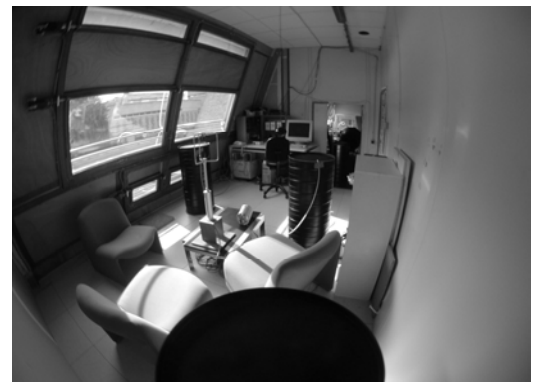
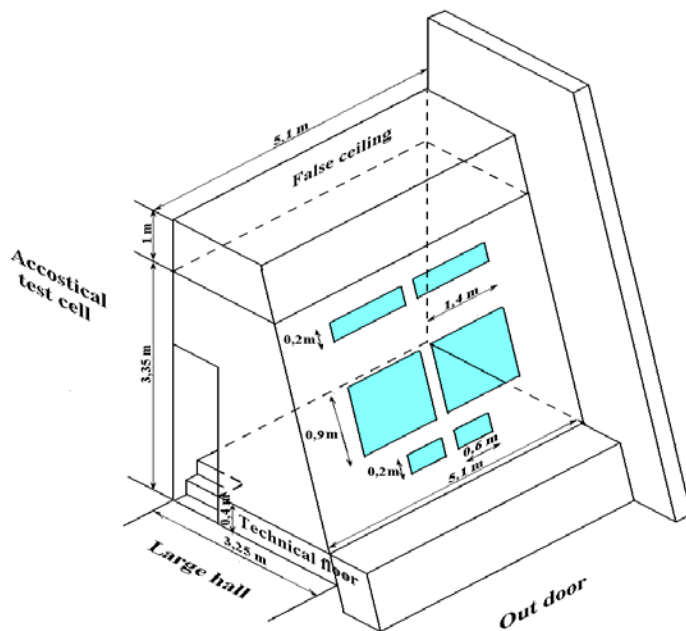


Figure 2. HYBCELL test cell architecture and equipment.

- Qualify the relative impact of control parameters;
- Generate guidelines on control strategies for passive cooling.

PHACES is an interactive tool that enables simulations by coupling a single-zone dynamic model, based on finite differences, and a pressure airflow model using the ‘onion’ approach, (El Mankibi 2003; El Mankibi et al 2006). This tool has been developed under the Mathworks MATLAB/SIMULINK environment, and several control strategies for passive cooling, based on temperature and CO₂, have been implemented. Schedule and occupation patterns were also taken into account in this model. Considerable possibilities were given to the user to adjust parameters for the simulations. Thus, the user can select climate (Rome, Lyon or Copenhagen), controllers (four levels of complexity) and different set-points and dead bands.

This tool has been used and evaluated by three generations of ENTPE students. Tests consisted of running simulations for a full week and the user has been offered the possibility to monitor various types of parameters and possibly modify manually some of them during the simulation. This tool also offers the possibility to display and to save information and a history of each simulation. Figure 1 shows the main window through which the user can access the different possibilities of PHACES. The main

window of PHACES also provides information on the selected strategies.

3. Building and Ventilation System

The building for which simulations are performed in this software is an experimental test cell called HYBCELL (El Mankibi et al 2001). In order to represent a large office or a meeting room, HYBCELL was created by totally retrofitting an enclosed area within a large hall whose temperature can be controlled to create an artificial climate around the test cell. The front of the cell consists of a sloped wall (70°) which communicates with the outdoor climate through six sash windows. The test cell is 5.1 m long by 3.5 m wide and it is 2.9 m high. The false ceiling and all walls are made of office building materials. The HYBCELL façade is equipped with two series of three openings controlled by actuators to ensure natural ventilation (see Figure 2).

4. Control Strategies

Various control strategies have been designed, whose purpose was to provide good thermal comfort and acceptable indoor air quality for the lowest energy consumption and maintenance cost. These strategies were implemented in the PHACES tool for the numerical evaluation of their performance after a tuning phase. These strategies focused on the control

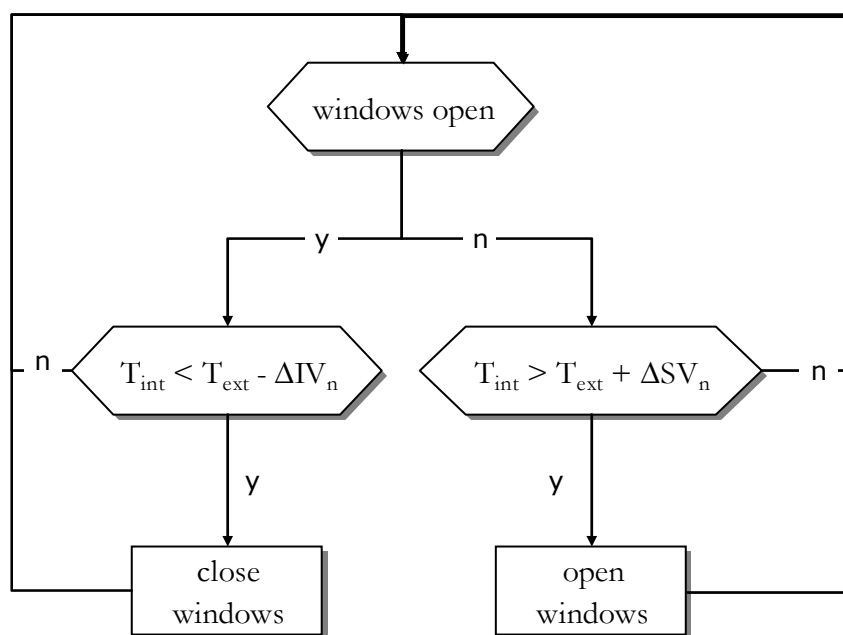


Figure 3. Basic passive cooling.

of façade components, i.e. windows and shading devices. Below are presented four different types of strategy, with particular interest in their robustness.

4.1 Basic Passive Cooling

This strategy uses natural ventilation as soon as the cooling power of the outside air exists, through an On-Off controller with a ΔSV_n (upper) - ΔIV_n (lower) dead band (see Figure 3):

- Start with windows open. If the temperature of the indoor air (T_{int}) is lower than the temperature of the outside air (T_{ext}), including a lower dead band ΔIV_n , the windows are closed;
- Start with Windows closed. If the temperature of the indoor air (T_{int}) is greater than the temperature of the outside air (T_{ext}), including an upper dead band ΔSV_n , the windows are opened.

4.2 Controlled Passive Cooling

Controlled passive strategies are On-Off controllers based both on cooling power (type A) and cooling needs, introducing a second ΔSR_p (upper) - ΔIR_p (lower) dead band (see Figure 4).

- Start with windows open. If the temperature of the indoor air (T_{int}) is lower than a set-point temperature T_c , including a lower dead band ΔIR_p , the windows are closed in order to avoid discomfort due to cold;
- Start with windows closed. If the temperature of the indoor air (T_{int}) is greater than a set-point temperature T_c , including an upper dead band ΔSR_p , the windows are opened in order to use the cooling power of the outside air and avoid overheating.

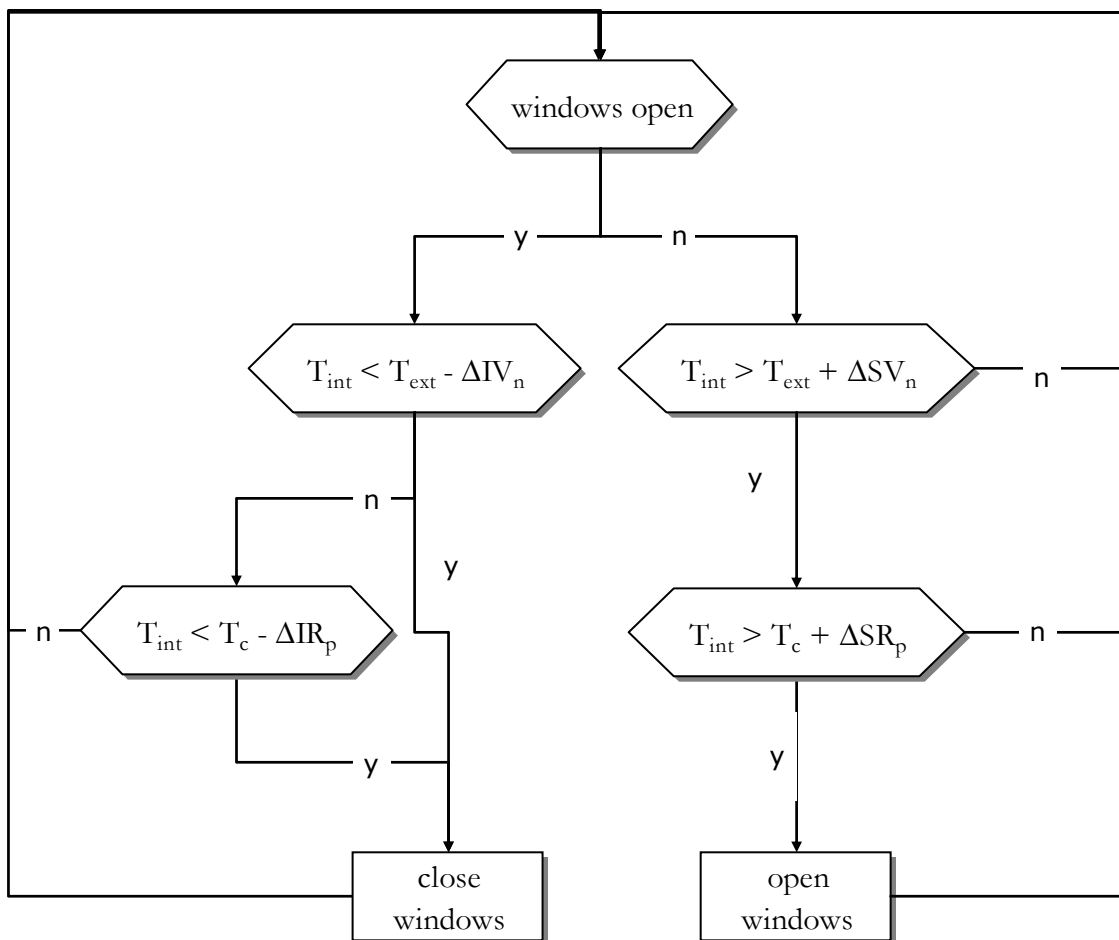


Figure 4. Controlled passive cooling.

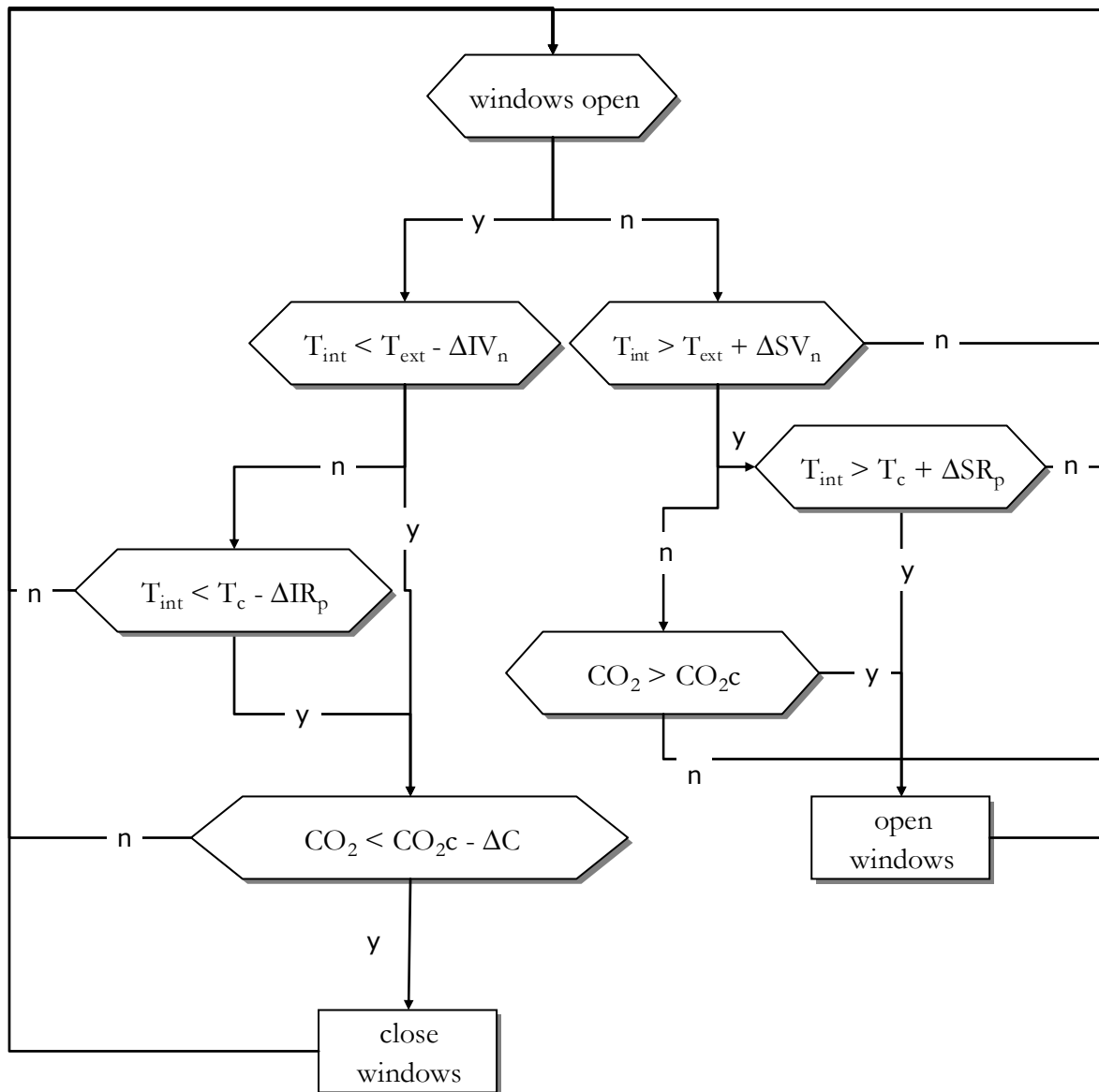


Figure 5. Advanced passive cooling.

4.3 Advanced Passive Cooling

Simulated strategies at this level are based on controlled passive cooling strategies introducing supplementary control for indoor air quality using time control, occupancy sensor or CO₂ sensor. Figure 5 illustrates a strategy including the control of indoor air quality.

- Start with windows open. If the CO₂ concentration is lower than a set-point concentration CO_{2c}, including a dead band ΔC, windows are closed in order to avoid cold discomfort while the indoor air quality is considered to be good.

- Start with windows closed. If the CO₂ concentration is higher than a set-point concentration CO_{2c}, the windows are opened to avoid heat discomfort only if passive cooling is required and if the cooling power of the outside air is available.

4.4 Global Passive Cooling

The most complex of the control strategies developed combines indoor air quality control during occupation and passive cooling control during unoccupied periods, using natural, assisted or mechanical ventilation, and based on On-Off or PI control. Figure 6 illustrates an example of such a

strategy including both manual and automatic controls. This strategy includes the same tests and the same parameters as the previous ones. Moreover, in order to prevent inadequate actions, automatic control is considered as impossible as soon as manual control is implemented by occupants and during a defined "no-action" time period. Afterwards and for the same reason, as soon

as automatic control is available again, manual control is considered as unavailable during a defined "no-action" time period. It is considered that occupants open windows if indoor temperature is above a set-point T_{open} temperature, and close them if the indoor temperature is below a set-point T_{close} temperature.

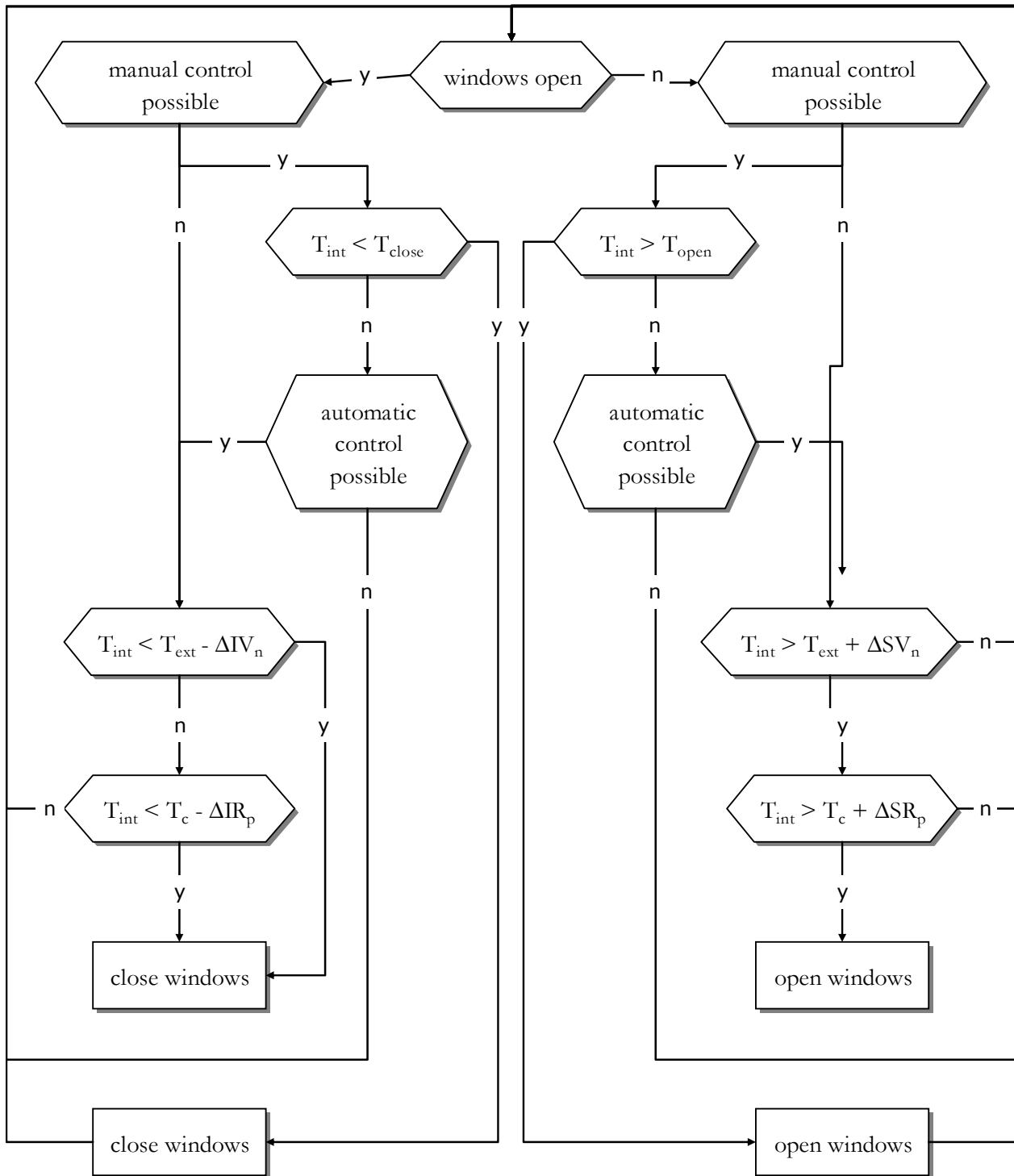


Figure 6. Global passive cooling.

Table 1. Lessons learnt.

| Strategy | Climate | Control parameters | Ventilation system | Occupancy management |
|---------------------------------------|--|---|----------------------------------|---------------------------------|
| A : Basic passive cooling | Cold discomfort. IAQ problems. Instabilities. | Low influence for thermal comfort. Instabilities. | High influence | Not tested |
| B : Controlled passive cooling | Cold discomfort reduced. Hot discomfort. Instabilities. IAQ problem. | Influence depends on climate and level of temperature set up. | Sensible Influence | Not tested |
| C : Advanced passive cooling | Risk of cold & hot discomfort. | Influence depends on climate and level of temperature set up. | Less influence for instabilities | Less instabilities and good IAQ |
| D : Global passive cooling | Risk of cold & hot discomfort. More instabilities. | Influence depends on climate and level of temperature set up. | Variable influence | Variable influence |

5. Lessons Learnt

The performances of the control strategies described above vary according to their degree of complexity, the number of control parameters taken into consideration and the aims they seek to achieve (i.e. simple cooling, controlled cooling, cooling and air quality). Other aspects have also been included in some of the developed control strategies, such as manual control, shading control and occupancy management.

Several simulations were carried out in order to evaluate the relative performance of the developed control strategies and to test their reaction to environmental variables and control parameters. The assessment process is based on thermal comfort, air quality and control stability.

The results obtained enabled the limits and advantages of each control strategy to be characterised. The observed thermal and airflow phenomena allow us to:

- Define the appropriate control strategies for each type of climate;

- Define the initial parameters for each control strategy;
- Anticipate the negative effects of the integration of other controllers (complex control strategy developed combines indoor air quality control during occupation and passive cooling).

Table 1 presents a synthesis of the lessons learnt from the simulations carried out.

6. Conclusion

The educational tool on passive cooling, PHACES, has been developed in order to generate guidelines on passive cooling strategies implementation and tuning. The potential users of this software are students, architects, engineers, teachers, building managers, planners and any other professional involved in building design.

Simulations carried out by engineering students within the framework of the ENTPE pedagogical programme have shown the possibilities of PHACES in optimising passive cooling by managing cooling potential, defining thermal

demand, defining the configuration of openings and taking into account solar shading.

PHACES can also be used to improve IAQ, reduce noise and prevent local discomforts while reducing instabilities and costs.

Examples of the use of this tool in passive cooling design have been demonstrated in this paper.

This tool has been largely appreciated and has contributed to a good understanding of the natural ventilation system process. Other numerical and experimental tools intended to teach natural ventilation techniques and advanced control strategies based on fuzzy logic control have also been combined with PHACES in order to initiate students in a global management of the building. Evaluation copies of PHACES are available from the authors.

References

Allard F and Santamouris M (Ed): (1998). "Natural ventilation in building", James & James, London

El Mankibi M: (2003). "Developpement et evaluation numérique et expérimentale de strategies de la ventilation hybride". Phd, INSA de Lyon, Lyon, France.

El Mankibi M, Michel P and Garracino G: (2001). "Control strategies for hybrid ventilation: development of an experimental device". *Proceeding of the 22nd Annual AIVC Conference, Bath, UK.*

El Mankibi M, Cron F, Michel P and Inard C: (2006). "Prediction of hybrid ventilation performance using two simulation tools". *Solar Energy*, **80**, (8), pp908-926.

Michel P and EL Mankibi M: (2000). "Advanced control strategies for hybrid ventilation", *Technical report, IEA-Hybvent project.*

Michel P and El Mankibi M: (2005). "Comparative analysis of control strategies for passive cooling", *Proceeding of Palenc, Santorini.*

Exergy Analysis as an Assessment Tool of Heat Recovery of Dwelling Ventilation Systems

P. Sakulpipatsin, E.C. Boelman and J.J.M. Cauberg

Climate Design Group, Building Technology, Faculty of Architecture, Delft University of Technology,
PO Box 5043, 2600 GA Delft, the Netherlands

Abstract

This paper presents steady-state energy and exergy analyses for dwelling ventilation with and without air-to-air heat recovery, and discusses the relative influence of heat and electricity on the exergy demand by ventilation airflows. Energy and exergy analysis results for De Bilt, NL, are presented in terms of heat and electricity use, on an instantaneous and a daily basis. The amount of electricity input to fans and the heat recovery unit (HRU) is much more significant in terms of exergy than of energy, due to the higher exergy value of electricity. From an exergy viewpoint, it could make sense to use the HRU only when environmental air temperature is low enough to compensate the additional need for electricity. When the air temperature is not too low, electricity input could be decreased by letting ventilation air bypass the HRU or by operating the HRU at low ventilation airflow rate, depending on outdoor temperatures and indoor occupancy conditions.

Key words: exergy, heat recovery, ventilation, winter, buildings, dwellings.

1. Introduction

In cold and moderate climates, improvements in building shell insulation and air-tightness imply a shift in heating loads from transmission and infiltration needs towards ventilation. Thus heat recovery from ventilation airflow plays an increasingly important role in minimising energy needs. Such heat recovery systems rely on the input of electric power (to drive fans, heat pumps, etc.) in order to recover thermal energy. Since the electricity input is relatively small compared to the amounts of thermal energy recovered, such systems are efficient from an energy viewpoint. One important yet often overlooked aspect, however, is the difference in 'quality' or 'exergy' between the high-grade electricity input and the lower grade thermal energy recovered. This paper analyzes the effectiveness of heat recovery from ventilation airflows from the viewpoint of exergy. The results provide a common basis for evaluating different forms of energy, considering their different abilities to produce work in relation to a given environment.

Exergy analysis provides a common basis for evaluating systems using heat and electricity, considering their different abilities to produce work in relation to a given environment (Boelman 2002; Wall 1990; Rosen and Dincer 2001; Ala-Juusela (ed.) 2004). Exergy can be defined as a measure of

the 'quality' of energy or the amount of work that can be obtained from the amount of energy considered. Thus while two sources have available the same amount of energy; more demanding tasks can be accomplished with a high quality energy source rather than with an equivalent low quality energy source. For example a high quality electrical source can be used to drive machinery while an equivalent low exergy warm water source would be restricted to providing space heating. To achieve optimum environmental performance it is important to match the quality of the required energy consuming tasks to the quality of the energy source.

The paper begins with an explanation of the system approach of energy and exergy analyses in relation to dwelling ventilation systems. It then describes the energy and exergy calculation methods and presents some characteristic climate data for De Bilt, in the Netherlands. After that, analysis results are presented and discussed in terms of an instantaneous and a daily basis. Finally, recommendations for the operation of dwelling ventilation systems are given in the conclusion.

2. Approach

Energy and exergy analyses were performed for the following dwelling ventilation systems:

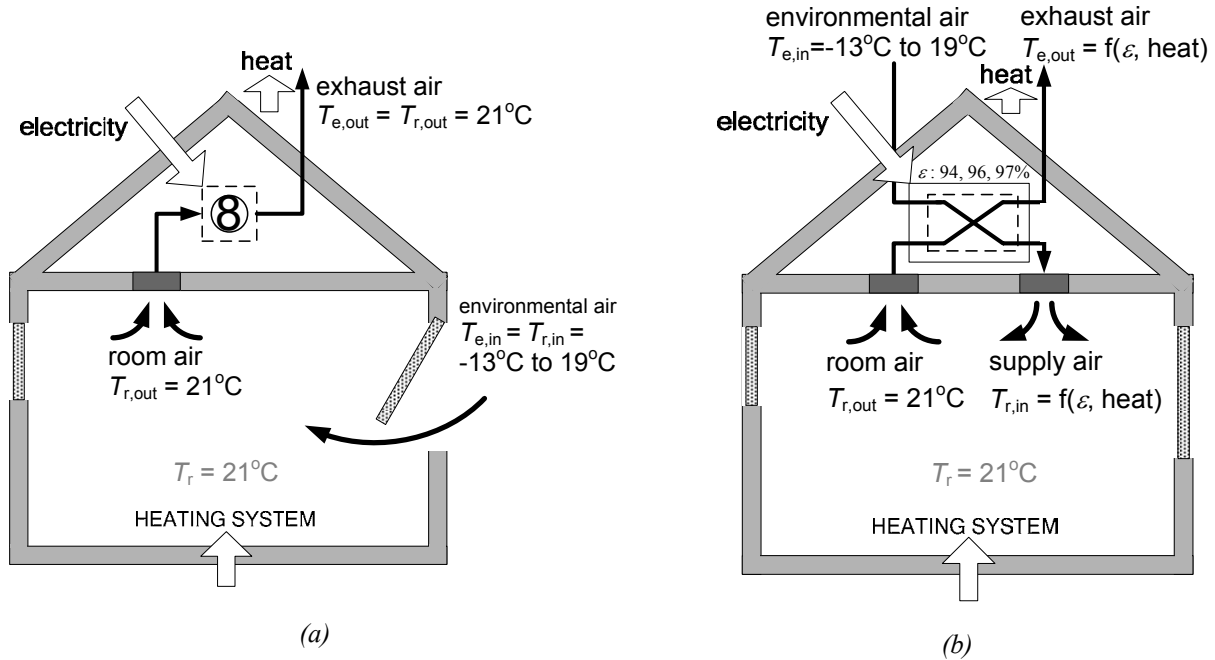


Figure 1. Dwelling ventilation: mechanical exhaust ventilation with natural air supply (a, left, reference case); balanced ventilation with heat recovery (b, right).

- Mechanical exhaust with natural air supply without heat recovery:
- Balanced ventilation with heat recovery.

The aim of the developed calculation method was to assess different systems of air to air heat recovery from exhaust air in terms of exergy. Infiltration air volumes, which can differ as a function of the ventilation system, were not considered.

The analysis assumed steady state operation and considered only dry air. It thus neglected latent heat exchange between ventilation airflows. The pressure difference between air entering and leaving the dwelling was ignored for the analysis. General calculation values, used for the exergy analysis in this paper, are given in Table 1.

Table 1. General calculation values (CEN 2000, 2005).

| Parameters | Values |
|--|---|
| air density (ρ) | 1.23 kg m ⁻³ |
| spec. heat capacity of air ($C_{p,air}$) | 1.008 kJ kg ⁻¹ K ⁻¹ |
| environmental air temperature (T_e) | from -13°C to 19°C |
| room air temperature (T_r) | 21°C |
| ventilation airflow rates (Q) | 0.028, 0.042, 0.063 m ³ /s |

The mechanical exhaust ventilation with natural air supply (hereunder “mechanical exhaust ventilation”) used an AC fan (Model: CVE 166 from Itho bv. 2005a) or a DC fan (Model: CVE ECO-fan 2 from Itho bv. 2005b). Environmental air enters the dwelling at temperature $T_{r,in}$ and goes through the exhaust fans at room air temperature $T_{r,out}$, as shown in Figure 1a.

The balanced ventilation with heat recovery case (Figure 1b) assumed a DC Heat Recovery Unit (Model: HRU ECO-fan 3 S B from Itho bv. 2005c). This contains two DC fans and a heat exchanger with high thermal effectiveness ε . The effectiveness and fan electricity input were calculated by interpolating from manufacturer’s data (Itho bv. 2005c) in relation to ventilation airflow rates (see Table 2). The environmental air gains heat from exhaust air entering the heat exchanger in the HRU at room air temperature $T_{r,out}$ and leaves the dwelling at temperature $T_{e,out}$.

Table 2. Thermal effectiveness ε versus airflow rates Q .

| Q [m ³ /s] | ε [-] |
|-------------------------|-------------------|
| 0.063 | 0.94 |
| 0.042 | 0.96 |
| 0.028 | 0.97 |

3. Exergy Analysis of Dwelling Ventilation

Different ventilation systems were compared on the basis of calculations of thermal energy and thermal exergy demands by ventilation airflows in relation to environmental air temperature and electricity input to a ventilation unit. The exergy analysis was carried out for the heating season. The calculations steps from Equations 1 to 4 (ASHRAE 2000) and Equations 5 and 6 (Wall 1990) apply to both mechanical exhaust ventilation and balanced ventilation. Equation 7 was used to calculate supply air temperatures at the HRU (ASHRAE 1993).

3.1 Electricity Input to Ventilation Unit

The relation between the pressure drop of the system P and the ventilation airflow rate Q was obtained according to Equation 1, where C is a coefficient. Average C values can be calculated from manufacturers' data (here we used CVE ECO-fan from Itho bv. 2005b and HRU ECO-fan 3 S B from Itho bv. 2005c).

$$P = P_{f,st} = CQ^2 \quad (1)$$

$$P_{f,ke} = \frac{1}{2} \rho \left(\frac{Q}{A_{duct}} \right)^2 \quad (2)$$

$$P_{f,tot} = P_{f,st} + P_{f,ke} \quad (3)$$

$$Pe_1 = Pe_2 \left(\frac{D_2}{D_1} \right)^4 \left(\frac{Q_1}{Q_2} \right)^3 \left(\frac{\rho_1}{\rho_2} \right) \quad (4)$$

The fan total pressures $P_{f,tot}$ for the AC and DC fans were calculated using equations 1 to 3, where $P_{f,st}$ is the fan static pressure, $P_{f,ke}$ is the fan kinetic pressure, ρ is the air density (assumed constant over the temperature range in Table 1), A_{duct} is the inner duct cross-section area and Q is the airflow rate given in Table 1.

The electricity Pe input to the AC and DC fans was calculated using the fan law in Equation 4 (ASHRAE 2000), where D is the fan impeller diameter. The fan law was used to predict performance of the fan when test data (data with subscript 2 in Equation 4) are available. The test data for Equation 4 was based on data at the intersection points where the system line (plotted by using Equation 1) intercepts the working line of the fans in the graph of fan static pressure versus airflow rate given by the fan producer (used Itho bv. 2005a, 2005b).

3.2 Thermal Energy and Exergy Demands by Ventilation Airflows

Thermal energy demand En_{th} and thermal exergy demand Ex_{th} by ventilation airflows were calculated by using Equations 5 and 6.

$$En_{th} = \rho_{air} Q C_{p,air} (T_{r,out} - T_{r,in}) \quad (5)$$

$$Ex_{th} = \rho_{air} Q C_{p,air} \left(T_{r,out} - T_{r,in} - T_e \ln \left(\frac{T_{r,out}}{T_{r,in}} \right) \right) \quad (6)$$

where $T_{r,out}$ is the temperature of the air leaving the room, equal to room air temperature ($T_r=21^\circ\text{C}$), $T_{r,in}$ is the temperature of air supplied to the room and T_e is environmental air temperature.

For the mechanical exhaust ventilation, $T_{r,in}=T_e$, between -13°C and 19°C . For the balanced ventilation with heat recovery, the supply air temperature $T_{r,in}$ was calculated by using heat exchanger thermal effectiveness ε (ASHRAE 1993) and heat balance equations, assuming the same airflow rates though the HRU for the supply air and the exhaust air.

$$T_{r,in} = T_e + \varepsilon(T_r - T_e) \quad (7)$$

where T_e is environmental air temperature and T_r is room air temperature.

3.3 Total Energy and Exergy Demands by Ventilation Airflows

The total energy demand by ventilation airflow En , was determined by adding thermal energy demand by ventilation airflow En_{th} (Equation 5) and electricity input to the ventilation unit Pe (Equation

Table 3. Electricity inputs to the fans and the HRU Pe versus ventilation airflow rates Q .

| | Q [m ³ /s] | Pe [W] |
|--------|-------------------------|----------|
| AC fan | 0.028 | 14 |
| | 0.042 | 35 |
| | 0.063 | 45 |
| DC fan | 0.028 | 6 |
| | 0.042 | 8 |
| | 0.063 | 22 |
| DC HRU | 0.028 | 28 |
| | 0.042 | 47 |
| | 0.063 | 110 |

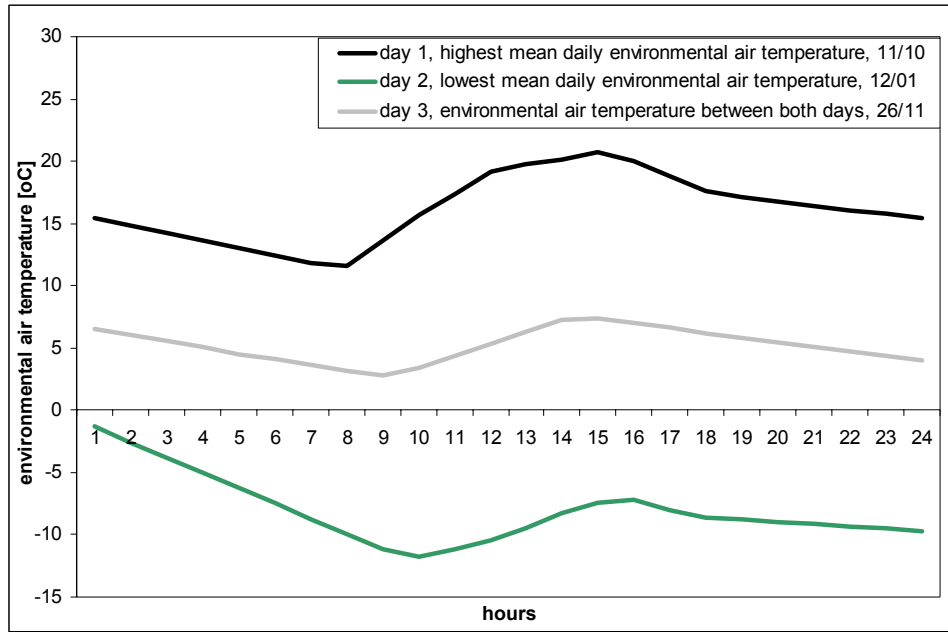


Figure 2. Hourly environmental air temperature profiles for 3 winter days in De Bilt, the Netherlands.

4). The total exergy demand by ventilation airflow Ex , was determined by adding thermal exergy demand by ventilation airflow Ex_{th} (Equation 6) and electricity input to ventilation unit Pe (Equation 4).

Table 3 shows electricity inputs in relation to the ventilation airflow rates of the applied fans and the HRU, calculated according to Equations 1 to 4.

The electricity input to the fans and the HRU depends on the ventilation airflow rate and on the pressure loss, but is not directly affected by environmental air temperature. The inputs of exergy and energy for electricity are identical because electrical energy can, in theory, be totally converted into mechanical work.

3.4 Daily Operation Profiles

Daily energy and exergy demands due to ventilation airflows for representative days in the heating season were calculated. In this paper, Figure 2 shows three hourly environmental air temperature profiles, for winter days of maximum, minimum and intermediate mean daily environmental air temperatures. Climate data for De Bilt, the Netherlands were taken from the TMY2 weather data (NREL 1995).

The hourly ventilation unit operation plan for these three days is given in Table 4.

4. Results and Discussion

This section presents the energy and exergy analysis results for the applied fans and the HRU in terms of heat and electricity, on an instantaneous and on a daily basis.

4.1 Thermal Energy and Thermal Exergy Demands by Ventilation Airflows

Figure 3 shows thermal energy En_{th} and thermal exergy Ex_{th} demands for ventilation airflows, as a function of environmental air temperature and ventilation airflow rate. Using the AC fan or DC fan in the mechanical exhaust ventilation has no effect on the demand for thermal energy or exergy as long as the fans operate between the same supply and exhaust air temperatures and at the same airflow rate. Ventilating at higher airflow rates increases

Table 4. Hourly operation plan for dwelling ventilation.

| hour | ventilation airflow rate [m ³ /s] |
|-------------|--|
| 0:00-8:00 | 0.028 |
| 8:00-9:00 | 0.042 |
| 9:00-17:00 | 0.063 |
| 17:00-18:00 | 0.042 |
| 18:00-24:00 | 0.028 |

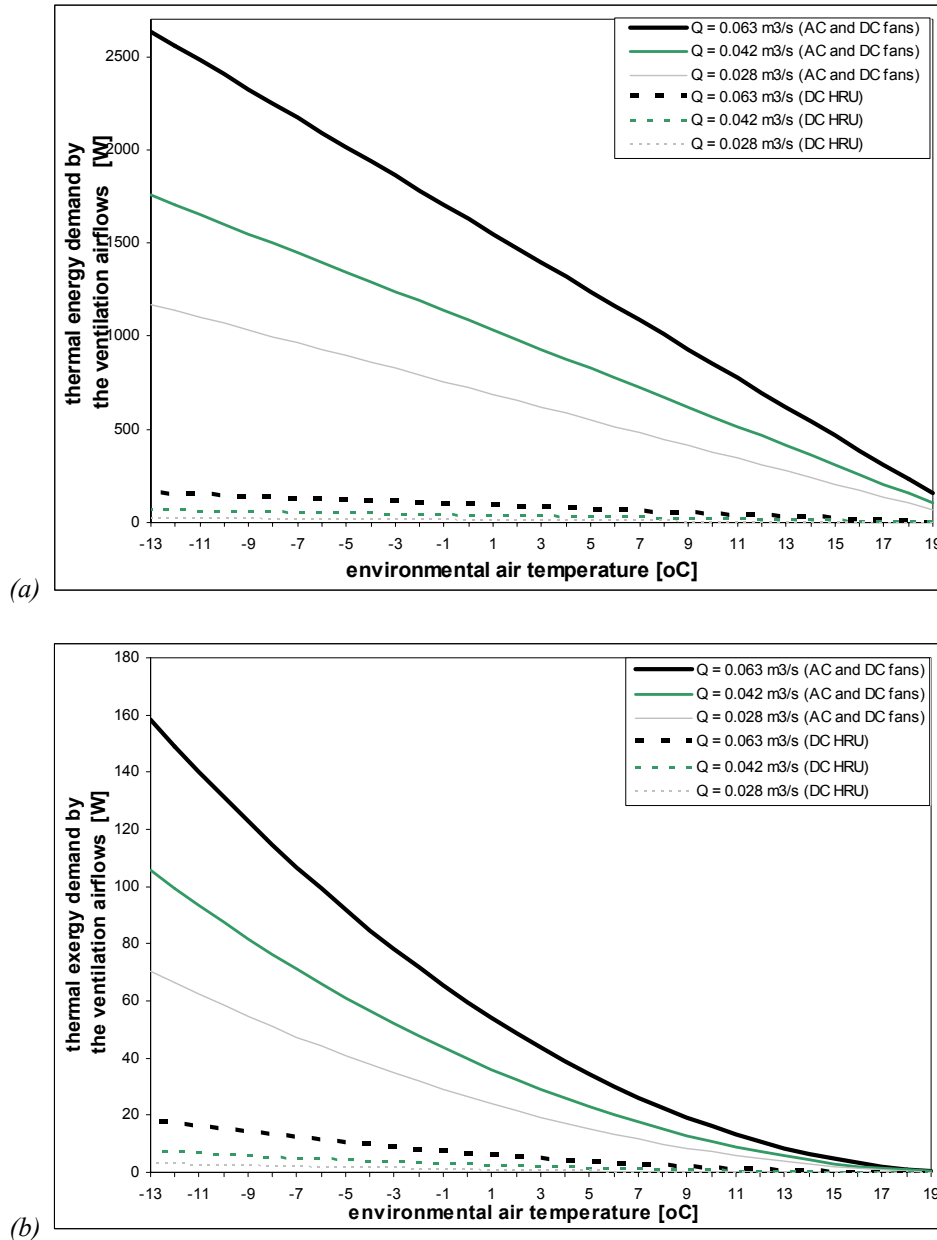


Figure 3. Thermal energy En_{th} (top graph) and thermal exergy Ex_{th} (bottom graph) demand by the ventilation airflows versus T_e .

thermal energy and exergy demands in all cases. This is because the ventilation heat demand depends on the ventilation airflow rate.

In absolute terms, the thermal exergy demand is much lower than the thermal energy demand because the temperature differences involved are relatively small (note that the graphs have different scales). However, the thermal energy demand varies linearly with environmental air temperature, while the thermal exergy demand does not. Hence, in relative terms the thermal exergy demand increases more strongly than the thermal energy demand for lower environmental air temperatures.

Figure 4 illustrates the total exergy demand by ventilation airflow Ex of the ventilation systems as a function of environmental air temperature and ventilation airflow rate. The smooth lines represent the total exergy demand of the mechanical exhaust ventilation using the DC fan. The dashed lines represent the total exergy demand of the mechanical exhaust ventilation using the AC fan (Figure 4a) and the total exergy demand of the balanced ventilation with heat recovery (Figure 4b).

As environmental air temperature T_e increases from -13°C to 19°C , the total exergy demand decreases for a given ventilation airflow rate. The sharpest

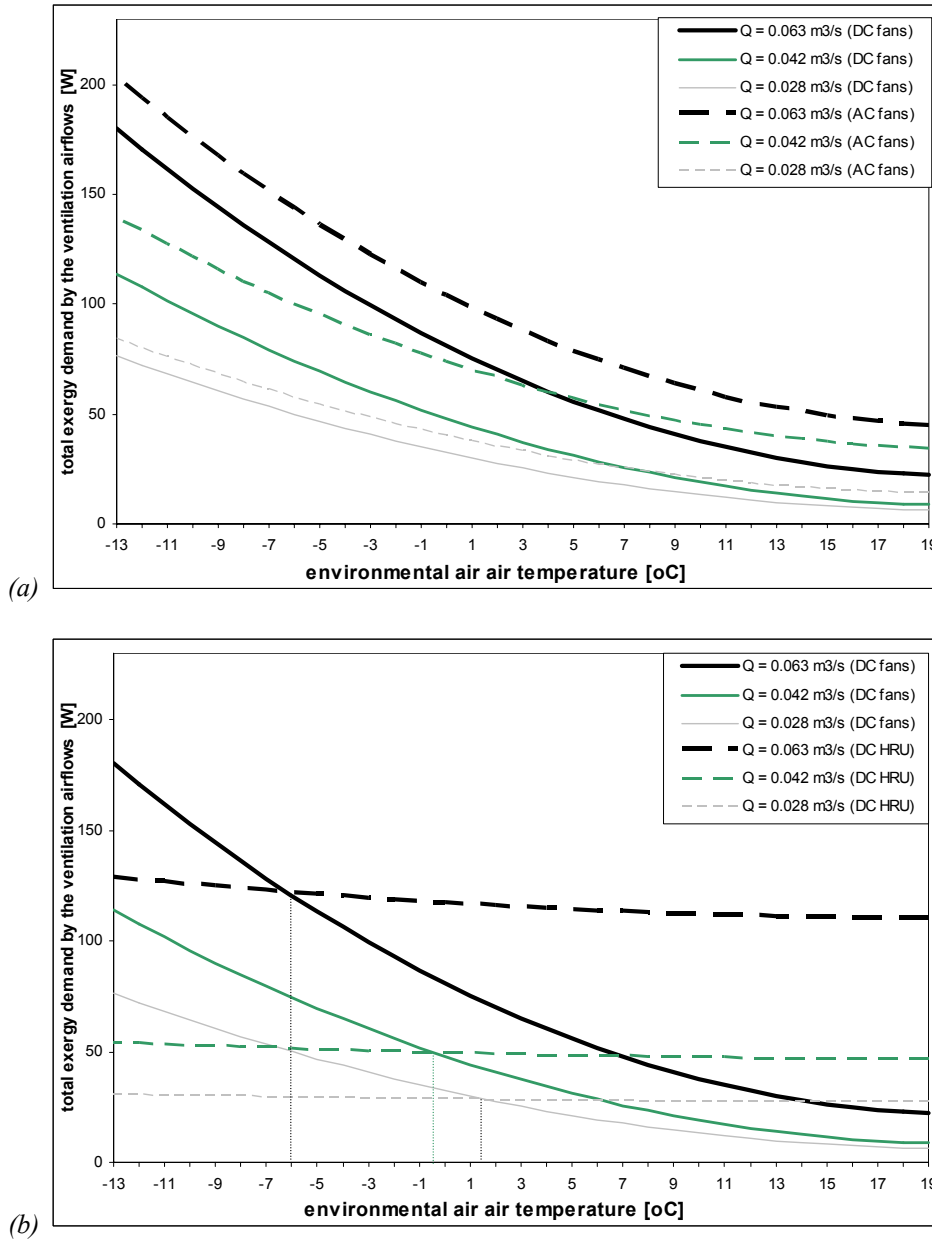


Figure 4. Total exergy demand by ventilation airflow (Ex) of the ventilation systems: mechanical exhaust ventilation with natural air supply (a, top); balanced ventilation with heat recovery (b, bottom) versus environmental temperature T_e .

decrease is for the DC fan, followed by the AC fan and lastly by the DC HRU.

The DC HRU lines in Figure 4b are less sensitive to T_e variations in the range of -13°C to 19°C because the DC HRU requires mainly electricity, while the exhaust ventilation systems using AC and DC fans require relatively more heat. The DC fan requires less exergy than the AC fan for the entire range of T_e . Compared to the DC HRU, the DC fan requires more exergy at lower T_e , and relatively less exergy as T_e increases towards the room air temperature T_r .

The total exergy demand lines (Ex) for the DC fan and the DC HRU intersect at a given environmental air temperature ($T_{e,intersect}$) for a given ventilation airflow rate (Figure 4b). $T_{e,intersect}$ shows at which environmental air temperature the total exergy demands of two different ventilation systems are equal. These Ex lines could be applied for evaluating the total exergy demands of different ventilation systems at different environmental air temperatures. For example, at $T_e = -10^\circ\text{C}$, the balanced ventilation with the DC HRU at $0.063 \text{ m}^3/\text{s}$ ventilation airflow rate uses approximately 125 W,

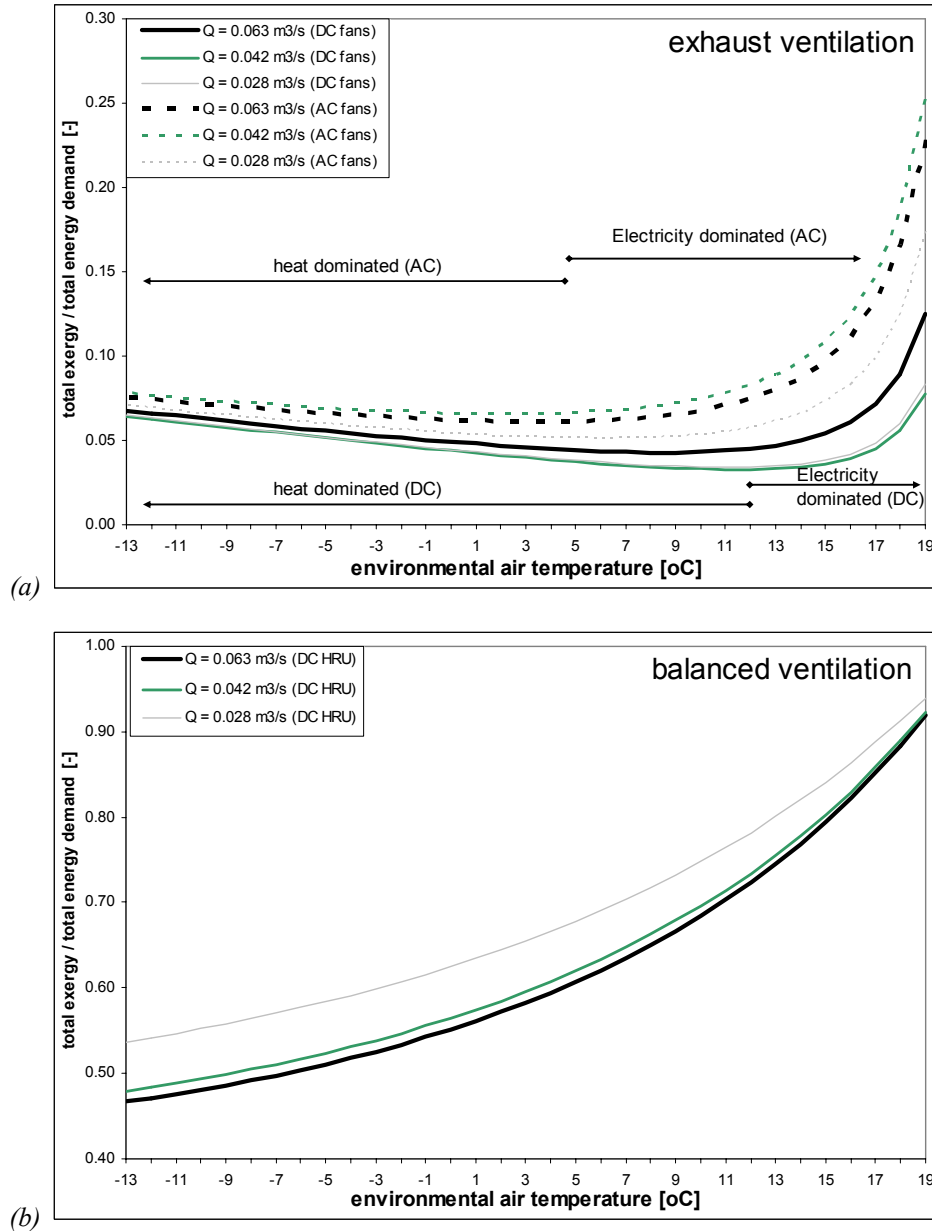


Figure 5. Ratios between the total exergy Ex and the total energy En demands by ventilation airflows of the dwelling ventilation systems: mechanical exhaust ventilation with natural air supply (a, top); balanced ventilation with heat recovery (b, bottom) versus environmental air temperature T_e .

while the mechanical exhaust ventilation with the DC fan at the same airflow rate uses about 150 W. Nevertheless, at $T_e = -3^\circ\text{C}$ the balanced ventilation with the DC HRU at the same airflow rate uses about 120 W, while the mechanical exhaust ventilation with the DC fan uses around 100 W. At $T_e > T_{e,intersect}$, using the mechanical exhaust ventilation with the DC fan results in less total exergy demand than using the balanced ventilation with the DC HRU at the same airflow rate. Moreover, $T_{e,intersect}$ increases when operating the ventilation units at lower airflow rates, since

electricity input to the DC HRU is less. For lower airflow rates, exergy demand for the balanced ventilation unit with the DC HRU is less than for the mechanical exhaust ventilation with the DC fan.

4.2 Ratio Between the Total Exergy and the Total Energy Demands by Ventilation Airflows

Figure 5 illustrates ratios between total exergy Ex and total energy En demands by ventilation airflows of the dwelling ventilation systems, for the range of environmental air temperature T_e from -13°C to 19°C .

In Figure 5a, the Ex/En ratio decreases with increasing environmental air temperature T_e , on the left part of the graph (heat dominated part). This reflects the fact that exergy demand due to ventilation and heat exchange Ex_{th} decreases with rising T_e . On the right part of the graph, the Ex/En ratio increases steeply as T_e rises. This is because of a significant increase in the relative share of electricity input: although the thermal exergy demand Ex_{th} decreases sharply, as shown in Figure 3b, the electric power Pe required for driving the fans remains unchanged. Because exergy assigns a higher value to electricity than to low grade heat, when T_e increases, the total exergy demand decreases at a much slower rate than the total energy demand.

In Figure 5b, the electricity input to drive the balanced ventilation with heat recovery always exceeds the thermal exergy required in ventilation and heat transfer, for the entire range of environmental air temperatures T_e between -13°C and 19°C .

4.3 The Total Energy and the Total Exergy Demands in a Winter Day

The previous items focused on instantaneous energy and exergy values in relation to environmental air temperatures. This section presents examples of cumulative energy and exergy demands by dwelling ventilation, in the course of three representative winter days in De Bilt, the Netherlands (Figure 2).

Daily energy and exergy demands by the dwelling ventilation units for the hourly ventilation plan (Table 4) are given in Table 5.

Thermal energy and exergy demands are highest on the coldest day (day 2) and lowest on the warmest day (day 1). Electricity for the AC fan, the DC fan, and the HRU are the same for all three days, because the hourly ventilation operation is the same in all three cases.

Within each day, the thermal exergy demand is the same for the AC and DC fans, because they operate between the same temperatures. For all three days, the total energy demand is lowest for the HRU, due to the significantly lower thermal energy demand. The total exergy demand, on the other hand, is lower for the HRU only on the coldest day (day 2). On the warmer (day 1) and average (day 3) days, the total exergy demand is lower for the DC fan, which uses the least electricity.

In terms of total exergy demand, these results indicate that it is worthwhile to reduce the thermal exergy demand on the colder day by using heat recovery. On milder days, however, the high-valued electricity required by the HRU exceeds the savings in low-grade heat obtained by using a HRU to preheat ventilation air.

These results consider the total exergy demand, which is different from the total exergy consumption. While demand is annotated to final use, consumption is considered as a flow from primary energy transformation to final energy delivery for end use. Because energy conversion flows could have different configurations for heat and electricity production, these forms of energy could thus have different impact on irreversibilities throughout the whole energy flows.

Table 5. Daily energy and exergy demands (heat and electricity).

| | | En_{th} [kWh] | Ex_{th} [kWh] | Pe [kWh] | Total En | Total Ex |
|---------------|-----|--------------------|--------------------|---------------|---------------|---------------|
| day 1 warm | AC | 4.891 | 0.054 | 0.565 | 5.456 | 0.618 |
| | DC | 4.891 | 0.054 | 0.193 | 5.084 | 0.247 |
| | HRU | 0.174 | 0.004 | 0.985 | 1.159 | 0.989 |
| day 2 cold | AC | 30.823 | 1.603 | 0.565 | 31.388 | 2.168 |
| | DC | 30.823 | 1.603 | 0.193 | 31.016 | 1.796 |
| | HRU | 1.126 | 0.112 | 0.985 | 2.111 | 1.097 |
| day 3 avg. | AC | 16.571 | 0.456 | 0.565 | 17.136 | 1.021 |
| | DC | 16.571 | 0.456 | 0.193 | 16.764 | 0.649 |
| | HRU | 0.601 | 0.032 | 0.985 | 1.586 | 1.017 |

5. Conclusions

Exergy analysis assigns values to thermal energy according to its temperature level: systems closer to environmental air temperature have lower thermal exergy. Electricity has a high exergy value because it can directly be converted into work. In terms of exergy the amount of electricity input to the fans and heat recovery unit (HRU) is much more significant than in terms of energy, because electricity has a higher exergy value than thermal energy.

This paper presented steady-state energy and exergy analyses for dwelling ventilation with and without air to air heat recovery from ventilation airflow, for dwelling ventilation systems using exhaust ventilation with and without air to air heat recovery in winter conditions in the Netherlands.

At lower environmental air temperatures T_e , mechanical exhaust ventilation with natural air supply has higher total exergy demand than balanced ventilation with heat recovery. In this range, there is relatively more demand for thermal exergy than for electricity. This trend reverses as T_e increases towards the room air temperature, as the heat demand decreases. The balanced ventilation with heat recovery is less sensitive to T_e , since it requires mainly electrical exergy.

From the viewpoint of total exergy consumption at room level, it could make sense to use the HRU only when T_e is low enough to compensate the additional need for electricity and let ventilation air bypass the HRU, or if possible to operate the HRU at low ventilation airflow rate in order to decrease the electricity input when T_e is not too low. Nevertheless, the ventilation airflow rate must be sufficient to satisfy indoor occupancy conditions.

In terms of energy demand, the balanced ventilation system with HRU is a better alternative for dwelling ventilation in the heating season in the Netherlands, since the system needs less energy. However, in terms of exergy demand, the HRU requires more exergy because of the additional electricity input. The thermal exergy recovered from the exhaust air is relatively small, since the exhaust air is relatively close to the environmental air temperature, and thus has low thermal exergy.

This analysis considered the final exergy demand at room level, without focusing on the efficiency of energy conversion and delivery processes (electricity, heating system). This conclusion may change, if instead of the exergy demand, the exergy consumption is considered, including the exergy efficiencies of electricity and heat production.

Acknowledgements

Financial support for this research was provided by the Faculty of Architecture at the Delft University of Technology, and is gratefully acknowledged.

References

- Ala-Juusela M (ed.): (2004). "Guidebook to IEA ECBCS Annex 37 - Low Exergy Systems for Heating and Cooling of Buildings". VTT Technical Research Centre of Finland, Finland.
- ASHRAE: (1993). "1993 ASHRAE handbook fundamentals", SI ed. Atlanta: ASHRAE: American Society of Heating, Refrigerating, and Air-Conditioning Engineers, Inc.
- ASHRAE: (2000). "ASHRAE handbook - HVAC systems and equipment", SI ed. Atlanta: ASHRAE: American Society of Heating, Refrigerating, and Air-Conditioning Engineers, Inc.
- Boelman EC: (2002). "Exergy Needs for Winter Ventilation in Buildings". *Proceeding of the Sustainable Building 2002 Conference*. Oslo, Norway, 23- 25 September, 2002, paper No.489.
- CEN: (2000). "EN12524 - Building materials and products - Hygrothermal properties - tabulated design values". Brussels: European Committee for Standardisation.
- CEN: (2005). "EN15251 - Criteria for the Indoor Environment including thermal, indoor air quality, light and noise". Brussels: European Committee for Standardisation.
- Itho bv.: (2005a). "Afzuigunit CVE 166 - Technische documentatie". <http://www.itho.nl/> (in dutch).
- Itho bv.: (2005b). "Afzuigunit type CVE ECO-fan 2 - Technische documentatie". <http://www.itho.nl/> (in dutch).
- Itho bv.: (2005c). "Warmteterugwinunit HRU ECO-fan 3 - Technische documentatie". <http://www.itho.nl/> (in dutch).
- NREL: (1995) "User's Manual for TMY2s (Typical Meteorological Years)". NREL/SP-463-7668, Colorado: National Renewable Energy Laboratory.
- Rosen MA and Dincer I: (2001). "Exergy as the confluence of energy, environment and sustainable development". *The International Journal of Exergy*, 1, pp3-13.
- Wall G: (1990). "Exergy Needs to Maintain Real Systems Near Ambient Conditions". *Proceeding of the Florence World Energy Research Symposium*. Pergamon, Florence, Italy, pp261-270.

Potential of Natural Ventilation in a Tropical Climate

Leopoldo Eurico Gonçalves Bastos¹ and Cláudia Barroso-Krause²

PROARQ-FAU/UFRJ, Programa de Pós-graduação em Arquitetura,
Universidade Federal do Rio de Janeiro, CEP 21941-590 Rio de Janeiro, Brazil

Abstract

Sustainable architecture design for tropical climates requires the use of natural ventilation combined with other strategies including: the use of appropriate materials, site location, orientation of façades and solar shading, etc. Requirements for thermal performance and indoor thermal comfort also depend on the geographical site where the building is located. The new Brazilian standard “Norma ABNT NBR 15220-3” has established seven bioclimatic zones and some architectural guidelines for low-income houses. Perhaps, due to the lack or scarcity in relation to wind data, certain regions such as the Amazon and Northeast coast were inserted in the same bioclimatic zone. This will pose problems for the distinct ventilation strategies required for each region. As a means to overcome this challenge, a potential yearly average wind zoning map for all the country is proposed. This overlaps with the map of bioclimatic zones defined by the Brazilian standard. In addition, to aid design, yearly average wind velocity values for each region are presented which consider two heights from the ground; i.e. 1.5 m and 6 m. Calculations were performed using a logarithm profile defined from theoretical-empirical data charts (meteorology data + WasP simulations) at 50 m height, used for selection of available sites for wind driven electricity generation.

Key words: natural ventilation, Brazilian climate, tropical climate comfort, sustainable architecture, wind velocity, wind profiles.

1. Introduction

Nowadays, in order to accomplish a sustainable building approach, the architect needs to consider, in addition to the site microclimatic analysis, other important subjects including socio-cultural aspects, energy adequacy use, and environmental impacts.

When dealing with the Brazilian architectural design of low-income houses, a challenge exists due to the diversity of problems encountered which include: uncomfortable indoor environments (non-adequacy to the site climate); socio-cultural aspects and the use of low quality and non-compliance performance materials (Barroso-Krause, 2005). When considering this range, the wind resource comes to play an important role for such buildings since this is needed for occupant health, cooling the envelope and improving indoor thermal comfort. Thus, natural infiltration and ventilation need to be taken in account by the architect in tropical climates.

Despite the importance of natural air infiltration and ventilation to provide health and comfortable indoor ambiances for Brazilian low-income houses, it is observed that there is a lack or scarcity of available wind data that is appropriate for this purpose.

This problem was found in the new Brazilian standard “Norm NBR 15220-3” (2005) which has established eight bioclimatic zones and some building guidelines for low-income houses. However, it does not consider the wind resource regional diversity. Furthermore, certain bioclimatic zones comprise regions with distinct wind characteristics. For example the Amazon and the Northeastern coast were inserted in the same climate zone Z8. This will pose problems to architects, because the wind fields and flow regimes are not the same for these regions.

To overcome this problem the present paper introduces a method to determine a potential yearly average wind zoning map for Brazil. This map overlaps that of the existing eight zones defined by the Brazilian standard. Also, two heights from the ground are considered, these being 1.5 m and 6 m. For each height the calculated yearly average wind velocity values have been determined for use in estimating house aperture areas for natural ventilation. This solution was based upon the analysis of available wind charts used to select wind turbine sites for electricity generation (Eletrobras, 2001; Rio de Janeiro State, 2005).

2. Available Wind Data

The general wind distribution over Brazil is controlled by large atmospheric scales (synoptic and general planetary). This general profile presents large meso-scale variations (regional level) and micro-scale variations (local level) due to the site characteristics including topography, altitude and water masses. The factors acting upon the small scale can generate local wind regimes with specific patterns, which vary in time (hours or days). This occurs under a predominant daily regime dictated by local and regional influences. The annual and seasonal wind regimes depend on the large atmospheric scales.

In the present paper several wind data charts were utilised based on values given at 50 m height from the ground. These were published in Brazil between 2001 and 2005. These charts contain regional wind regime distributions including yearly average wind speeds, main directions and terrain roughness. Wind turbines for electricity generation operate at average wind velocities of between 2.5 to 15 m/s, and are placed at 50 m height or more from the ground. The wind regime distribution is presented through seven regional meso-scales.

3. Wind Regional Meso-Scales

3.1 Eastern and Central Amazon Basin

This region is located between 10°S and 5°N latitudes and 55°W to 77°W longitudes. The climate is equatorial humid, with an average temperature of 25°C and a precipitation of 2000 mm/year. The atmospheric pressure gradients are low and the trade winds from the east have low intensity. The wind speed at 50 m height from the ground is under 3.5 m/s, and the average terrain roughness $Z_o = 0.8$ m. The wind is calm during night-time periods. During the day, there are localized winds due to the non-uniform heating of vegetation and water reservoir surfaces. On the North part of this basin there is a hill region known as Serra da Paracaima (Roraima State). This has constant winds from East to Northeast, reaching average yearly velocities of 6 to 9 m/s at 50 m height, and a terrain roughness $Z_o = 0.2$ m.

3.2 Eastern Amazon Basin

This region comprises a 100 km band width from the 55°W longitude, Santarém City (Pará State) up

to the Atlantic coast region of the Amapá and Maranhão States. On the North part there are trade winds from East to Northeast. On the South part the winds are from East to Southeast. The yearly average wind speed at 50 m height is under 3.5 m/s, and the terrain roughness is $Z_o = 0.5$ m. Over some hills near the ocean coast, average velocities reach 7.5 m/s to 9 m/s at 50 m height from the ground.

3.3 North - Northeastern Atlantic Coast

The Coast region is 100 km wide stretching from the Amapá State to the São Roque cape, Rio Grande do Norte State. The dominant trade winds are from the East; also there are breezes. On the North part (Amapá and Pará) the yearly average wind velocities at 50 m height reach 5 m/s to 7.5 m/s, for a terrain roughness $Z_o = 0.4$ m. On the South portion, (Maranhão, Piauí, Ceará and Rio Grande do Norte States) due to land-breeze effects, the wind velocities reach 6 to 9/s at a height of 50 m, and terrain roughness $Z_o = 0.2$ m.

3.4 Northeastern - Southeastern Coast

This region is of 100 km width and stretches from the São Roque cape up to Rio de Janeiro State. On the North part, the average wind velocity varies from 8 to 9 m/s toward the South direction at 50 m height and $Z_o = 0.3$ m. More to the Southeast the wind velocity range is reduced from 6.0 to 3.5 m/s. On the part situated between the latitudes 21°S and 23°S at 50 m height, the yearly average velocities are 3.5 to 4.0 m/s from East-Southeastern direction, and $Z_o = 3$ m. On the hill region, Serra do Mar, the yearly average velocity is around 6.5 m/s at 50 m height and terrain roughness $Z_o = 1$ m. For the marshy coast region the velocities are from 6 to 7 m/s, $Z_o = 0.005$ m. Considering the Rio de Janeiro city region, the yearly average velocities at 50 m height are from 3.5 m/s to 4 m/s, towards the South quadrant, $Z_o = 3$ m.

3.5 Northeastern - Southeastern Hills

This region is composed of hills and an elevated interior plateau situated 1000 km from the Atlantic coast. This extends from the Rio Grande do Norte State up to Minas Gerais State (Diamantina e serra do Espinhaço). The yearly average velocities are 6.5 to 8.5 m/s on the Central and Southern parts, and 5.5 to 7.7 m/s for the other sites, at 50 m height and $Z_o = 0.4$ m.

3.6 Central Plateau Region

This region is situated from the Amazon Basin and the left side of the São Francisco river up to the Bolivia and Paraguay frontiers. The winds blow toward the East-Southeastern directions. On the North part, Amazon Basin boundary, the yearly average wind velocities at 50 m height are from 3.5 to 4 m/s, and more to the South (Mato Grosso do Sul State) the velocity range increases from 5 to 6 m/s, $Z_o = 0.2$ m.

3.7 South Plateau Region

This region extends from the 24°S latitude (São Paulo) up to the Southern Brazilian frontier (South of the Rio Grande do Sul State). The winds are towards the Northeast and are 5.5 to 6.5 m/s (50 m height) and in hilly regions reach 7.0 to 8.0 m/s, $Z_o = 0.45$ m. On the South coast there are land-breezes and the wind blows East-Northeastern. The yearly average wind velocities reach values above 7 m/s (50 m height) and $Z_o = 0.1$ m.

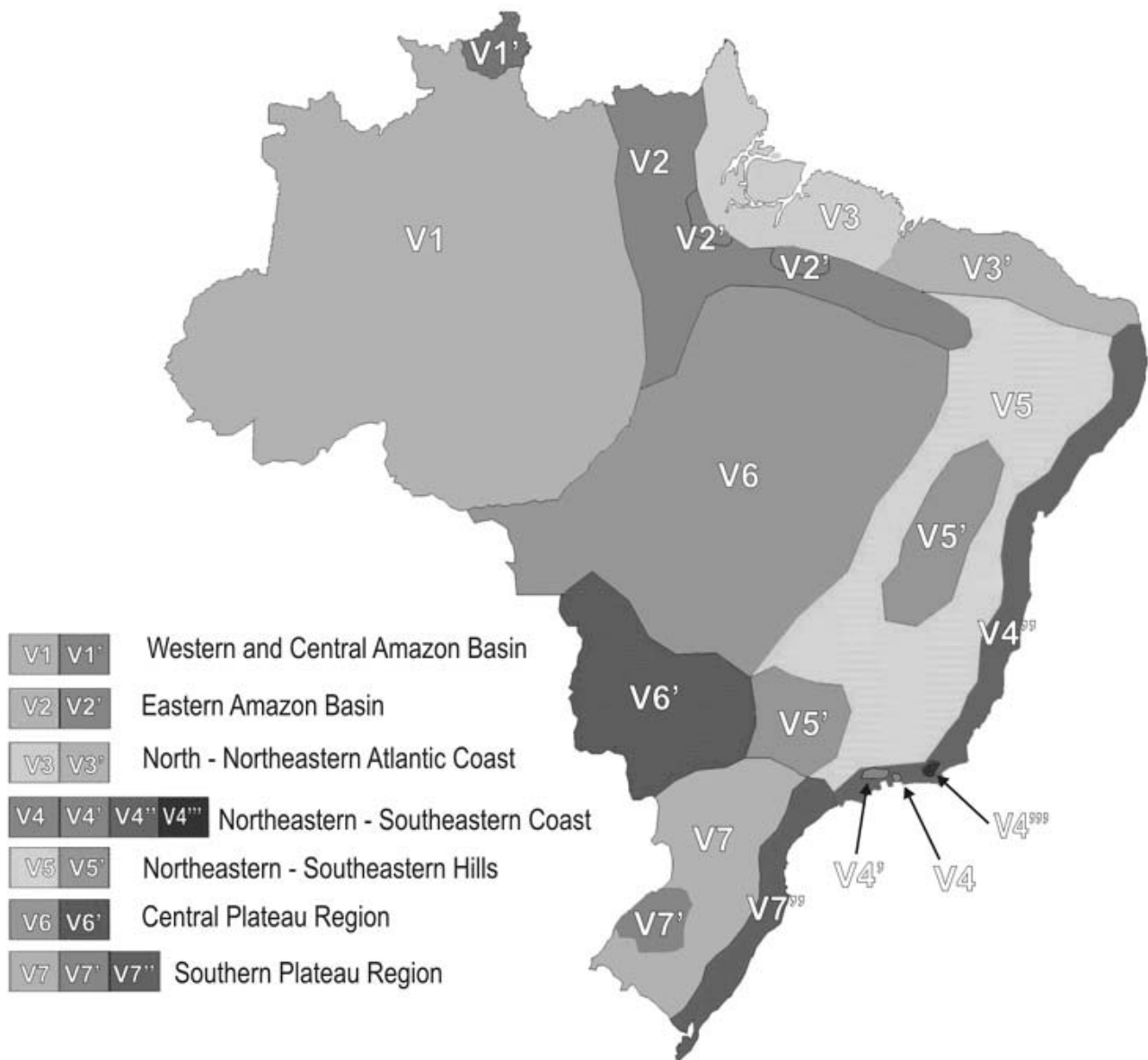


Figure 1. Regional and sub-regional Brazilian wind distribution.

4. Wind and Bioclimatic Maps Overlapping

Considering the previously described Brazilian regional and sub-regional wind characteristics, it is possible to design a map as shown in Figure 1. This identifies seven regions and various sub-regions having distinct wind characteristics.

In order to compare the regional wind map presented in Figure 1 with the eight bioclimatic zones defined by the Brazilian standard, it was possible to generate eight overlap maps as illustrated in Figures 2 to 9.

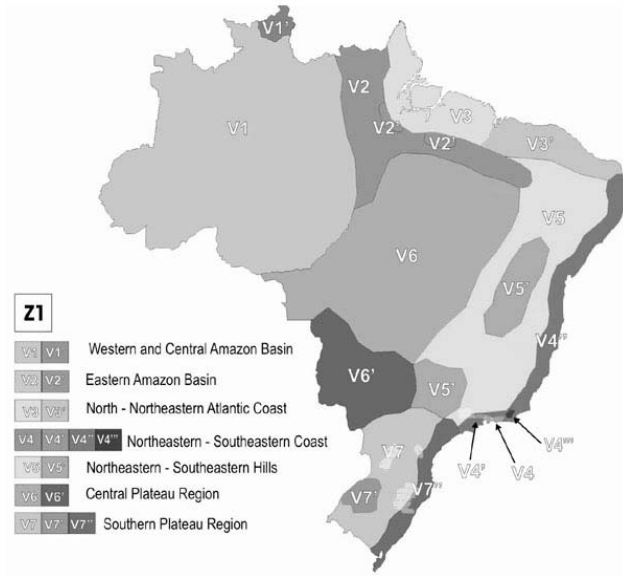


Figure 2. Bioclimatic Zone 1 + Wind Regions.

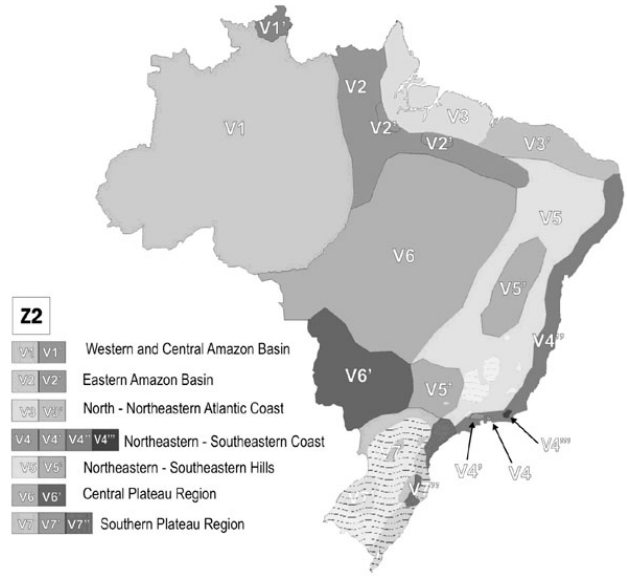


Figure 3. Bioclimatic Zone 2 + Wind Regions.

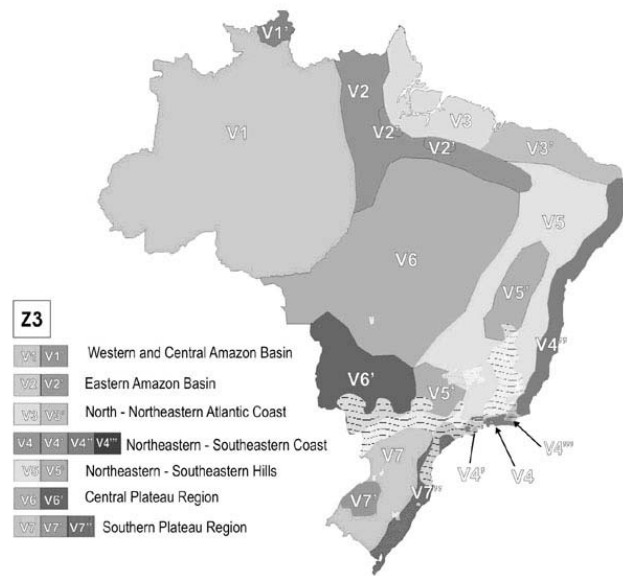


Figure 4. Bioclimatic Zone 3 + Wind Regions.

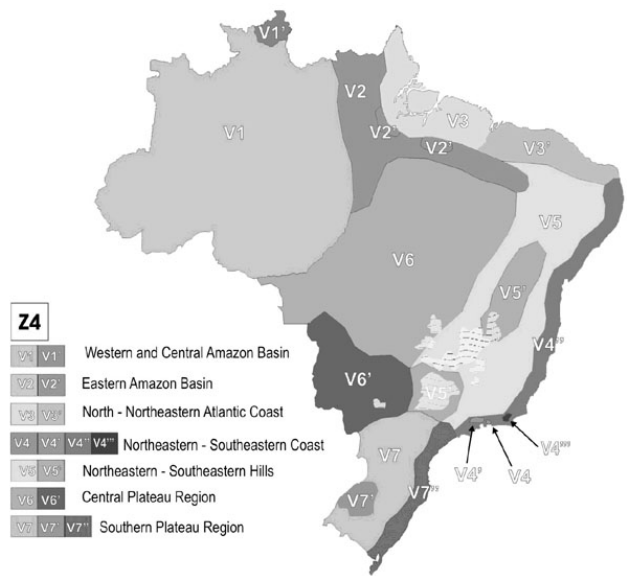


Figure 5. Bioclimatic Zone 4 + Wind Regions.

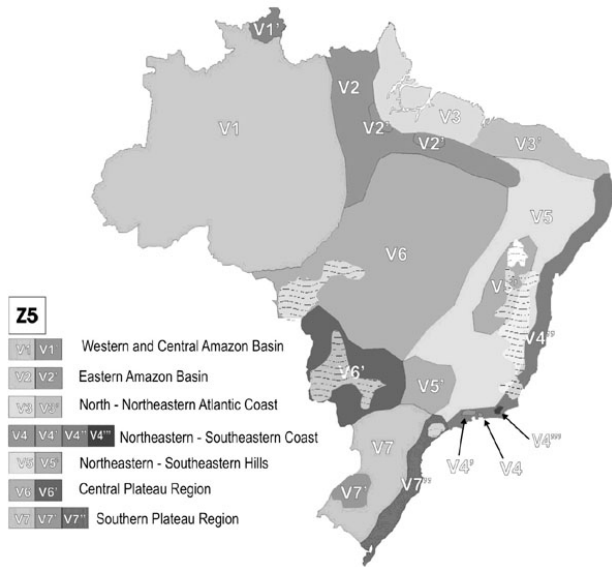


Figure 6. Bioclimatic Zone 5 + Wind Regions.

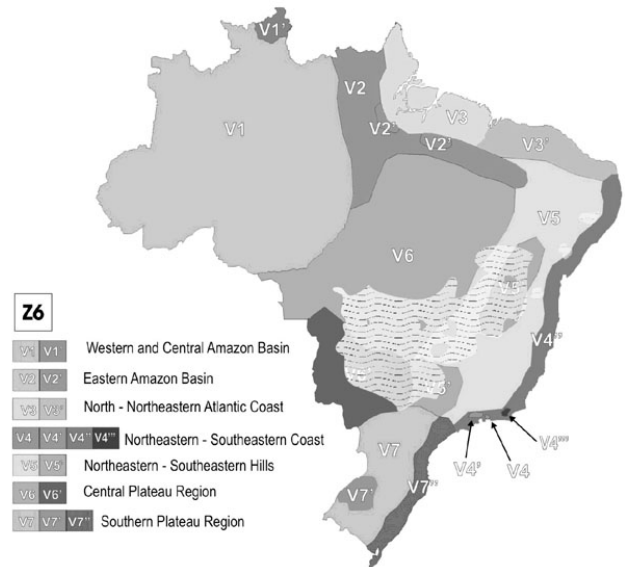


Figure 7. Bioclimatic Zone 6 + Wind Regions.

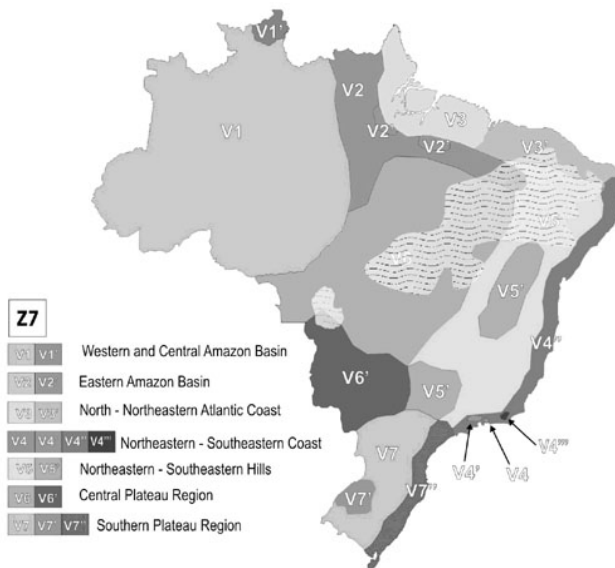


Figure 8. Bioclimatic Zone 7 + Wind Regions.

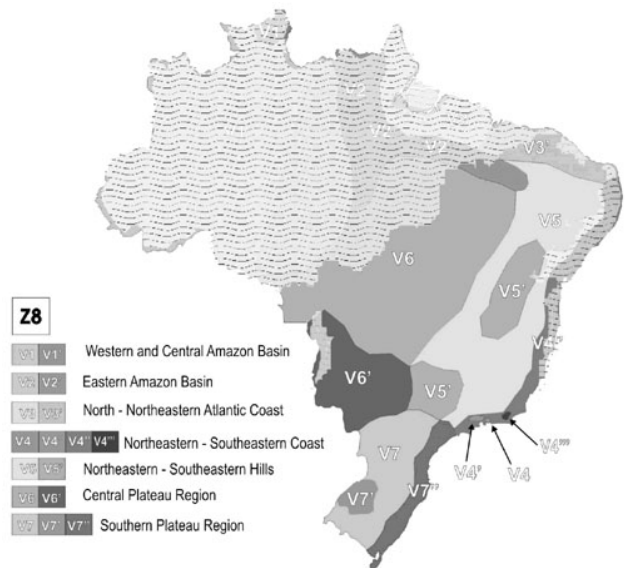


Figure 9. Bioclimatic Zone 8 + Wind Regions.

5. Yearly Average Wind Velocities for Architecture

In order to examine the potential of natural ventilation for low-income houses, two reference heights above the ground were selected for the natural ventilation apertures; i.e 1.5 m for one-family houses and 6 m for multi-family houses.

Calculations were performed using the available yearly average wind velocities data chart (meteorology and WasP simulations) at 50 m height for all the country (Eletrobrás, 2001; Rio de Janeiro State, 2005).

The yearly average wind velocity profile was approximated by a logarithmic law, Equation 1:

$$U(Z) = (U_0/k) \ln(Z/Z_0) \tag{1}$$

where:

$U(Z)$ = wind velocity at the height Z ;

Z_0 : = terrain roughness;

k : = Von Kármán constant;

U_0 : = shear velocity (square root of the shear stress to air specific mass ratio).

This equation can be written for two heights from the ground Z_1 and Z_2 for a same site position, to give Equation 2:

$$U(Z_2)/U(Z_1) = \ln(Z_2/Z_0) / \ln(Z_1/Z_0) \tag{2}$$

The required wind speed $U(Z_2)$ for ventilation purposes at several heights, Z_2 , can be obtained from Equation 2, where $Z_1 = 50$ m; $U(Z_1)$ is the available velocity at this level, and Z_0 is the terrain roughness.

These presented results are an estimate for the wind potential near the ground, and are not considered

specific site conditions since boundary interferences, envelope form, local topography, etc can influence these results. Also, from these calculated velocity values incident on the house surfaces, it is possible to estimate the average indoor air velocity.

As an example assume that a single storey house has equal open windows on opposite walls, with the normal surface oriented to the wind direction. From Givoni (1978), Equation 3 can be used to calculate the average indoor air velocity, V_i (m/s), where x is the window area/ wall area ratio.

$$V_i = 0.45[1 - \exp(-3.48x)] U(Z_2) \tag{3}$$

Thus, for each of the seven Brazilian wind regions described, it is possible to estimate the yearly average velocity profile at heights near the ground. The obtained results are presented in Table 1.

Table 1. Potential range of wind velocity for regional Brazilian housing.

| Region | Region portion | Wind at 1.5 m (m/s) | Wind at 6 m (m/s) |
|-----------------------------------|-----------------------|---------------------|-------------------|
| Western and Central Amazon Basin | V1 General | < 0.53 | <1.7 |
| | V1' North | 2.2 – 3.3 | 3.7 – 5.5 |
| Eastern Amazon Basin | V2 General | < 0.8 | < 1.9 |
| | V2' Hills | 1.8 – 2.0 | 4.0 – 5.0 |
| North-Northeastern Atlantic Coast | V3 North | 1.4 – 2.0 | 4.2 – 6.3 |
| | V3' South | 2.6 – 3.9 | 4.4 – 6.6 |
| Northeastern-Southeastern Coast | V4 Rio (RJ) | - | 1.4 |
| | V4' Serra do Mar | 0.67 | 3 |
| | V4'' North | 2.5 – 2.9 | 4.7 – 5.3 |
| | V4''' NE(RJ), S(ES) | 3.1- 4.7 | 4.2 – 6.0 |
| Northeastern-Southeastern Hills | V5 General | 1.5 – 2.0 | 3.1 – 4.2 |
| | V5' Central and South | 1.6 – 2.0 | 3.6 – 4.5 |
| Central Plateau Region | V6 North | 1.1 – 1.5 | 1.8 – 2.5 |
| | V6' South | 1.8 – 2.2 | 3.1 – 3.7 |
| Southern Plateau Region | V7 General | 1.4 – 1.7 | 3.0 – 3.6 |
| | V7' Hills | 1.8 – 2.0 | 3.8 – 4.4 |
| | V7'' South Coast | > 3.0 | > 4.6 |

6. Conclusions

Sustainable architecture design for low-income houses in tropical climates is a real challenge. Several constraints are posed to the architect designer, and one is related to the lack of available regional wind data for ventilation purposes. This paper has shown the potential, for architectural purposes, of applying regional wind maps based upon charts developed to select appropriate sites for the wind generation of electricity. Also, these wind maps were combined with the bioclimatic zones defined by the Brazilian standard, by means of a series of 8 overlapping maps. Considering the Brazilian standard alone, it is evident that the assumed zoning is far from the climate reality encountered, and will pose problems to someone following this standard. Thus, this standard needs to be reviewed.

In addition, this paper has shown the possibility to estimate the Brazilian regional outdoor yearly average wind velocity for low-income houses, and to infer an estimate for the indoor air velocity. In tropical climates, infiltration and ventilation are necessary to improve thermal comfort and indoor air quality.

References

- Allard F and Santamouris M (Eds): (1998). "Natural Ventilation in Buildings". James & James, London, UK.
- Barroso-Krause C. et al.: (2005) "Eficiência Energética em Habitações de Interesse Social"; Caderno MCidades 9; Ministério das Cidades/Ministério de Minas e Energia,. Brazil.
- Brazilian Standard NBR 15220-3 (2005) "Bioclimatic Zones for Low-Income Houses", Associação Brasileira de Normas Técnicas ABNT. Rio de Janeiro, Brazil.
- Eletrobrás: (2001) Atlas do Potencial Eólico Brasileiro, Ministério de Minas e Energia. Brasília, Brazil.
- Givoni B: (1978) "L'Homme, l'Architecture et le Climat". Eyrolles, Paris, France.
- Rio de Janeiro State: (2005) "Atlas Eólico- Estado do Rio de Janeiro", Secretaria de Estado de Energia, Industria Naval e do Petróleo, Rio de Janeiro, Brazil.

The Real Life Efficiency of Gas Phase Filters Used in General Ventilation and their Influence on the Indoor Air Quality of an Office Building

Alain Ginestet and Dominique Pugnet

CETIAT, Centre Technique des Industries Aérauliques et Thermiques, Domaine Scientifique de la Doua, 25 avenue des Arts, BP 2042, 69603 Villeurbanne cedex, France

Abstract

Gas phase filters were installed within the air handling unit of a HVAC system feeding 100 % fresh (outdoor) air to an office building. The filter efficiency for ozone (O₃) and nitrogen oxides (NO₂ and NO) was measured continuously over a one year period as a function of time (filter's life) and outdoor air parameters (temperature and relative humidity). The results show that the filter efficiency varies with time and depends on the temperature and relative humidity of air. It was also shown that the use of this kind of filter improves the indoor air quality as the indoor / outdoor concentration ratio is lower with the use of the gas phase filters than without.

Key words: gas phase filters, filtration, real life efficiency, ozone, nitrogen oxides, indoor air quality.

1. Introduction

In urban cities, there are many pollutants amongst which ozone (O₃) and nitrogen oxides (NO₂ and NO) penetrate indoors through mechanical ventilation systems. In these environments, ozone is mainly produced by photochemical reactions. Most of the nitrogen dioxide (NO₂) in the air of these environments comes from the reaction of nitrogen oxide (NO) with oxygen and ozone especially in the presence of sunlight and other pollutants (Yocom, 1982). NO is emitted from a wide range of combustion processes and the amount of NO₂ initially produced by these processes is generally small compared to the amount of NO formed.

There are health risks of breathing ozone and nitrogen oxides and these chemicals can react with other indoor pollutants to produce compounds that can affect health and comfort. From Zhang's point of view (1994), the reactions of ozone with nitrogen oxides and the reactions of ozone with unsaturated VOCs (volatile organic compounds containing unsaturated carbon-carbon bonds) present indoors can be considered to be by far the most important reactions in indoor ozone chemistry or even in indoor air chemistry. Among the many reactions which can occur indoors, Weschler's results (1999) show that reactions of ozone with selected terpene (d-limonene, α -terpinene, α -pinene) can be a significant source of sub-micron particles in indoor spaces. More or less the same conclusions were

formulated in a paper published by Wolkoff et al (2000) after the authors studied the airway irritants produced by the reaction of ozone with terpene. Ozone can also react with building products and the results published by Nicolas et al (2005) show that increased emissions of formaldehyde, hexanal, heptanal, octanal and decanal have been measured during exposure to ozone of several products frequently used indoors (carpet, PVC flooring, paint, etc.). Also, according to the results recently published by Tamas et al (2006), it has been shown that the reaction of ozone with limonene can decrease the perceived air quality. Ozone passing through used particulate filters (loaded with atmospheric dust) can be responsible for oxidation processes resulting in the generation of products that contribute to the deterioration of the perceived air quality (Bekö et al, 2006). Finally, a comprehensive overview of indoor ozone chemistry, is presented by Weschler (2000). In summary, there are many examples (mainly for ozone and, to a lesser extent, for nitrogen oxides) showing that molecular compounds should be removed before they enter ventilation systems.

General ventilation filters exist on the market for gas phase removal but there are very few publications reporting on the real life performances of this kind of filter. The aim of this work was to study (for one year) the real life efficiency for O₃, NO₂ and NO of gas phase filters installed within an air handling unit of a HVAC system feeding 100 %

fresh (outdoor) air to an office building and to assess their impact on the indoor air quality of the building.

2. Gas Phase Filtration: Literature Review

More than thirty years ago, Sabersky et al (1973), on the basis of the results of their experiments, explained that certain filters, especially those using activated carbon, can be used to reduce indoor levels of ozone.

A few years later, the results published by Shair (1981) are probably the first showing very clear results on how gas phase filters installed within a ventilation system can remove ozone (and sulphur dioxide). These results showed the (positive) influence of gas phase filters (protected by prefilters) on the indoor ozone concentration (less than 0.2 times the outdoor concentration) after 1, 2 and 3 years of use (the air handling unit was running only when the outdoor ozone concentration exceeded 0.2 ppm, mainly in summer time) but this influence was not correlated with any of the parameters of the air (temperature, relative humidity, etc.).

Gas phase filters (protected by coarse and fine filters) installed in three separate air handling units were studied by Shields et al (1999) regarding their ability to remove ozone after extensive use. For the first air handling unit, it decreased by only 5 % after 5 years of use (95 to 90 %). The filter efficiency of the second air handling unit decreased by 25 % after 3 years of use (from 85 to 60 %) and remained at this efficiency after 8 years of use. The efficiency of

the third air handling unit also decreased by 25 % (from 95 to 70 %) over 7 years of use. In this case the efficiency was unchanged during the first 3 years. The authors report that the efficiency may sometimes decrease for a short period and they explain this by an increase of the relative humidity of (outdoor) air (this parameter was not measured). Similar results were published, in more detail, by Weschler (1992 and 1994).

Other interesting results have been published by Partti-Pellinen et al (2000). These authors studied the effect of ventilation and air filtration on indoor air quality in a children's day care centre. Nitrogen oxides readily penetrate indoors without gas phase filters, while 50 to 70 % were removed when gas phase filters (carbon and aluminium oxide saturated with potassium permanganate) were used.

From the above literature review it can be concluded that although the use of gas phase filters in ventilation systems has been studied there are very few data dealing with the performance of the filters and such data are not correlated to any other parameters except the life-time of the filters. However, the indoor / outdoor concentration ratio has been more extensively studied (mainly for ozone) and this point is discussed later in this paper.

3. Method

The gas phase filters were studied when installed in an air handling unit providing 100 % fresh (outdoor) air to an office building located in Lyon (France). The air handling unit was located on the roof of the building, 9th floor, and air was distributed to the

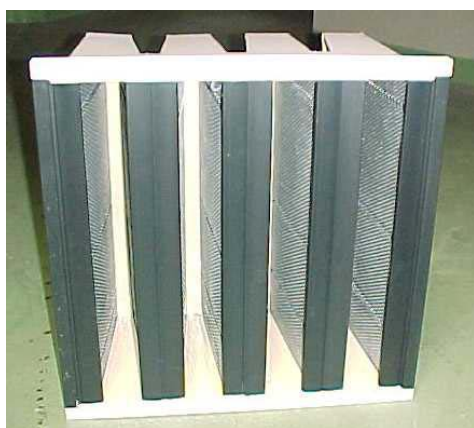


Figure 1. The gas phase filter.



Figure 2. Filters within the air handling unit.

offices through ceiling air diffusers. Air exhausts, also on the ceiling, were connected to a separate air handling unit. Four full size and two half size gas phase filters (26 kg per filter including 12.5 kg of activated carbon, provided by France Air company, Figure 1) were installed in parallel and were each protected by pleated F6 (EN 779) prefilters (glass fibre medium, provided by Camfil Farr company) installed just upstream (Figure 2). The activated carbon was coconut based, 95 % by mass of the grains had a diameter greater than 2.5 mm, and the specific surface area of the activated carbon was 800 m²/g. The air handling unit operated continuously 5 days a week (Monday to Friday) from 6:00 am to 8:00 pm.

O₃, NO₂ and NO gas concentration measurements were carried out just upstream of the filters (outdoor air), just downstream of the filters (supplied air) and on the exhaust air duct (indoor air). These measurements were made with automatic specific analyzers (UV absorption analysis for O₃ and chemiluminescence for NO₂ and NO). The filtration efficiency was calculated from the results of the gas concentrations measured upstream and downstream of the filters. The temperature and relative humidity of the air were also measured upstream of the filters. These measurements were performed each month during a one week period. Gas analyzers were connected to sample lines and electric valves allowed alternated sampling between the 3 measurement points. Data were collected by an acquisition system connected to a computer. The airflow rate of the air handling unit was calculated from the air velocity profile in the duct measured with an anemometer.

For comparison purposes, measurements were made during a one week period just before the prefilters and the gas phase filters under study were installed (June 3, 2005).

4. Results and Discussion

4.1 Airflow Rate of the Air Handling Unit

The airflow rate of the air handling unit remained more or less constant during 3 months then began to decrease as the filters (mainly the prefilters) became loaded by particles. The airflow rate increased back to its initial value after the prefilters were changed after more than 6 months of use. The airflow rate of the air handling unit ranged between 12500 and 16900 m³/h meaning that, per full size filter, the airflow rate ranged between 2500 and 3400 m³/h.

4.2 Gas Concentrations with and without Gas Phase Filters

Figures 3 to 8 show gas concentration measurement results for O₃, NO₂ and NO before (the air handling unit was at that time equipped with G4 and F6 particulate air filters in series) and after the new filters (prefilters and gas phase filters) were installed.

Outdoor O₃ concentration values show a typical trend for summer time with a continuous increase from the beginning to the middle of the day. Before the installation of the gas phase filters, the efficiency of the filters was equal to zero as the O₃ concentration downstream of the filters was the

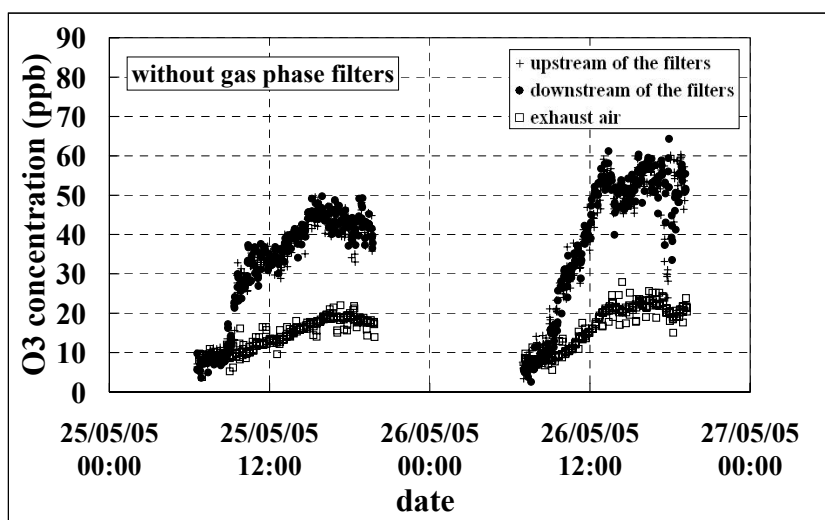


Figure 3. O₃ concentrations without gas phase filters.

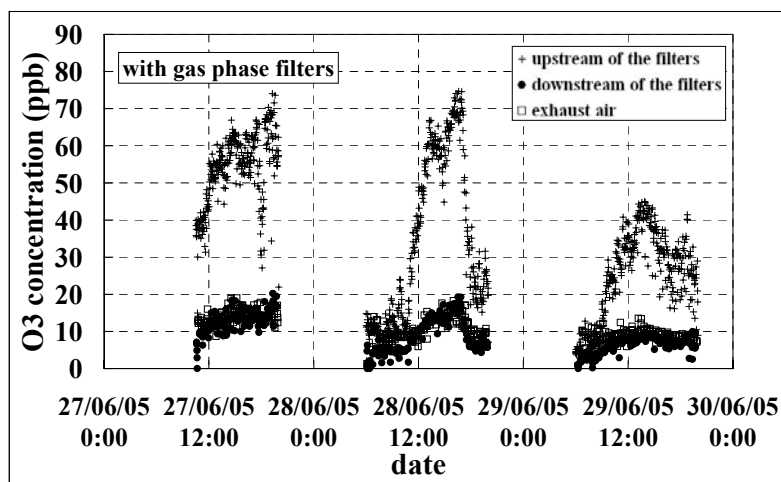


Figure 4. O_3 concentrations with gas phase filters.

same as that upstream (Figure 3). Sometime it has been shown that particulate air filters can remove a small amount (a few percent) of the incoming ozone (Bekö et al, 2006) but this phenomenon was not observed in our study. The O_3 concentration was lower indoors than outdoors but the trend indoors (increase or decrease) was the same as outdoors. Ozone does not disappear indoors but reacts with material surfaces and other chemicals. The efficiency of the gas phase filters is evident as the concentration was lower downstream than upstream (Figure 4).

For NO_2 and NO , the maximum outdoor concentration is generally obtained twice a day during automotive traffic peaks, first early in the morning and then at the end of the afternoon

(Figures 5 to 8). Before the installation of the gas phase filters, the filter efficiency was equal to zero as the NO_2 and NO concentrations downstream of the filters were the same as upstream (Figures 5 and 7). NO_2 and NO penetrate readily indoors with a short time delay. For NO_2 , the efficiency of the gas phase filters is evident as the concentration is lower downstream than upstream (Figure 6). The gas phase filters are ineffective at removing NO and the concentration is sometimes higher downstream than upstream (Figure 8). This phenomenon is not due to NO desorption as NO had not been previously adsorbed by the gas phase filters but is due to the chemical transformation of NO_2 into NO in the filters. Ekberg and Strindehag (1999) reported on this phenomenon but no data were presented in their paper.

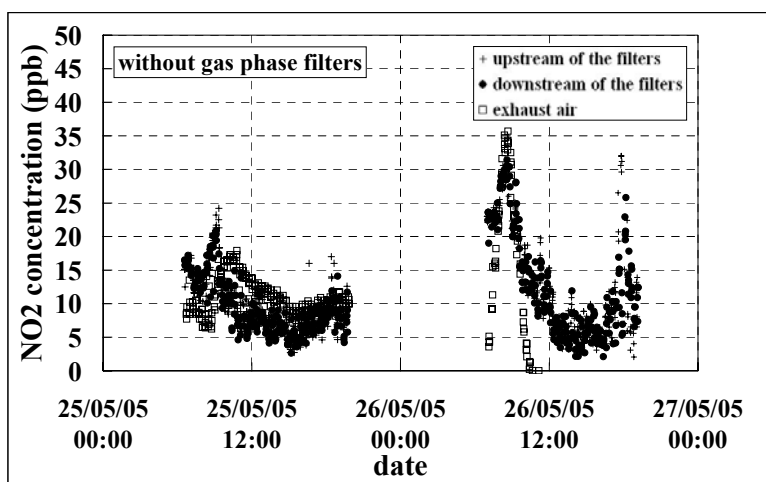


Figure 5. NO_2 concentrations without gas phase filters.

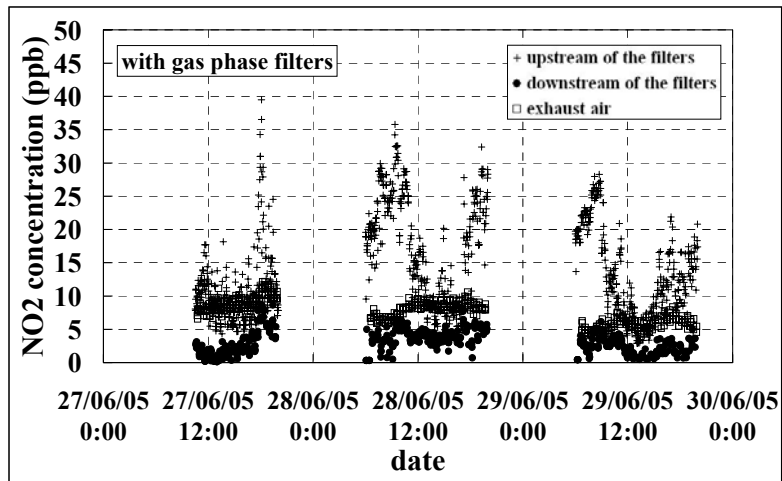


Figure 6. NO₂ concentrations with gas phase filters.

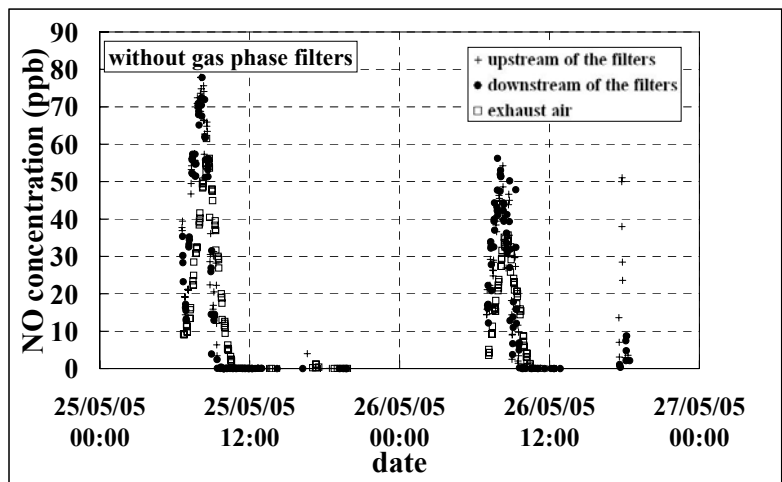


Figure 7. NO concentrations without gas phase filters.

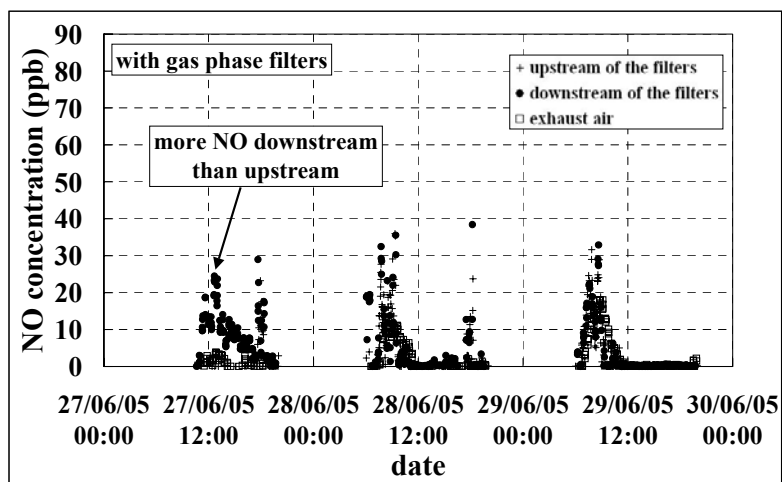


Figure 8. NO concentrations with gas phase filters.

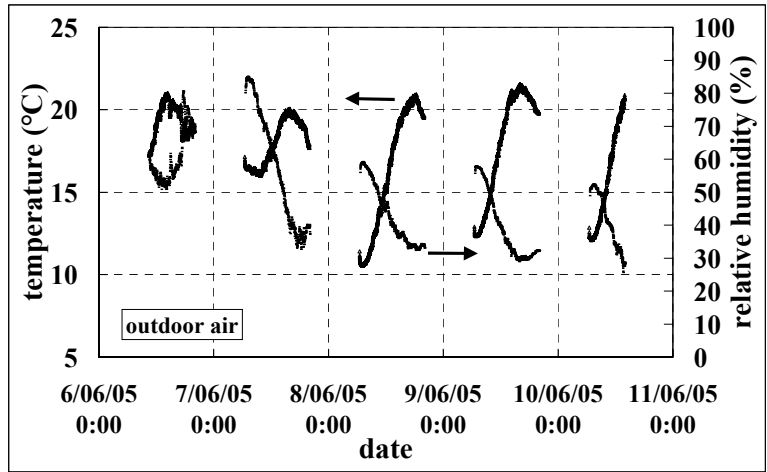


Figure 9. Climatic conditions (June 2005).

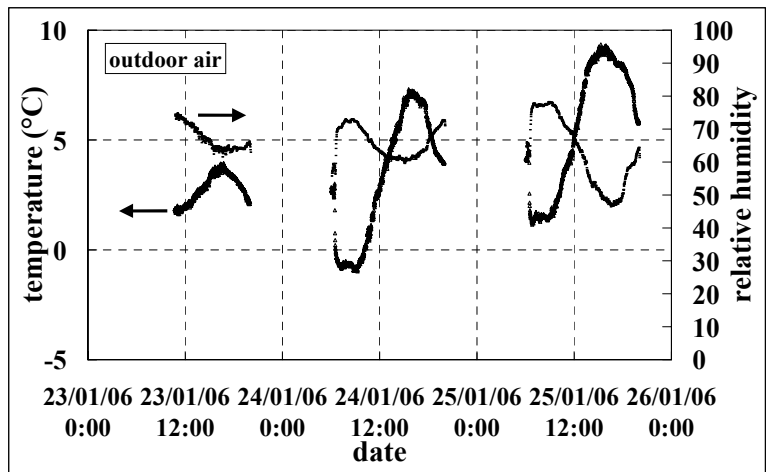


Figure 10. Climatic conditions (January 2006).

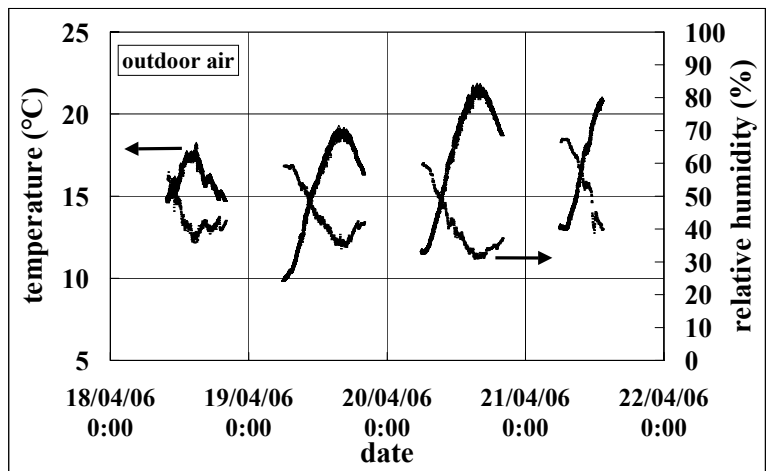


Figure 11. Climatic conditions (April 2006).

4.3 Efficiency of Gas Phase Filters

The climatic conditions (outdoor air) encountered during the measurements carried out when the gas phase filters were in place are shown in Figures 9, 10 and 11.

For O_3 , the initial efficiency of the filters (June 2005) ranged between 60 and 80 % (Figure 12) and reduced after several months of use (Figures 13 and 14). The efficiency was lower during winter time (Figure 13).

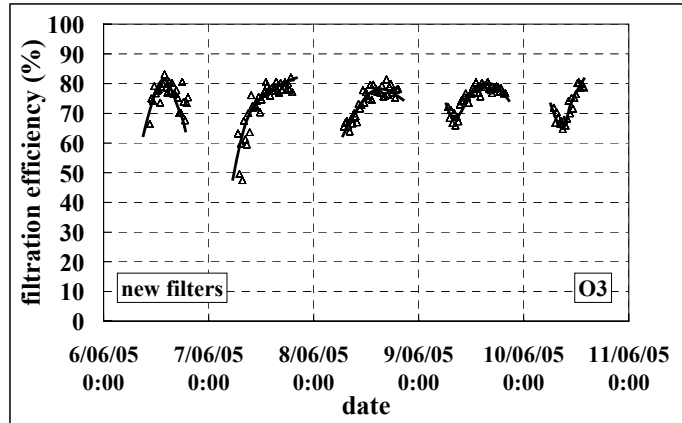


Figure 12. Filtration efficiency (O_3) (June 2005).

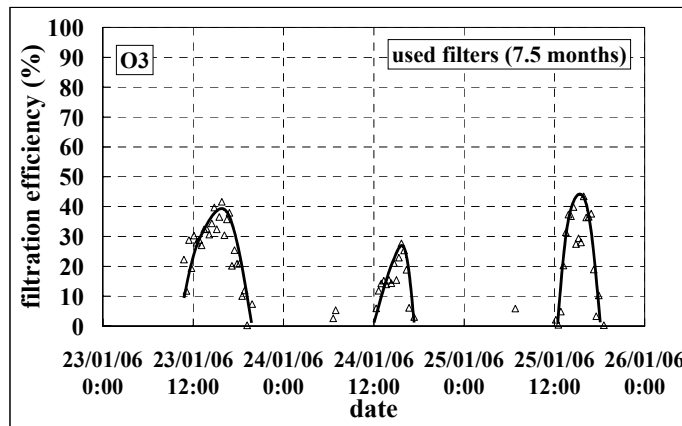


Figure 13. Filtration efficiency (O_3) (January 2006)

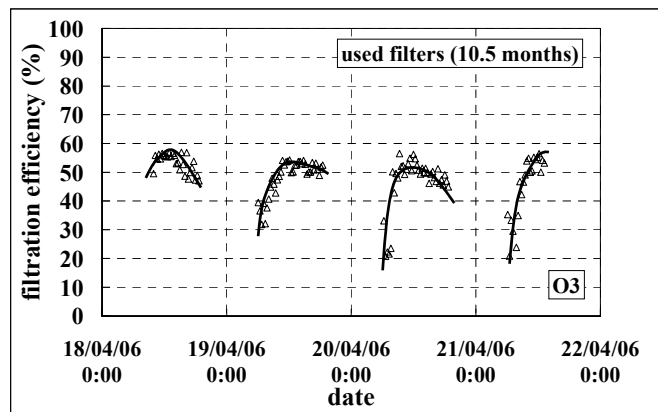


Figure 14. Filtration efficiency (O_3) (April 2006).

The results based on monitoring in June 2005 and April 2006 showed that:

- For constant relative humidity, the O₃ filtration efficiency increased with temperature as shown in Figure 15. This implied that the main mechanism for ozone removal is chemical reaction (ozone reaction with the activated carbon and with molecular compounds, especially VOCs, adsorbed on the activated carbon).
- For constant air temperature, the O₃ filtration efficiency remained constant with increasing relative humidity up to a value of approximately 70%. Thereafter it decreased (see Figure 16). In this case, O₃ would probably not be able to react with molecular compounds that cannot be adsorbed onto the activated carbon (competition between water and molecular compounds).

Trying to establish a relationship between the efficiency of the gas phase filters on ozone and the air characteristics (temperature and relative

humidity) does not mean that other parameters (presence of other chemicals for example) have no effects. According to the results presented in Figures 15 and 16, it can be concluded that the efficiency of the gas phase filters on ozone had decreased by only 20% after 10 months of use. During this period the pressure drop across the gas phase filters only increased from 203 to 235 Pa thus indicating that they were well protected by the prefilters against loading by atmospheric dust.

In the case of NO₂ filtration, the initial efficiency (June 2005) ranged between 60 and 90% (Figure 17) and appeared to be lower at 7.5 and 10.5 months later (Figures 18 and 19). There was found to be no clear relationship between the filtration efficiency and the climatic conditions but sometimes it looked as if the efficiency increased for decreasing air temperature and increasing relative humidity (Figure 18). However, because of the wide scatter of results it was difficult to establish any definite relationship of NO₂ filtration efficiency with air temperature and relative humidity.

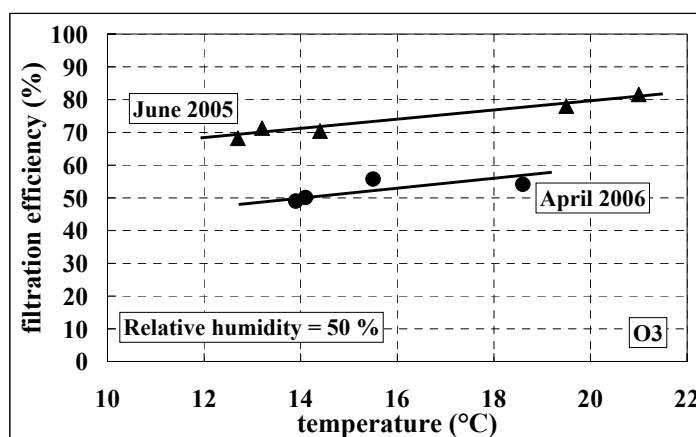


Figure 15. Filtration efficiency (O₃) at constant relative humidity (50%).

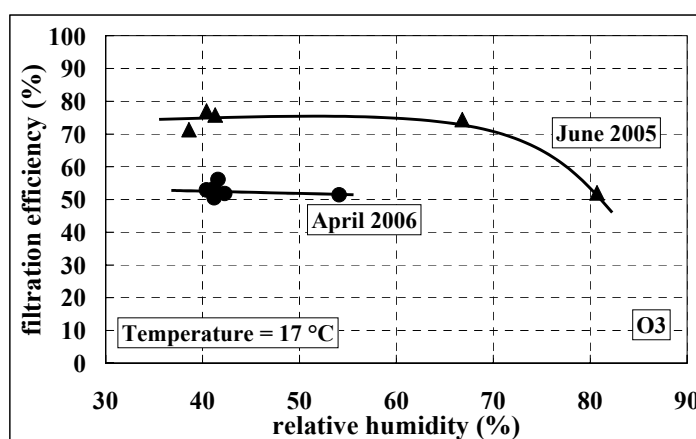


Figure 16. Filtration efficiency (O₃) at constant temperature (17°C).

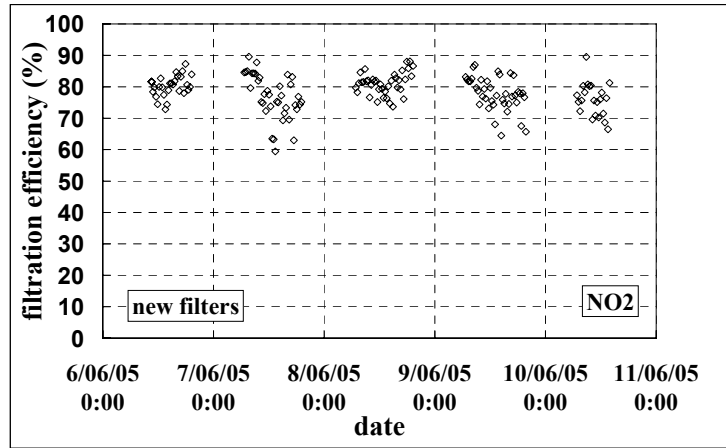


Figure 17. Filtration efficiency (NO₂) for new filters.

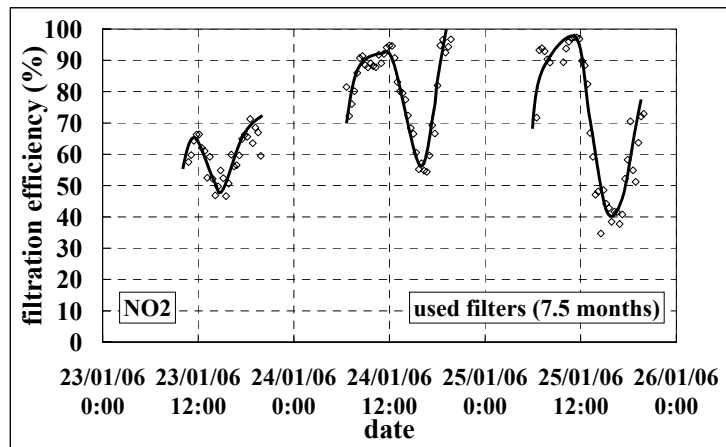


Figure 18. Filtration efficiency (NO₂) for used filters (after 7.5 months).

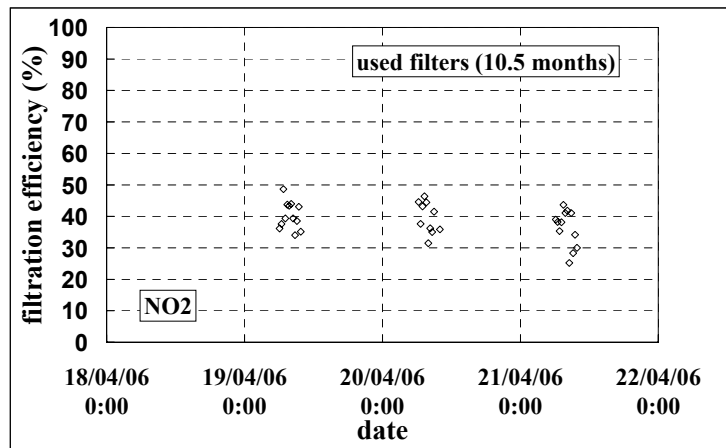


Figure 19. Filtration efficiency (NO₂) for used filters (after 10.5 months).

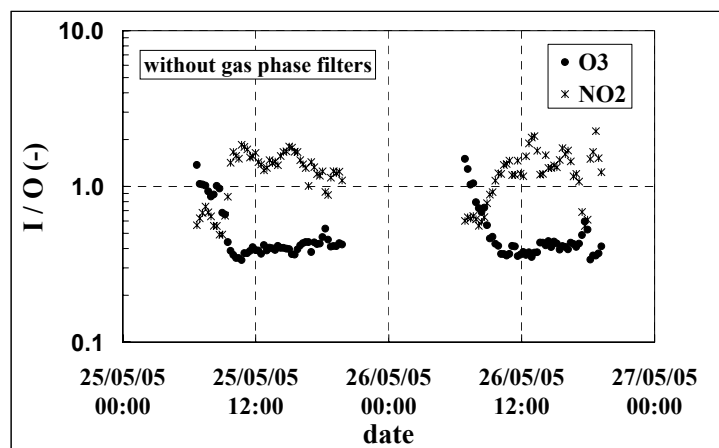


Figure 20. Indoor / outdoor concentration ratio (without gas phase filters).

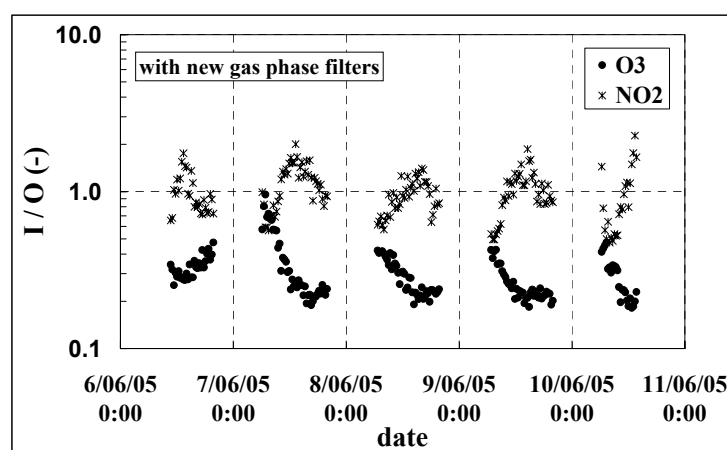


Figure 21. Indoor / outdoor concentration ratio (with new gas phase filters).

4.4 Indoor / Outdoor Concentration Ratio

The results presented in Figures 20 and 21 show that by using gas phase filters the indoor / outdoor concentration ratio is lowered.

In the case of ozone, this ratio decreases as the day proceeds and as the outdoor ozone concentration increases. The ratio reaches 0.4 without gas phase filtration with this ratio mainly being dependent on the airflow rate (air exchange rate) and the chemical reactions between ozone and indoor surfaces and indoor chemicals. With gas filtration, using new filters, the ratio reduces to 0.2. The results also show that there is a background level of ozone inside the building even if there is no ozone outside. These results compare with the literature review of Weschler (2000), which concludes that ranges between 0.2 and 0.7 are observed for non filtered air

while values as low as 0.05 can be achieved in buildings that are tightly sealed or use gas phase filters.

For further comparison, in a project aimed at the protection of works of art from atmospheric ozone, Cass et al (1989) studied the indoor / outdoor concentration ratio in museums with different air conditioning and ventilation systems. Results showed that the ratio ranged between:

- 0.69 and 0.84 in buildings with a high air exchange rate and no air conditioning;
- 0.10 and 0.59 in buildings with a low air exchange rate;
- 0.33 and 0.49 in a naturally ventilated building;
- 0.24 and 0.40 in buildings with a conventional air conditioning system and no gas phase filters;

- 0.03 and 0.17 in buildings with gas phase filtration systems.

The indoor / outdoor concentration ratio for NO₂ starts below 1 as the indoor concentration is low (it is assumed that there are no indoor sources). It then increases as the day progresses. When the outdoor peak due to automotive traffic penetrates indoors via the ventilation system (part of the total amount of NO₂ breaks through the gas phase filters), ratios above 1 can be recorded before the value returns to below 1 when the indoor NO₂ is removed by ventilation. There are not many data available in the literature for this kind of building (except for those from Partti-Pellinen et al, 2000, discussed earlier). Almost all the data available concern homes and kitchens

5. Conclusions

In relation to O₃ the efficiency of gas phase filters was found to be closely dependent on the temperature and the relative humidity of air. Performance also decreased by about 20 % after 10 months of use.

In relation to NO₂, there was no clear relationship between the filtration efficiency and climatic conditions but, again, efficiency decreased after 10 months of use.

Gas phase filters were found to be ineffective at removing NO and the NO concentration was sometimes found to be higher downstream than upstream. This was not due to a desorption phenomenon since NO had not been previously adsorbed. Instead, it was considered to be as a result of chemical transformation of NO₂ into NO. Additional work is necessary in order to better understand this phenomenon and to know which parameters have an effect on it.

The use of gas phase filters has a positive effect on indoor air quality since the indoor / outdoor concentration ratio was found to be lower than when they were not installed.

The use of gas phase filters may be recommended for general ventilation applications.

The method and apparatus presented in this paper can be used in real situations to assess the efficiency of gas phase filters.

Acknowledgements

This study was sponsored by the French HVAC system manufacturing companies which are members of CETIAT. The authors are grateful to Camfil Farr and France Air for supplying the filters.

References

- Bekö G, Halas O, Clausen G and Weschler CJ: (2006). "Initial studies of oxidation processes on filter surfaces and their impact on perceived air quality", *Indoor Air*, 16, pp56-64.
- Cass GR, Druzik JR, Grosjean D, Nazaroff WW, Whitmore PM and Wittman CL: (1989). "Protection of works of art from atmospheric ozone", *Research in Conservation*, The Getty Conservation Institute.
- Ekberg LE and Strindehag O: (1999). "Long-term testing of gas adsorption filters for ventilation systems", *AIVC, 20th Annual Conference, Ventilation and Indoor Air Quality in Buildings*, Edinburgh, Scotland, 8-13 August 1999.
- Nicolas M, Ramalho O and Maupetit F: (2005). "Reactions between ozone and building products: impact on primary and secondary emissions", *The 9th International Conference on Indoor Air Quality and Climate Indoor Air 2005*, Beijing, China, 4-9 September 2005.
- Partti-Pellinen K, Marttila O, Ahonen A, Suominen O and Haahtela T: (2000). "Penetration of nitrogen oxides and particles from outdoor into indoor air and removal of the pollutants through filtration of incoming air", *Indoor Air*, 10, pp126-132.
- Sabersky RH, Sinema DA and Shair FH: (1973). "Concentrations, decay rates and removal of ozone and their relation to establishing clean indoor air", *Environmental Science Technology*, 7, (4), pp347-353.
- Shair FH: (1981). "Relating indoor pollutant concentrations of ozone and sulfur dioxide to those outside: economic reduction of indoor ozone through selective filtration of the make-up air", *ASHRAE Transactions*, Part 1, pp116-139.
- Shields HC, Weschler CJ and Naik D: (1999). "Ozone removal by charcoal filters after continuous extensive use (5 to 8 years)", *The 7th International Conference on Indoor Air Quality and Climate*

Indoor Air'99, Edinburgh, Scotland, 8-13 August 1999.

Tamas G, Weschler CJ, Toftum J and Fanger PO: (2006). "Influence of ozone-limonene reactions on perceived air quality", *Indoor Air*, 16, pp168-178.

Weschler CJ, Shields HC and Naik DV: (1992). "An evaluation of activated carbon filters for the control of ozone, sulfur dioxide and selected volatile organic compounds", *ASHRAE IAQ'92 Conference, Environments for People*, San Francisco, USA, 18-21 October 1992.

Weschler CJ, Shields HC and Naik DV: (1994). "Ozone removal efficiencies of activated carbon filters after more than three years of continuous service", *ASHRAE Transactions*, Part 2, pp1121-1129.

Weschler CJ and Shields HC: (1999). "Indoor ozone/terpene reactions as a source of indoor particles", *Atmos Environ.*, **33**, (15), pp2301-2312.

Weschler CJ: (2000). "Ozone in indoor environments: concentration and chemistry", *Indoor Air*, 10, (4)pp269-288.

Wolkoff P, Clausen PA, Wilkins CK and Nielsen GD: (2000). "Formation of strong airway irritants in terpene/ozone mixtures", *Indoor Air*, 10, pp82-91.

Yocom JE: (1982) "Indoor outdoor air quality relationships", *J Air Pol.*, **32**, (5).

Zhang J and Liroy PJ: (1994). "Ozone in residential air: concentrations, I/O ratios, indoor chemistry and exposures", *Indoor Air*, 4, pp95-105.

The Air Infiltration and Ventilation Centre was inaugurated through the International Energy Agency and is funded by the following ten countries:

Belgium, Czech Republic, Denmark, France, Greece, Japan, The Netherlands, Norway, South Korea and United States of America.

The Centre provides technical support in air infiltration and ventilation research and application. The aim is to provide an understanding of the complex behaviour of the air flow in buildings and to advance the effective application of associated energy saving measures in both the design of new buildings and the improvement of the existing building stock.

Air Infiltration and Ventilation Centre
Operating Agent and Management
INIVE EEIG
Boulevard Poincaré 79
B -1060 Brussels - Belgium



Tel: +32 2 655 77 11
Fax: +32 2 653 07 29
inive@bbri.be
www.inive.org